UNIVERSITÀ DEGLI STUDI DI NAPOLI "FEDERICO II"

DOTTORATO DI RICERCA IN BIOLOGIA APPLICATA
XXVI CICLO

The Serotonin Receptor 7: a key regulator of neuronal cytoarchitecture in the Central Nervous System

COORDINATOR:
PROF.
EZIO RICCA

CO-TUTOR:
PROF.
CARLA PERRONE CAPANO

TUTOR:
PROF.
MARIANNA CRISPINO

CANDIDATE:
LUISA SPERANZA

ANNO ACCADEMICO 2013-2014

INDEX

1. INTRODUCTION

1.1 The neurotransmitter serotonin and the serotonergic system in the mammalian brain

Neurotransmitters have the well known role of mediators in synaptic neurotransmission: they are released by the nerve endings of presynaptic neurons, diffuse across the synaptic cleft and interact with specific receptors on postsynaptic neurons, inducing a response identified as modification of membrane potential. Besides their key role in neurotransmission, these compounds have also additional functions not only in neurons, but also in other cells. An increasing body of evidence indicates that neurotransmitters are acting as signals during the development of the nervous system, modulating the architecture and plasticity of brain circuits.

Serotonin (5-hydroxytryptamine or 5-HT) was the first neurotransmitter for which a developmental role was suggested. It is a phylogenetically ancient signaling molecule (Hay-Schmidt, 2000) and it is the most widely distributed neurotransmitter in the brain (Steinbusch, 1981). The activation of 5-HT signaling pathways is involved in several brain functions, including sensory processing, cognitive control, emotion regulation, autonomic responses, and motor activity. In addition, the 5-HT pathways are target of many physiological regulators, such as modulators of gene transcription, neurotrophic factors, and steroids, as well as psychotropic compounds. Serotonin is involved in basic morphogenetic activities during brain development and in the life-spanning adaptive capacity of the brain, including modulation of neural cell proliferation, migration and differentiation as well as neurite outgrowth, axonal guidance, synaptogenesis, and efficiency of transsynaptic signaling (Azmitia and Whitaker-Azmithia, 1997; Daubert and Condron, 2010; Gaspar et al, 2003).

Several evidence link dysfunction of 5-HT transmission to neurodevelopmental and subsequent psychiatric disorders characterized by compromised function of the so-called “social brain” (Blakemore, 2008; Frith and Frith, 2012). These disorders comprise a spectrum of diseases ranging from schizophrenic psychoses to autism and attention-deficit-hyperactivity disorders.

In addition to the 5-HT role in synapse and neuronal network formation during development, increasing evidence implicate 5-HT in the regulation of cell adhesion molecules critically involved in the plasticity of the developing and adult brain (Dalva et al., 2007; Yamagata et al., 2003).

The 5-HT system of the mammalian brain originates from the raphe located in the midline of the rhombencephalon and in the reticular formation, where 5-HT neurons are clustered into nine nuclei numbered B1-9 on a rostrocaudal axis (Azmitia and Whitaker-Azmitia, 1997). These clusters are subdivided into rostral and caudal sections with the rostral subdivision comprising the caudal linear

nucleus (CLi), the dorsal raphe nucleus (DR: B6, B7) and the median raphe nucleus (B9 and MR:, B8, B5). 5-HT neurons from the rostral subdivision project primarily to the forebrain where the extensive collateralization of their terminal densely innervates virtually all regions (Calizo et al, 2011; Hensler, 2006). The caudal portion, which projects mainly to the spinal cord and cerebellum, consists of nuclei termed as raphe pallidus (B1), raphe obscurus (B2), and raphe magnus (B3) and is involved in motor activity, pain control, and regulation of the autonomic nervous system.

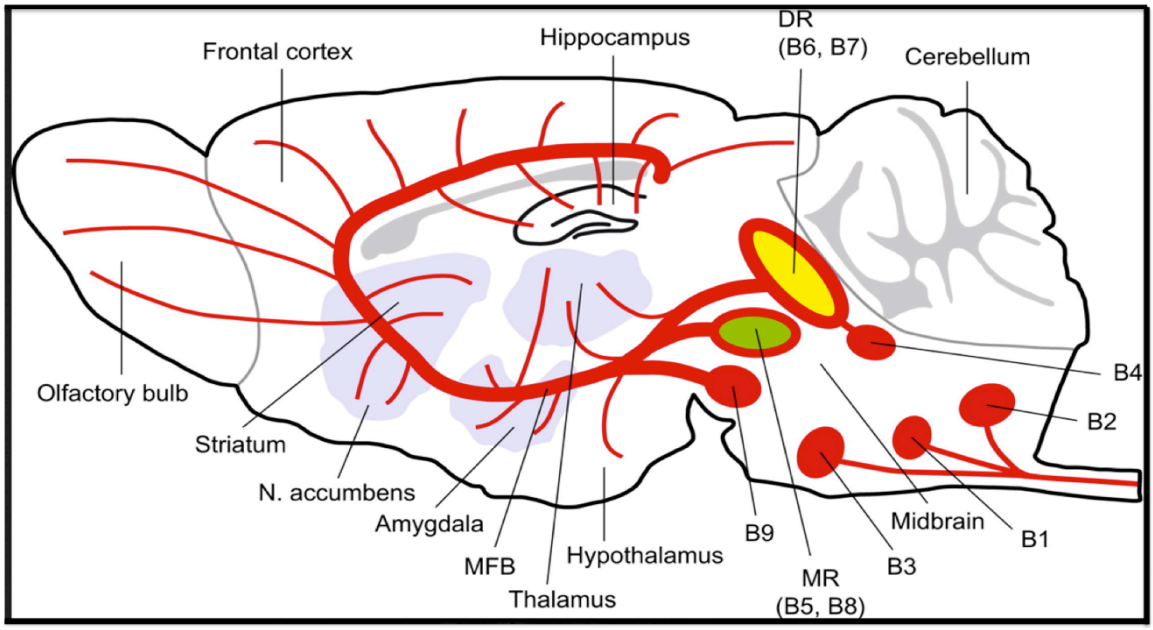

Figure 1. Rodent Brain 5-HT System.

5-HT neuron clusters are organized in the nine raphe nuclei, B1-B9. The more caudal nuclei (B1-B3) in the medulla project axons to the spinal cord and the periphery, whereas the more rostral raphe nuclei contain the principal dorsal raphe group (B6 and B7; depicted in yellow) and the median raphe group (B5 and B8; depicted in green), which project to different but overlapping brain areas. DR, dorsal raphe nucleus; MFB, medial frontal bundle; MR, median raphe nucleus. Image from (Lesch and Waider, 2012).

1.2 Serotonin biosynthesis and trafficking in nerve endings

Serotonin is synthesized from a diet-derived indole-containing precursor, the amino acid tryptophan (TRP, Figure 2). The initial and rate limiting step is the conversion of L-tryptophan to 5-hydroxy-L-tryptophan (5-HTP) by tryptophan 5-hydroxylase (TPH), which has two isoforms. Tph1 is primarily localized in the enterochromaffin cells (EC cells), whereas Tph2 is mainly found in the central and enteric neurons (Walther et al. 2003; Yu et al. 1999). The second and final step is the conversion of 5-HTP to serotonin by aromatic L-amino acid decarboxylase (AADC, Figure 2). As serotonin is a very basic molecule, once formed it quickly gets transported into vesicles via a vesicular monoamine transporter (VMAT). There are two isoforms: VMAT1, which is only present in neuroendocrine cells, and VMAT2, which is the neuronal isoform (Erickson et al., 1996). The synaptic vesicles release serotonin via exocytosis into the synaptic cleft, where it binds to pre- and/or post-synaptic serotonin receptors. To avoid desensitizing serotonin's receptors, reuptake of serotonin via the Na^+/ Cl^- dependent transporter Serotonin Reuptake Transporter (SERT) is required (Fuller and Wong, 1990; Wade et al., 1996). When SERT is knocked out, organic cation transporters can function as low affinity backup serotonin transporters (Chen et al., 2001). Upon reuptake, serotonin is broken down primarily by monoamine oxidase A (MAOA) into 5-hydroxyindoleacetic acid (5-HIAA) (Figure 2). Alternatively it can be metabolized into N-methyl, N,N-dimethyl or O-methyl tryptamine and then into melatonin (Siegel et al., 2011). Metabolism to melatonin occurs mainly in the pineal gland though it can also occur in the gastrointestinal tract (Raikhlin et al., 1975).

SERT regulates the extracellular serotonin concentration in most brain regions through reuptake of this neurotransmitter (Benninghoff et al., 2012). The serotonin transporter belongs to the family of monoamine transporters and serves the high affinity reuptake of 5-HT into presynaptic terminals. After being released by activity of 5-HT neurons, it is assumed that the majority (90%) of 5-HT is removed by controlled reuptake via SERT whereas diffusion serves the clearance of the remaining 10% (Stoltenberg 2005). The activity and the amount of SERT within the synapse significantly determine the length of time for the chemical signal to remain in the synaptic cleft. By internalizing 5-HT into presynaptic neurons and enabling a successive storage of 5-HT into presynaptic vesicles SERT furthermore mediates the maintenance of the 5-HT pool available for subsequent release (see Figure 2). The highest density of SERT occurs in serotonergic cell bodies in the raphe complex but

also in regions receiving serotonergic projections such as neocortical regions, entorhinal cortex, the CA3 region of the hippocampus, the amygdala, the striatum, the hypothalamus and the substantia nigra (Hensler et al., 1994; Ravindran et al., 1994). Disruption of SERT has been implicated in development, appetite and insulin sensitivity (Marston et al., 2011).

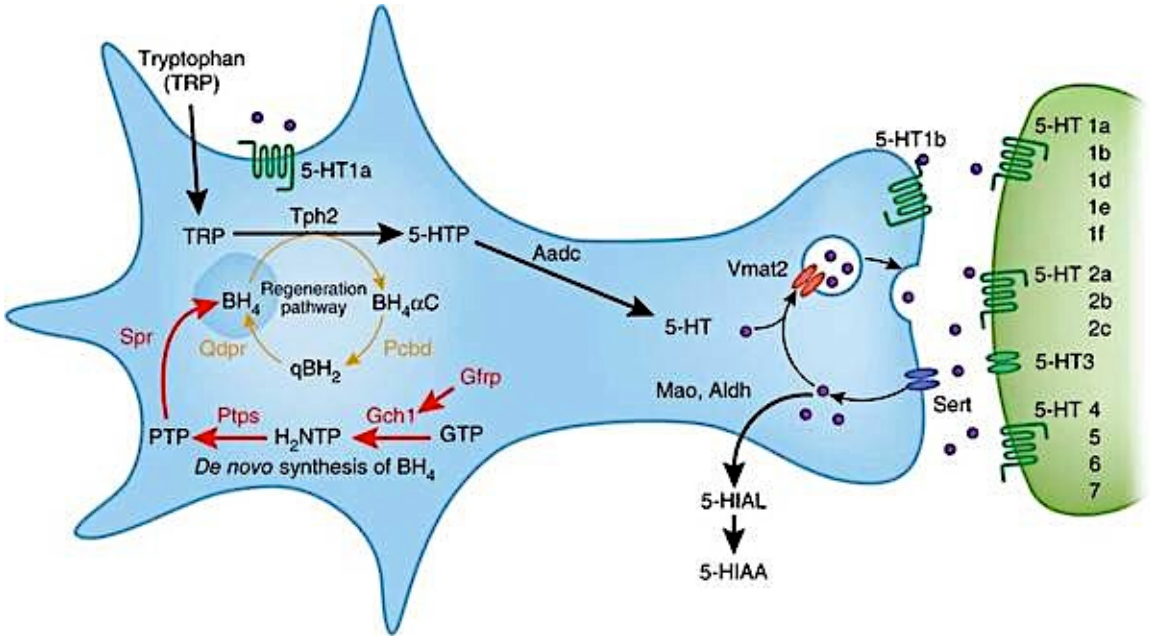

Figure 2. Serotonergic neuron identity.

5-HT neurons co-express genes directing 5-HT synthesis (Tph2, Aadc, Gch1, Gfrp, Ptps, Qdpr), reuptake (Sert), vesicular transport (Vmat2), autoreceptor signaling (Htr1a, Htr1b) and metabolism (Maoa, Maob).

1.3 Classification of 5-HT receptors

Over the years, with the development of new pharmacological and molecular tools such as radioligand binding, availability of potent and selective ligands and sequencing, it became clear that there must be more 5-HT receptor (5-HTR) subtypes. The current classification scheme takes into account not only operational criteria, such as drug-related characteristics, but also information about intracellular signal transduction mechanisms and amino acid sequence of the receptor protein (Hoyer et al., 1994; Hoyer and Martin 1997).

Currently, eighteen serotonin receptor genes have been identified in vertebrates (Marston et al., 2011), and classified into 7 different families (Filip and Bader, 2009), and all of them are, except one, members of the G-protein coupled receptor (GPCR) superfamily. The exception is the 5-HT_3 receptor, a Cys-loop ligand-gated ion channel (LGIC) that in evolutionary terms arose independent of the GPCR 5-HT receptors along with other members of this superfamily (e.g. the nicotinic acetylcholine receptor, $GABA_A$ receptor). Further receptor heterogeneity is generated through alternative splicing (e.i. 5-HT_3, 5-HT_4 and 5-HT_7 receptors), RNA editing (the 5-HT_{2C} receptor), and the putative formation of homo- and heterodimers (Nichols and Nichols, 2008). Biochemical, structural and functional evidence collected during the last decade indicates that GPCRs can form oligomers (Bulenger et al., 2005). Oligomerization can occur between identical receptor types (homodimerization) or between different receptors of the same or different GPCR families (heterodimerization). Heterodimerization is of particular interest because it can specifically modulate receptor properties. It can lead to significant changes in receptor pharmacology, either by affecting the ligand binding on individual protomers or by the formation of new binding sites (Franco, 2009; Rozenfeld and Devi, 2011). Serotonin receptors 5-HT_{1A} and 5-HT7 are highly co-expressed in brain regions implicated in depression. In a recent study, it is showed that 5-HT7 receptor forms heterodimers with the 5-HT_{1A} both in vitro and *in vivo* (Renner et al., 2012).

Receptor Subtype	Distribution	Post-receptor mechanism
5-HT1 (A-F)	Raphe nuclei, hippocampus, substantia nigra, globus pallidus, basal ganglia, cortex, putamen	G_i/G_o –protein coupled, ↓ cAMP
5-HT2 (A-C)	Cerebral cortex, hippocampus, substantia nigra, stomach fundus, choroid, platelets, smooth muscle, sensory and enteric nerves	G_q/G_{11} –protein coupled, ↑ IP_3
5-HT3	Area postrema, sensory and enteric nerves	Receptor is a Na^+ -K^+ ion channel
5-HT4	CNS and myenteric neurons, smooth muscle	G_s- protein coupled, ↑ cAMP
5-HT5 (A, B)	Brain	G_i/G_o –protein coupled, ↓ cAMP
5-HT6	Brain	G_s- protein coupled, ↑ cAMP
5-HT7	Brain	Gs- protein coupled, ↑ cAMP

Table 1. Classification of serotonin receptors.

1.4 The 5-HT7 receptor

The 5-HT7 receptor is the most recently identified member of the family of G-protein-coupled 5-HT receptors. It is coupled to G_s (activating adenylyl cyclase) and is widely distributed in the mammalian brain.

1.4.1 The 5-HT7 receptor gene

The 5-HT7 receptor gene is located on human chromosome 10q21-q24 and contains three introns. Alternative splicing only occurs at the second and third intron and gives to at least five splice variants in man, mouse and rat, which differ in their C-terminal tail. So far, three splice variants have been described in human (a, b and d) and in mouse (a, b and c) and four in rat (a, b, c, and e). No major differences in their pharmacology or functionality have been detected (Gellynck et al., 2008; Heidmann et al., 1998; Krobert and Levy, 2002). Two isoform are homologous in mouse, rat and human; they are designed 5-$HT_{7(a)}$ and 5-$HT_{7(b)}$ and are caused by two alternative donor sites located in tandem at the end of exon II. The use of the second splice donor site in the isoform 5-$HT_{7(b)}$ results in a 5bp insertion within the coding sequence, which introduces an in-frame stop codon. This shortens the C-terminal tail by 13 amino acids compared to the 5-$HT_{7(a)}$. The h5-$HT_{7(d)}$ contains an extra 98bp exon cassette at the exonII-exonIII boundary (Gellynck et al., 2008; Heidmann et al., 1997). In rat, a similar, yet distinct, exon (named exon C) provides the 5-$HT_{7(c)}$ splice variant (Figure 3). The different splice variants in each organism differ only in the length and sequence of theirs carboxy-terminal tail and in the number of phosphorylation sites (Vanhoenacker et al., 2000).

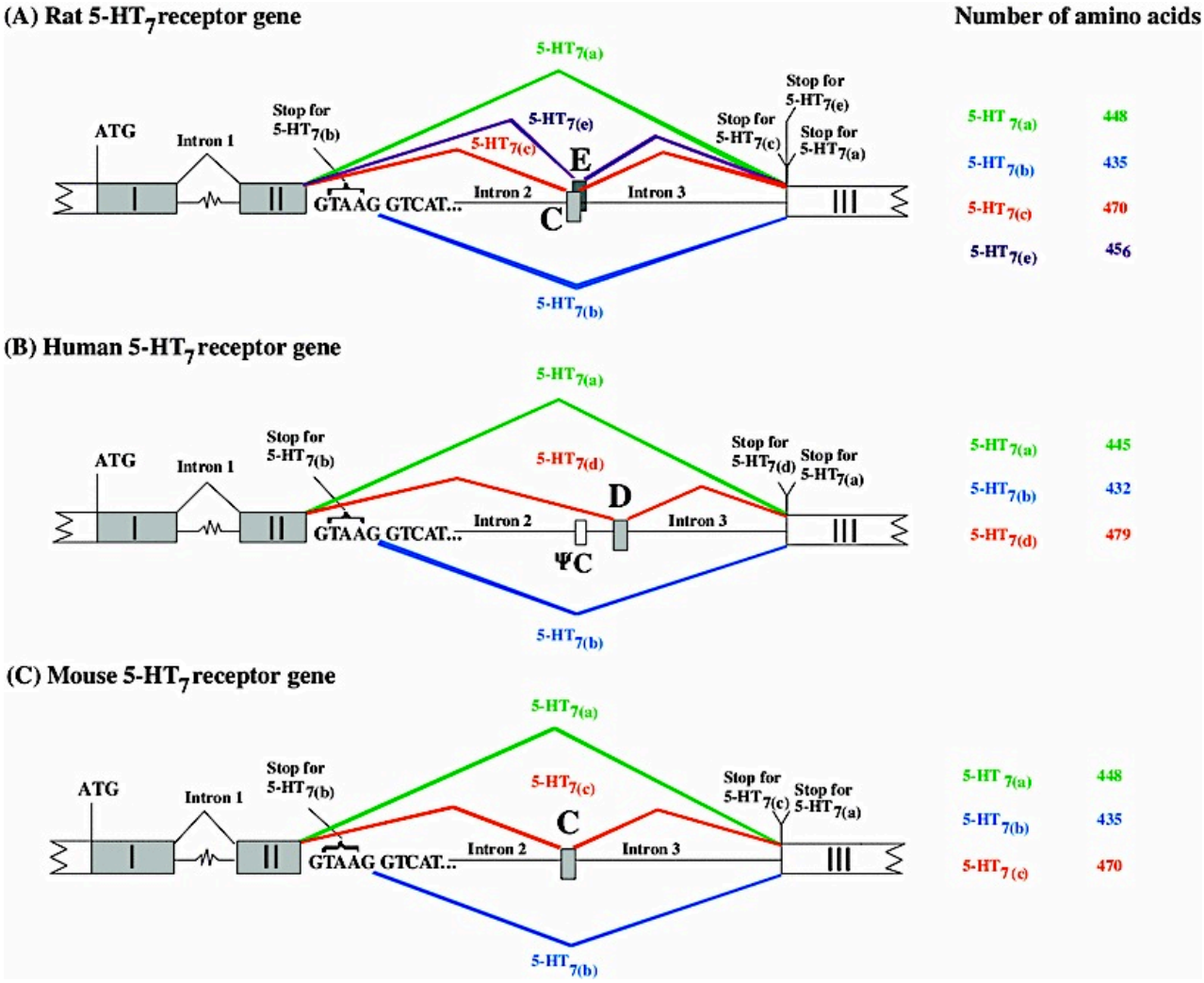

Figure 3. 5-HT7 receptors splice variants in rat, human and mouse. Images from (Gellynck et al., 2013)

The human isoforms 5-HT$_{7(a)}$ and 5-HT$_{7(b)}$ are present in brain, heart, kidney, liver, lung, placenta, small intestine, skeletal muscle, colon, ovary, testis, prostate, spleen and thymus tissues without difference in their relative abundance, with exception of 5-HT$_{7(b)}$ receptors not being present in the colon, whereas 5-HT$_{7(d)}$ receptor was not detected in kidney, skeletal muscle, prostate, thymus and it has lower expression in the other tissues than 5-HT$_{7(a)}$ and 5-HT$_{7(b)}$ receptors (Krobert et al., 2001). The 5-HT$_{7(b)}$ receptor variant is the most expressed of all variants in the hypothalamus, and 5-HT$_{7(d)}$ receptor is the least frequently expressed isoform and is mostly present in smooth muscle (Guthrie et al., 2005; Heidmann et al., 1997).

All variants display identical G protein, Adenylyl Cyclase (AC) coupling and high affinity for 5-HT; this similar pharmacological profile and binding abilities show that the difference in the C-tail does not influence ligand binding or receptor activation (Krobert et al., 2001). Additionally they are

constitutively active and display identical responses to constitutive AC activity. 5-HT7 receptors also behave as if they are pre-associated with G protein in the absence of ligand (Krobert et al., 2001).

The 5-HT7 receptor promoter contains regulatory elements for AP2 (adipocyte protein 2), Egr-1 (early growth response 1) and MAZ (MYC-associated zinc finger protein) and an Sp1/Sp3 consensus motif. In addition, Sp factors were shown to be essential for transcription of the 5-HT7 receptor (Leanen et al., 2007).

1.4.2 5-HT7 receptor signaling

Although coupling of the 5-HT7 receptor to cAMP formation has been known since the discovery of the receptor, recent studies have elucidated the functional coupling of the 5-HT7R in more detail. The 5-HT7 receptor can also activate extracellular signal-regulated kinase (ERK) (Errico et al., 2001); however, the involved signaling pathway seems to differ substantially depending on the cell system. In PC12 cells, 5-HT7 receptor-mediated ERK activation was shown to be dependent on a cAMP-activated guanine nucleotide exchange factor, briefly called Epac, and Rap (Lin et al., 2003), while in HEK293 cells, the 5-HT7 receptor couples to ERK through protein kinase A (PKA) and Ras (Norum et al., 2003). By inducing the rapid phosphorylation of ERK and IKBα in naive T cells, the 5-HT7 receptor appeared to interact synergically with T cell receptor signaling in the promotion of T cell activation and proliferation (Leon-Ponte et al., 2007). Finally, stimulation of the 5-HT7 receptor was also shown to induce expression of IL-6 in both an astrocytoma and a microglial cell line (Mahe et al., 2005; Lieb et al., 2005). In astrocytoma cell line, this was shown to be dependent on p38 MAPK and PKCε. Preliminary data indicate that the 5-HT7 receptor can reside in lipid rafts, more specifically caveolae, and internalize in a caveolin-dependent way (Sjogren et al., 2006; Sjogren and Svenningsson 2007). The 5-HT7 receptor was also shown to interact with eukaryotic initiation of translation factor 3, subunit k, which seems to play a role in transport of the receptor to the plasma membrane (De Martelaere et al., 2007).

Besides $G\alpha_s$, the receptor was also shown to interact with $G\alpha_{12}$. Activation of the 5-HT7 receptor/G α_{12} signaling pathway led to stimulation of Cdc42 and RhoA, resulting in serum response element-mediated gene transcription, which in turn led to filopodia formation and cell rounding (Kvanchina et al., 2005) (Figure 4).

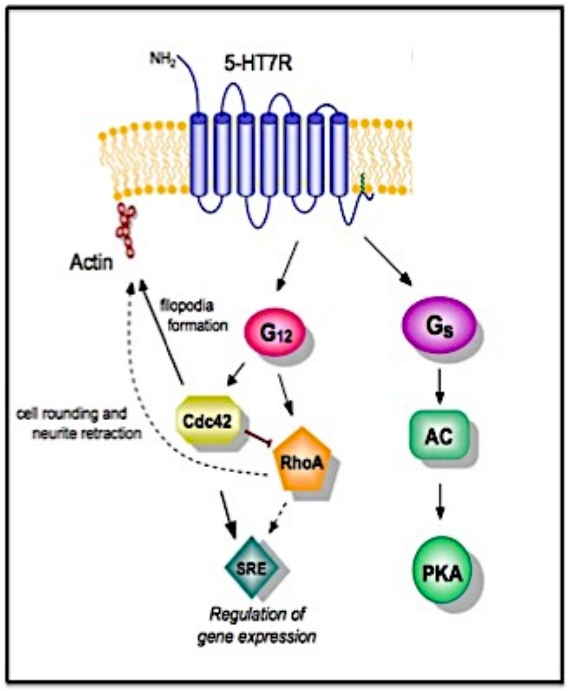

Figure 4. Molecular model for the 5-HT7 receptor-mediated signaling. The receptor couple to the stimulatory G_s protein leading to activation of different types of adenylyl cyclases and to Gα12 protein resulting in activation of small GTPases of the Rho family, RhoA and Cdc42. *Arrows* indicate activation and lines with a blunt end indicate inhibition. AC adenylyl cyclase, PKA protein kinase A, SRE serum response element.

1.4.3 Distribution of the 5-HT7 receptor

Early and more recent studies, using *in situ* hybridization, demonstrated that, in rat brain, 5-HT7 receptor mRNA is most abundant in thalamus, hippocampus and hypothalamus (Lovenberg et al., 1993; Gustafson et al., 1996; Neumaier et al., 2001). It is noteworthy that 5-HT7 receptor mRNA is present in all of the CA fields of the hippocampus and in the suprachiasmatic nucleus (SCN) of the hypothalamus.

The protein distribution of the 5-HT7 receptor in mice and rats, analyzed by immunohistochemical techniques, is similar to that observed for the mRNA, with the highest abundance in the thalamus, hypothalamus and hippocampus and with low levels of immunoreactivity in the rat striatum (Neumaier et al., 2001; Muneoka et Takigawa, 2003). In particular, in the hippocampus, the pyramidal cell layer of all CA regions exhibits immunoreactivity for the 5-HT7 receptor (Neumaier et al., 2001; Bickmeyer et al., 2002), while in the cerebellum, the 5-HT7 receptor protein is located exclusively in Purkinje cells (Geurts et al., 2002). In the mouse CNS, the 5-HT7 receptor is located in both dendrites and axon terminals of mostly GABA-containing neurons (Belenky and Pickard., 2001).

An important issue for any receptor is, of course, whether the expressed protein exhibits agonist/antagonist functional binding. Indeed, studies on knockout mice using radiolabeled selective 5-HT7 receptor antagonists and agonists (i.e. [3H] SB269970, [3H] 5-CT) confirm the protein and mRNA distribution pattern showing highest binding densities in the thalamus, hypothalamus and hippocampus (Bonaventure et al., 2002; Bonaventure et al., 2004). Additional studies, using radioligands, indicate notable differences between rats and human with high binding density in the human caudate and putamen nuclei and low level binding in rat striatum (Martin-Cora and Pazos, 2004).

The localization of 5-HT7 receptors in the brain depicts the functions in which they are implicated that are summarized in the Figure 5, and are described in the next paragraph.

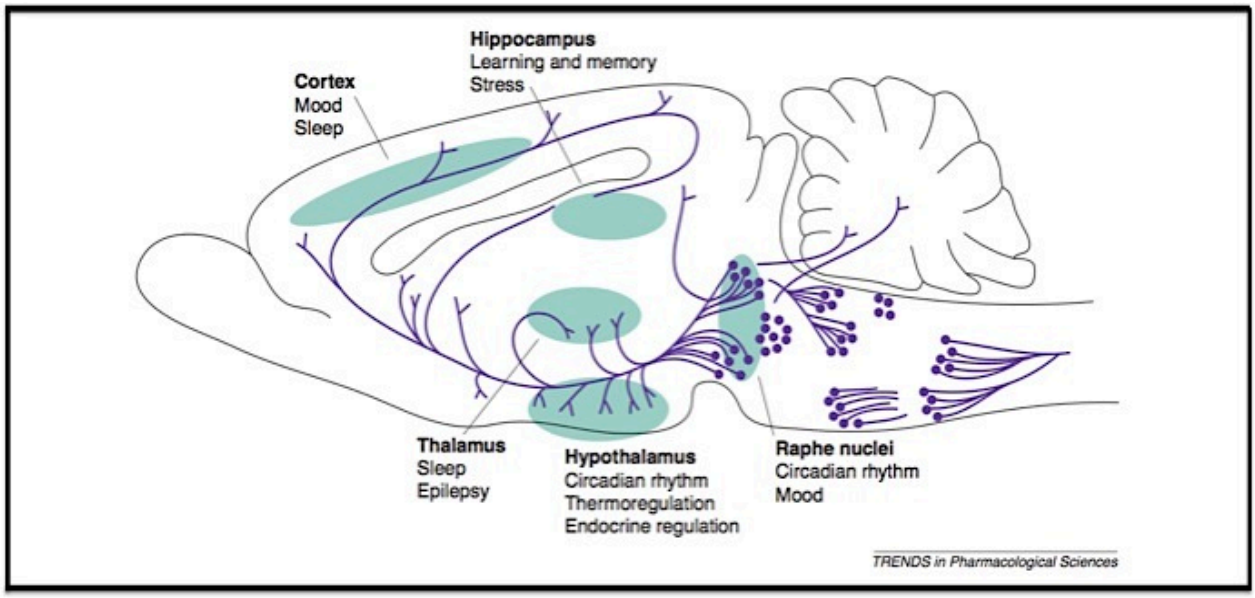

Figure 5. A sagittal view of the rodent brain, showing the 5-HT-producing neurons of the brain stem with their ascending and descending projections (purple). Regions that are relatively rich in 5-HT7 receptor expression (green) and their putative correlation with 5-HT7 receptor-mediated functions are indicated. Image from (Hedlund PB. and Sutcliffe GJ., 2004).

1.4.4 Role of the 5-HT7 receptor in the Central Nervous System

Being among the most recently discovered receptors for serotonin, the 5-HT7 receptor is also one of the least characterized. Nevertheless, during the last several years a large amount of information has been collected about this receptor. In the CNS, a physiological role for the 5-HT7 receptor has been demonstrated in circadian rhythm regulation (Glass et al., 2003), in thermoregulation (Hedlund et al., 2004) and in neuroendocrine regulation (Jørgensen 2007). Interesting findings have also indicated the involvement of this receptor in specific aspects of hippocampus-dependent contextual learning and memory processing (Roberts et al., 2004; Gasbarri et al., 2008; Eriksson et al., 2008; Sarkisyan and Hedlund, 2009). In the periphery, 5-HT7 receptor is expressed in smooth muscle cells and may play a role in irritable bowel syndrome (Beattie and Smith, 2008), in the control of micturition (Read et al., 2003; Recio et al., 2009), and in the reproductive system (Graveleau et al., 2000).

The early finding that several antipsychotics (Roth et al., 1994) and antidepressants (Monsma et al., 1993; Mullins et al., 1999) have high affinity for the 5-HT7 receptor, as well as the demonstration of its presence in relevant regions of the brains (Bonaventure et al., 2004), has prompted several preclinical studies evaluating its possible involvement in psychiatric disorders and other pathological processes of the nervous system. These studies took advantage from pharmacological

tools (mainly antagonists as SB-269970, Hagan et al., 2000) and/or transgenic mice lacking functional 5-HT7 receptors as behavioral models for human disorders.

The results of these studies indicate that several psychiatric and neurological disorders, such as anxiety, schizophrenia and epilepsy, involve deregulation of the 5-HT7 receptor, but specially this receptor plays a key role in depression. For instance, a recent study is indicating that the antidepressant effect of amisulpride is due to its action at 5-HT7 receptor (Abbas et al., 2009). In addition, it was shown that inhibition of the 5-HT7 receptor potentiates the effect of clinically used antidepressants (Abbas et al., 2009). Together, these results confirm that 5-HT7R mediates key aspects of serotonergic transmission in mood regulation.

Moreover, chronic MPH exposure to adolescent rodents produces enduring structural rearrangement of neural pathways involved in reward-based behavior, in terms of synaptic contacts and accumbal 5-HT7 receptor upregulation. Both the 5-HT7 receptor transcript and the protein were found to be persistently up-regulated following adolescent MPH exposure (Leo et al., 2009).

The MPH is a common psychostimulant used for the treatment of attention deficit hyperactivity disorder (ADHD), which is one of the most common childhood disorders and can continue through adolescence and adulthood.

Another pathological conditions involving 5-HT7 receptor is Fragile X syndrome. Fmr1 KO mouse, an animal model of Fragile X syndrome, exhibit spatial memory impairment and synapse malfunctioning in the hippocampus, with abnormal enhancement of long-term depression mediated by metabotropic glutamate receptors (mGluR-LTD). Although physiological LTD is crucial for hippocampal-dependent memory, abnormal LTD might lead to excessive synapse elimination. It was demonstrated that, in Fmr1 KO mouse, the activation of 5-HT7 receptor by the selective agonist LP-211, was able to rescue hippocampal synaptic plasticity, correcting excessive mGluR-LTD. These data suggest that activation of 5-HT7 receptor may represent a new therapeutic approach for Fragile X syndrome (Costa et al., 2012).

Several recent data are also indicating the involvement of 5-HT7 receptor in many aspects of neuronal development, such as neurite outgrowth, remodeling of neuronal morphology and dendritic shape and density. In particular has been demonstrated that the stimulation of endogenous 5-HT7 receptor in hippocampal neurons resulted in a marked elongation of neurites (Kvachnina et al., 2005).

In a recent study, Kobe and coworkers found that the activation of 5-HT7R/G_{12} signaling pathway promotes formation of dendritic protrusions and synaptogenesis in cultured hippocampal neurons, leading to enhanced spontaneous synaptic activity. In organotypic hippocampal cultures from

juvenile mice, the 5-HT7 receptor signaling potentiates formation of dendritic spines, increases the basal neuronal excitability and modulates synaptic plasticity.

1.4.5 Pharmacological profiles

5-HT7 receptors are defined pharmacologically by their high affinity for 5-CT (5-carboxamidotryptamine), 5-HT (5-hydroxytryptamine), 5-MeOT (5-Methoxytryptamine) and methiothepin, moderate affinity for 8-OHDPAT (8-hydroxy-N,N-dipropylaminotetraline) and ritanserin and low affinity for pindolol, sumatriptan and buspirone.

In recent years considerable efforts have been dedicated to the development of selective 5-HT7 receptor agonists and antagonists (Leopoldo 2004; Pittalà et al., 2007). The selective antagonists are: SB-258719 ((R)-3,N-dimethyl-N-[1-methyl-3-(4-methyllpiperidin-1-yl)propyl]benzene sulfonamide) and SB-269970 ((2R)-1-[3-hydroxy-phenyl)sulfonyl]-2-[2-(4-methyl-1-piperidinyl)ethyl]pyrrolidine), with SB-269970 considered to date the standard selective 5-HT7 receptor antagonist.

On the agonists' side, the mixed 5-HT1A/5-HT7 ligand 8-OH-DPAT has been used to activate 5-HT7 receptors in the presence of the 5-HT1A receptor antagonist WAY100635 (N-[2-[4-(2-methoxyphenyl)-1-piperazinyl]ethyl]-N-(2-pyridyl)cyclohexanecarboxamide) (Eriksson et al., 2008). Recently a series of arylpiperazine derivative have been developed as potential 5-HT7 receptor agonists. Among these N-(4-cyanophenylmethyl)-4-(2-diphenyl)-1-piperazinehexanamide (LP-211) displayed potent 5-HT7 receptor agonist activity (Leopoldo et al., 2008) with pharmacodynamics and pharmacokinetic properties suitable for both *in vitro* and *in vivo* studies aimed to characterize the functional role of this receptor (Hedlund et al., 2010).

1.4.6 Post-translational modifications

Several 5-HTRs display N-glycosylation at the N-terminal extracellular domain (Abramowski and Staufenbiel, 1995; Monk et al., 2004; Dutton et al., 2008).

The 5-HT7R contains two consensus sequences for N-linked glycosylation sites in the extracellular N-terminus (Figure 3) (Bard et al., 1993; Lovenberg et al., 1993). It has been recently demonstrated that N-glycosilation of the 5-HT7R does not influence the affinity for the 5-HT but receptors deprived of the glycosilation sites displayed a reduced expression (Gellynck et al., 2012).

Palmitoylation of GPCRs can be involved in the regulation of different processes including membrane targeting, interaction with G proteins, basal and agonist-dependent activity as well as phosphorylation and desensitization. Most 5-HTRs have cysteine residues in their carboxyl termini that may be palmitoylated (Carrel et al., 2006; Kvanchina et al., 2009) thus creating potential membrane anchors that can form a putative fourth intracellular loop in order to modulate the conformation of the GPCR (Gellynck et al., 2013).

The intracellular domain also has phosphorylation sites for several serine/threonine kinases (Backstrom et al., 2000; Wu et al., 2002; Parker et al., 2003; Turner and Raymond, 2005). The 5-HT7R splice variants differ in the length of their C-termini and in the number of phosphorylation sites. This can have important functional consequences, such as different G protein-coupling efficiency or different susceptibility to desensitization (Heidmann et al., 1998) as it has been shown in functional studies with point mutations in the 5-HT_{2C}R C-terminus (Backstrom et al., 2000) and in the 5-HT_{1A}R IL2 (Wu et al., 2002). So far, no significant differences in ligand binding, signaling, receptor regulation, have been described for the different 5-HT7R splice variants.

2. AIM

In the last decade, several data indicate the involvement of 5-HT7 receptor in many aspects of neuronal development, such as neurite outgrowth, modulation of neuronal morphology and changes of dendritic shape and density. In particular, it was demonstrated that stimulation of endogenous receptor in embryonic hippocampal neurons resulted in a marked elongation of neurites (Kvanchina et al., 2005) and the activation of 5-HT7R/G12 signaling pathway in postnatal hippocampal cultures promotes formation of dendritic protrusion, synaptogenesis and modulates synaptic plasticity (Kobe et al., 2012).

In line with these results, my PhD project aims to characterize the role of 5-HT7 receptor in remodeling of neuronal cyto-architecture and connectivity during the early and late development, in behavioral relevant CNS circuits. In particular, the main goal of my PhD thesis project is to study the cellular and molecular mechanisms of the neurite outgrowth induced by the stimulation of 5-HT7 receptor and to reveal the associated signaling transduction pathway. The occurrence of these mechanisms will be evaluated during the embryonic development of the CNS by *in vitro* approaches, and in the postnatal period by *in vitro* and *in vivo* approaches.

The comprehension of the molecular basis of 5-HT7 receptor involvement in modulation of neuronal connectivity will open the way to the second aim of my project. Indeed I plan to examine whether the pharmacological modulation of 5-HT7 receptor may improve the altered neuronal connectivity of specific cerebral circuits, observed in several neurodevelopmental disease (X-fragile, ADHD, Rett syndrome).

To this aims, I have used two different approaches:

1) For the *in vitro* approach I used primary cultures from different embryonic and early postnatal areas of CNS, to examine the effects of 5-HT7 receptor stimulation on neuronal morphology during the early phases of the development, and the signal transduction pathway activated by it.
2) For the *in vivo* approach, I administered a specific 5-HT7 receptor agonist to one month-old mice to evaluate the effect produced by *in vivo* stimulation of 5-HT receptor on the structural remodeling of rodents cerebral circuits. These experiments will be also performed on Mecp2-/y mice, animal model of Rett syndrome, characterized by defects in synaptic organization, to assess the possible beneficial effects induced by stimulation of 5-HT7 receptor on the altered connectivity of these cerebral circuits.

3. MATERIALS AND METHODS

3.1 Neuronal primary cultures

Timed pregnant Sprague-Dawley rats (Charles River, Italy), C57 BL/6 mice and Mecp2-/y mice, animal model of Rett Syndrome (Bertulat et al., 2012) were housed, cared for and sacrificed in accordance with the recommendations of the European Commission. The embryonic age (E) was determined by the date of insemination (i.e. the appearance of vaginal plug was considered as day E0). About 15-20 embryos from different dams were pooled (at E16 for rats, and at E15 for mice) and were used for preparation of the monolayer cultures. The striatum (STR) and cortex (CTX) were quickly dissected, under a stereoscope in sterile conditions, from rat and C57 mouse embryos. For Mecp2-/y mice, only the cortex was dissected from single embryos, obtained by breeding heterozygous female (Mecp2 +/-) with WT male mice; genotypization was performed by PCR on the tail of embryos. The tissues were placed in PBS without calcium and magnesium, supplemented with 33 mM glucose, and cells were dissociated from embryonic STR or CTX and cultured as previously described (di Porzio et al., 1980). Briefly, the dissected areas were enzymatically dissociated by incubation for 30 minutes (min) at 37°C in a papain solution (Worthington, 20 U/ml) in Earle's balance salts containing 1mM EDTA, 1mM cysteine and 0.01% pancreatic DNAse. After addition of 1mg/ml of bovine serum albumin (Sigma-Aldrich) and 1 mg/ml ovomucoid (Sigma-Aldrich) the cells suspensions were centrifuged 5 min at 800 g, resuspended in plating medium and counted (Fiszman 1991). For the viable count, cell suspension was diluted 1:1 with 0.1% trypan blue dye and loaded into a disposable cell counting chamber-slide. Cell concentration was determined on the basis of the total cell count, the dilution factor and the trypan blue dye exclusion.
Dissociated cells were plated at a density of $1.5x10^5/cm^2$ in 2 cm^2 Lab-Tek chamber slides (Nunc) for morphological analyses, and at a density of $3x10^5/cm^2$ in 9,5 cm^2 cell culture dishes (Corning) for RNA purification and Western blot analyses. Both chamber slides and cell culture dishes were coated with 15 μg/ml of poly-D-Lysine (Sigma-Aldrich).
Cells were grown in serum-free Neurobasal medium (Invitrogen), supplemented with B27 (Invitrogen), 2 mM L-glutamine, penicillin (50 U/ml) and streptomycin (50 μg/ml). Cultures were maintained at 37°C in a humidified incubator for 3 days before experimental manipulation. For each experimental point, cultures were prepared at least in independent triplicates, and experimental points were repeated using independent cell preparations.

3.2 Drugs and reagents

The cell cultures were treated with 100 nM of the 5-HTR (1A/7) agonist 8-OH-DPAT (Tocris), 100 nM of the selective 5-HT7R agonist LP-211 (gift of M. Leopoldo, University of Bari, Italy), 100 nM of the HT7R antagonist SB-269970 (Tocris), or with a combination of these drugs. Drugs were added to cultures 72 hours (h) after cell plating and incubated for appropriate time. Pretreatment of cells with the 5-HTR1A antagonist, WAY 100635 (Tories;) was performed at the final concentration of 30nM for 30 min (Corradetti et al., 1998). Pretreatment of the cells with the ERK 1/2 inhibitor U0126 was performed at the final concentration of 10 μM, for 30 min, as recommended by manufacturer (Cell Signalling). Pretreatment of the cells with cycloheximide (Sigma-Aldrich), an inhibitor of eukaryotic protein synthesis was performed at the final concentration of 50 μM, for 30 min. Roscovitine (Sigma-Aldrich), a Cdk5 inhibitor, was used at the final concentration of 20 μM for 2 h.

Treatment of cells with cytochalasin D (100 nM), latrunculin (2 μM) and jasplakinolide (2 μM) was performed for 2 hours.

3.3 Morphological characterization and measurement of neurite outgrowth

For immunofluorescence analysis, cells in culture were fixed in 4% paraformaldehyde in phosphate buffered saline (PBS), for 30 min at room temperature (RT), washed three times in PBS, and then permeabilized for 15 min in PBS containing 0.1% Triton-X-100 and 10% normal goat serum (NGS). The cells were blocked to room temperature with blocking solution (10% NGS, 0,1% BSA in PBS) for 1 h and incubated with the primary antibody (in PBS containing 0,1% BSA) overnight at 4°C. The following antibodies were used at the indicated dilutions: polyclonal GAD2 antibody (Cell Signalling) 1:100, monoclonal antibody Tuj1 (Covance) 1:500 and polyclonal antibody 5-HT7 receptor (Imgenex) 1:70, MAP1B (Chemicon) 1:500, MAP2 (Chemicon) 1:500.

The cells were washed 3 times in PBS, and then incubated for 2 hours with fluorescent-labeled secondary antibodies (Texas red goat anti-rabbit, 1:400, Invitrogen; goat anti-mouse fluorescein-conjugated, 1:400, Invitrogen) in PBS containing 5% NGS.

Cells were then counterstained with DAPI (nuclear stain, 1:1000) for 10 min, washed with PBS and mounted with oil mounting solution (Vectashield, Vector Lab Inc).

As negative controls, some cells were processed as described above, but without primary antibody.

For morphological analyses, cells fixed and permeabilized as above, were incubated for 2 h at RT with the monoclonal antibody against neuron specific class III β-tubulin (anti-Tuj1, 1:750, Covance) diluted in PBS containing 10% NGS. Cells were then rinsed in PBS and stained

according to the standard avidin-biotin immunocytochemistry procedures (Vectastain Elite, Vector Lab Inc) using peroxidase substrate kit (diaminobenzidine).

After Tuj1 staining, cell-culture slides were analyzed with a Leica microscope (Leica DM6000B) using the software Leica Application Suite (LAS). Images were obtained using a 40x objective and analyzed by the image-processing software Image J, for the perimeter and the area of the soma, neurites' number and length. Only clearly visible cells were subjected to analysis to prevent inaccurate scoring. A total of 15 fields for each cell-culture condition were selected from at least three independently treated culture wells. A total of 300 neurites/well were traced from Tuj1 positive neurons to measure their length. The analyses were carried out "blind" to avoid any subjective influences during the measurements.

Morphometric parameters were always compared to controls from the same batch of dissociated cells treated with vehicle alone. Significant agonist-induced increase in neurite length varied always between 1.2 and 2 fold compared to controls (CTRL). For easy comparison of the results among various cell preparations, data were expressed as percentage of the average CTRL.

3.4 RNA isolation and RT-PCR analyses

RNA was extracted from primary cells cultured in 4 cm^2 wells, 3 days after seeding, using the Tri-Reagent isolation system (Sigma-Aldrich). The analyses were always carried out in triplicates for each experimental point. The yield and the integrity of RNA were determined by A_{260} determinations and agarose gel electrophoresis respectively. For reverse transcriptase (RT)-PCR analyses, RNA was treated with DNA-free kit (Ambion Inc., Milan, Italy) to prevent false results by DNA contamination. Briefly, 2 μg of RNA were reverse transcribed using random hexanucleotides as primers (New England Biolabs Inc., 6 μM) and 200 U of Moloney-murine leukemia virus reverse transcriptase (New England Biolabs Inc.). Negative amplification control was performed in the absence of template.

Quantitative Real time PCR was performed by using gene specific primer sets (Table 1) that were designed with OLIGO 6 software, to obtain amplicons fragments with comparable size (around 100 bp).

SYBR Green Real-time PCR reactions were performed in 96-well plates using 7900HT Fast Real-Time PCR System (Applied Biosystem). Each cDNA sample was amplified in triplicate and every reaction included a negative control (having no template) to eliminate the possibility of contamination. Thermal cycling conditions comprised initial step at 50°C for 2 min and 95°C for 10 min, followed by 40 cycles at 95°C for 15 seconds and 60°C for 1 min. Gene expression levels were

quantified by the comparative threshold cycle (*CT*) method (Schmittgen and Livak, 2008) using hypoxanthine phosphoribosyltransferase (HPRT) as an internal control gene. The fractional number of PCR cycles *CT* required to obtain a given amount of amplified product in the exponential phase of amplification was determined for the gene of interest and for HPRT in each cDNA sample. The relative expression level of the gene of interest was then expressed as $2^{-\Delta CT}$ where $\Delta CT = CT$ gene of interest - *CT* HPRT.

Table 1. Primers used for Real-time PCR analyses

Genes	**Primers**	**Annealing temperature**	**Length**
5-HT7R	F: GCGGTCATGCCTTTCGTTAGT R: GGCGATGAAGACGTTGCAG	62°C	83bp
NF-M	F: CGTCGCACATCACCGTAGAG R: CGCCTGGTGCATGTTC	55°C	113 bp
Vimentin	F: GCCGAGGAATGGTACAAG R: TCTCCGGTATTCGTTTGACT	55°C	105 bp
B-III-tubulin	F: GTCCACCTTCATCGGCAACAG R: GCCTTCGCCCGTGTACCAGT	59°C	115 bp
Map2	F: CTCAGCCGGACACAAGTAAAA R: CTGCGCAAATGGACTGG	54°C	89 bp
MAP1B	F: AGCAACATGCAGGTGACTCT R: GTGAGGTCTTGCTGCTTCT	57 °C	93 bp
HPRT	F: TGGGAGGCCATCACATTGT R: AATCCAGCAGGTCAGCAAAGA	58 °C	71 bp

3.5 Gel Electrophoresis and Western Blot analyses

For mono-dimensional polyacrylamide gel electrophoresis (PAGE), culture dishes were lysed in RIPA Buffer in presence of protease inhibitors (Roche, Milan, Italy). Proteins (20 µg/lane) were separated on 12% SDS-polyacrilamide gel and transferred to PVDF membranes (Amersham, Milan, Italy). Filters were blocked for 30 min in 5% (w/v) non-fat milk in Tris-buffered saline Tween-20 (TBST; 0.1% Tween, 150mM NaCl, 10mM Tris-HCl, pH 7.5) and probed for 2 h at room temperature with the following antibodies: anti-5-HT7 receptor (Imgenex, 1:300), anti-β-actin (Sigma-Aldrich, 1:1000), anti-p-ERK1/2 (Cell Signalling, 1:750) and anti-ERK 1/2 (Santa Cruz Biotechnology, 1:1000). After washing, immunoblots were incubated with goat anti-rabbit IgG (Amersham ECL, 1:10000) or anti-mouse IgG antibodies (Amersham ECL, 1:10000) conjugated to horseradish peroxidase (HRP) and visualized on autoradiographic film, using enzyme-linked chemiluminescence (ECL; Immobilion Western, Millipore). The relative protein levels were determined by densitometry and compared with the protein level of the appropriate standard (ERK1/2 for p-ERK1/2 blots, and β-actin for 5-HT7R blots) probed on the same membrane, after stripping of the antibody previously used. Net intensity value of each band was calculated by subtracting the background of each area from the total intensity.

For 2D-PAGE, monolayer cultures of LP-211 treated and untreated striatal cells were harvested and cell pellets were washed three times with PBS and lysed in the lysis buffer (40 mM Tris-HCl pH 8.0, 8 M urea, 4% CHAPS, 65 mM DTT and 1 mM PMSF). Total proteins were extracted by repeated freezing and thawing with liquid nitrogen and pooled from 6 independent culture dishes. Samples were centrifuged at 17 500 g for 15 min at 4 °C to eliminate cellular debris and sonicated into an ultrasonic bath for 15 min. Samples were then further centrifuged at 17 500 g for 15 min at 4 °C to eliminate cellular debris. The supernatant was collected and protein concentration determined by the Bradford method, according to manufacturer's instructions (Biorad). Lysates were aliquoted and stored at -80 °C until use. 50 µg of lysate proteins were analyzed by 2D-PAGE, as previously described (Severino et al., 2010). Samples to be processed by isoelectrofocusing (IEF) were diluted with the rehydration buffer (8 M urea, 0.5% CHAPS, 0.2% DTT, 0.5% IPG ampholytes and 0.002% bromophenol blue) to a final volume of 125 µl. The precast IPG strips (3-10 linear pH gradient, 7 cm long, GE Healthcare), used for the first dimension, were passively rehydrated and loaded with the sample at room temperature for 12 h under low-viscosity paraffin oil. IEF was then performed using an IPGphor isoelectric focusing cell (GE Healthcare), according to the following protocol: 50V for 3 h, 100V for 2 h, 500V for 2 h, 1000V for 2 h, 3000V for 2 h, 4000V for 2 h, 5000V for 2 h, 6000V for 2 h, 8000V until about 25000V/h total. Strips were then equilibrated twice for 15 min under gentle shaking in the equilibration solution (6 M urea, 50 mM Tris-HCl buffer pH 8.8, 30%

glycerol, 2% SDS, 0.002% bromophenol blue) containing 1% DTT (to reduce disulfide bonds), in the first equilibration step, and 2.5% iodoacetamide (to alkylate thiols), in the second step. The second-dimension separation was performed on 12% polyacrylamide gels (0.75 mm x 7.5 x 10 cm) by using a Miniprotean II apparatus for the detection of Vimentin, β-tubulin, Neurofilament L and MAP1B. For the detection of MAP2 and Neurofilament M, 10% polyacrylamide gels were used for protein separation. The strips were fixed with 0.5% agarose and 0.002% bromophenol blue dissolved in SDS/Tris running buffer. The run was carried out at constant power (10 mA/gel for 15 min; 20 mA/gel until the end of the run). After the second dimension, 2D-gels were electroblotted onto nitrocellulose membranes by using a TransBlot Turbo system (BioRad, Milan, Italy) following the manufacturer's instructions. The membrane was blocked with 5% milk in TBS-0.1%Tween (TTBS) for 1 h at room temperature and washed with TTBS. Subsequently, membranes were incubated with primary antibodies diluted in 2.5% milk in TTBS overnight at 4 °C. The following antibodies were used: anti-β-tubulin (Covance, 1:1000); anti-Vimentin (Millipore, 1:100); anti-MAP1B (Millipore, 1:500); anti-Neurofilament L (Millipore, 1:1000); anti-MAP2 (Chemicon, 1:2000), anti-Neurofilament M (Chemicon, 1:1000), anti-Cofilin (Cell Signaling, 1:1000), anti-actin (Chemicon, 1:5000) and anti-βtubulin (Covance, 1:1000). Membranes were then washed with TTBS, incubated with the appropriate HRP-conjugated secondary antibody diluted 1:5000 in 2%milk in TTBS for 1 h at room temperature. Immunoreactive protein bands were visualized by the ECL Plus Western Blotting Detection System (GE Healthcare) according to the manufacturer's instructions.

3.6 Embryonic hippocampal primary cultures and microfluidic chamber culture

Hippocampal neuron cultures were prepared from 18-day old (E18) mouse embryos. The hyppocampi were dissected in cold HBSS 1X and 3mM HEPES (Gibco, Life Technologies Ltd, Paisley, UK), containing antibiotics (100 unit/ml penicillin and 0.1 mg/ml streptomycin) (Sigma-Aldrich, Milano, Italy), and transferred into a 15 ml tube. After a rinse in buffer, specimens were incubated, for 30 min at 37°C, with 40 ml/hippocampus of 0.5% trypsin (EuroClone SpA, Pero, Italy) (equivalent to 0.2 mg trypsin/hippocampus) and 100 mg/ml DNAase. After an extensive wash, hippocampi were mechanically dissociated and cell density was determined using a counting chamber. Cells were re-suspended in 100ml of the appropriate medium and plated in microfluidic chambers (Xona Microfluidics LLC, Temecula, California USA) (Taylor et al., 2005; Park et al., 2006). Chambers were prepared as suggested by manufacturer's instructions: briefly, 35 mm Petri dishes were coated overnight with 100 mg/ml poly-L-lysine (Sigma-Aldrich) at 37°C and then washed and air dried under a sterile hood. Poly(dimethylsiloxane) (PMDS) chambers were placed

on the Petri dishes with their micro-channel side down, sealed to the dish by gentle pressure and filled with 20 mg/ml laminin (Sigma-Aldrich), for 2 h at 37 °C. Laminin was removed just before plating cells, approximately 100.000 cells were pipetted directly into one compartment (the soma compartment) and then both compartments were filled with NeuroBasal (Gibco, Life Technologies Ltd), containing 1X B27 supplement (Gibco, Life Technologies Ltd,), 0.5 mM glutamine, 25 mM glutamate and antibiotics. Cells were exposed to DMSO (control) or DMSO + LP-211, added to both compartments (somatic and axonal), and maintained *in vitro* for 6 days (6 DIV). Medium was changed every 24 h and the number of axons reaching the axonal compartment was counted blindly by three researchers, from 1 to 6 DIV. At this last date, cells were fixed and processed for Tuj1 immunofluorescence.

Cultured cells were fixed in 4% formaline and 4% sucrose in phosphate buffered saline (PBS) for 30 min at room temperature (RT), added directly to both compartments, without removing the microfluidic chambers. After fixation, cells were blocked in 1 % bovine serum albumin (BSA) (Sigma-Aldrich), 10 % normal goat serum (NGS) (Jackson ImmunoResearch Europe Ltd, Suffolk, England) and 0.5 % Triton X-100 in PBS, for 1 h at RT, and then incubated overnight at 4 °C with the primary antibodies diluted in 1 % BSA, 1 % NGS and 0.2 % Triton X-100 in PBS. Antibodies used were: mouse anti-neuron specific bIII-tubulin (Tuj1) (Covance, Emeryville, CA, USA) (1:3000), in co-localization with either rabbit anti Map2 (AbCam, AbCam, Cambridge, UK) (1:400), to visualize dendrites, or rabbit anti Tau (AbCam) (1:50), to visualize axons. After a rinse with buffer, cells were incubated, for 1 h at RT, with the appropriate secondary antibodies: goat anti-mouse IgG Alexa Fluor 488 (Molecular Probes, Life Technologiers Ltd) and goat anti-rabbit IgG Cy3 (Jackson ImmunoResearch) both diluted 1:1000. ProLong Gold Antifade Reagent (Invitrogen, Life Technologiers Ltd) was added to both compartments to visualize and store immunolabed cells.

3.7 Treatment *in vivo* with LP-211

Young male C57 BL/6 mice (40-days old) were housed in group on standard 12:12 light:dark cycle with food and water *ad libitum,* cared for and sacrificed in accordance with the recommendations of the European Commission. Animals were divided into two groups: one group (n=4) was intraperitoneally injected for 2 days with 0,25 mg/Kg LP-211; a second group (n=4) received the treatment with the vehicle alone (DMSO). At the third day, mice were intraperitoneally anesthetized with avertine and intracardially perfused with PBS, followed by fresh 4% PFA in PBS (pH 7.4). Brains were carefully removed from the skull and post-fixed in the same fixative solution for 24

hours at 4°C. After rinsing in PBS, brains were coronally sectioned in 100 μm thick slices with a vibratome (Leica VT1000S) and collected in PBS.
Sections were subsequently labeled with solid DiI crystals (1,1=-dioctadecyl-3,3,3=,3=-tetramethylindocarbo- cyanine perchlorate; Molecular Probes).

3.8 Labeling of neuronal projections with lipophilic carbocyanine dyes

The lipophilic carbocyanines DiI is highly fluorescent and quite photostable when incorporated into membranes. Once applied to cells or tissue, the dyes diffuse laterally within the plasma membrane, resulting in staining of the entire cell. DiI crystals, mounted at the tip of a thin rod, were placed on the dorsolateral surface of the caudate-putamen under stereomicroscope. After application of the crystals, the sample were kept in a humid environment, in PBS, at 4°C for at least 3-4 weeks.
We acquired fluorescence of DiI-labeled dendrites of the striatal spiny neurons using a Leica SP2 confocal microscope. Images were 8-bit, resolution 512x512, em 562-634, ex 543, obj 63x (oil, NA 1.32), pinhole 1 Airy unit, zoom factor up to 5; the gain was adjusted image to image because the effective return fluorescence depended on the depth of the structure within the slice. The total number of slices was adjusted in order to capture the entire dendrite; the step size in the Z direction was set at 0.2 μm.
Dendrites were identified on the basis of the number of spines, excluding from the analysis all neurites with a low density of spines. For quantification, six segments of 15 μm-long dendrites were randomly chosen from each animal. Spine density was calculated by summing the total number of spines per dendritic segment length and calculating average number of spines/15 micron for each animal (three animals for each group). Anova unpaired t-test was used to evaluate statistical differences between untreated and LP-211 treated groups. All analyses were conducted under blind conditions. All images were then analyzed using ImageJ software.

3.9 RNA sequencing analyses

We used RNA-sequencing (RNA-seq) technology (Morozova et al., 2009) to sequence, map, and quantify the entire population of polyadenylated transcripts in cortical primary cultures obtained from WT and RTT E15 mouse embryos, treated for 2 h with LP-211 or with vehicle (DMSO). Triplicate RNA samples were extracted and sequenced for each culture condition (WT+ vehicle, WT + LP-211, MecP2 -/y + vehicle; MecP2 -/y +LP-211).
The RNA-seq protocol (Illumina) included a strand-specific library preparation followed by single-end 50bp sequencing. The bioinformatics analyses were performed in collaboration with

SequentiaBiotech (Barcelona, Spain). Only the high quality reads were aligned against the Mus *musculus* reference genome sequence (GRCm38) with TopHat (2.0.9); then, the gene expression values (read counts) were obtained with HTSeq-count (0.5.4p2). All statistical analyses were performed with R (3.0.1). Clustering of replicates showing a good separation between WT and null cell types were subjected to further analysis.

3.10 Statistical analyses

All the statistical analyses were performed using GraphPad Prism 3.0 (GraphPad Software). Drugs-treated cultures were compared to corresponding vehicle-treated cultures by un-paired Student's t-test; data were expressed as mean ± SEM. Significance threshold was set at $p < 0.05$.

4. RESULTS

4.1 Characterization of embryonic primary cultures

To test the potential involvement of 5-HT7 receptor in remodeling cytoarchitecture of neurons from various areas of the CNS, we used striatal and cortical primary cultures prepared from E16 rats' brain. Neuronal primary cultures have been a research tool for decades because they allow easy access to individual neurons for electrophysiological recording and stimulation, pharmacological manipulations, and high-resolution microscopy analyses.

These cultures are often heterogeneous and require characterization analysis to identify the cells.

The phenotype of our cells was investigated by immunofluorescence experiments performed with antibodies against Tuj1 (neuron specific class III β-tubulin, a widely used neuronal marker), GAD-65 (GABAergic neuron marker) and 5-HT7 receptor. As expected from the previous data (Leo et al., 2009), more than 98% of striatal and cortical cells in cultures were neurons, as judged by colocalization of the neuronal marker Tuj1 with the nuclear DAPI staining. In addition, more than 90% of striatal and cortical neurons were positive to 5-HT7 receptor. Most of neurons obtained from both areas were GABAergic (about 95% of Tuj1+/5-HT7 receptor + in striatal cultures and about 85% in cortical cultures) (Figure 6A).

The abundance of the 5-HT7 receptor protein in E16 striatal and cortical tissues was evaluated by Western blot and was similar in both areas (Figure 6B).

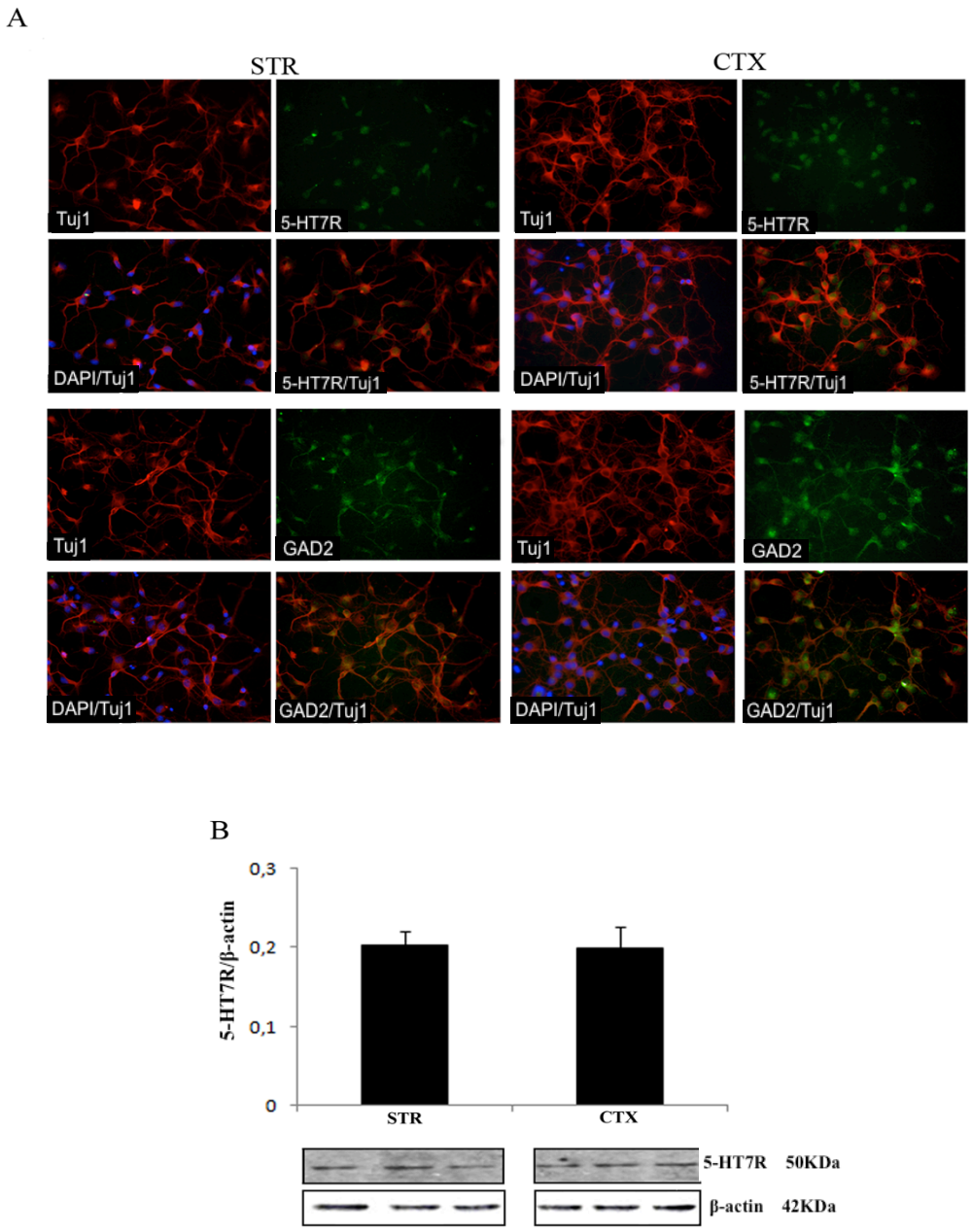

Figure 6. Characterization of striatal (STR) and cortical (CTX) primary cultures from rats E16 brain. (A) Photomicrographs of the cells from striatal and cortical cultures immunostained with specific antibodies against the neuronal marker Tuj1 (red), 5-HT7R (green) and GABAergic marker GAD2 (green), as indicated in each panel. Cell bodies were identified by counterstaining with the nuclear marker DAPI (blue). Magnification 40x. (B) Quantitation of 5-HT7R proteins in striatal and cortical regions of the E16 rat brain. The bars represent the densitometric values of 5-HT7R Western blot signals normalized with those of β-actin signals in the same samples (mean ± SEM; n=3).
The boxes below the graph display corresponding blots stained with antibody against 5-HT7R and β-actin.

4.2 Neurite outgrowth is induced by stimulation of 5-HT7 receptor in neuronal primary cultures.

Neurite outgrowth is a complex process that occurs in three stages: (1) initiation of neurite formation (sprouting), (2) elongation of neurites over long distances and guidance of their growth cones to the appropriate target (path finding) and (3) synapse formation and functional maturation of the newly formed connections. *In vitro* models of neurite outgrowth are very useful tools to study gene or compounds that play a key role during the development.

To evaluate the role of 5-HT7 receptor in remodeling neuronal circuits, the dissociated striatal cells from E16 rat brains, after 3 days in culture, were pharmacological stimulated with two 5-HT7 receptor agonists (8-OH-DPAT or LP-211) and with the selective antagonist SB-269970, at various time points. While 8-OH-DPAT is a mixed agonist for both 5-HT7 receptor 1A and 7, LP-211 is selective for 5-HT7 receptor (5-HT_7 K_i= 0.58 nM; $5\text{-HT}_{1\text{-}6}$ K_i>70 nM; Leopoldo et al., 2011).

After stimulation, the cultures were stained with Tuj1 antibody, and analyzed morphometrically by the software Image J.

As shown in Figure 7A, exposure of striatal cultures to 100 nM 8-OH-DPAT resulted in a significant increase in neurite length when compared to vehicle-treated control cultures (CTRL, set to 100%). The effect was highest after 30 min (150%), remaining significant after 2 h (120%), and diminished after 24 h. The effect of 8-OH-DPAT at 30 min was reversed by the addition to the culture medium of SB-269970 (100 nM), a highly selective 5-HT7 receptor antagonist, whereas treatment with the 5-HT7 receptor antagonist alone had no effect on the length of neurites. These results extend preliminary data previously obtained in my lab on striatal neurons in vitro (Leo et al., 2009), confirming that the effect of 8-OH-DPAT on neurite growth was induced by the selective stimulation of 5-HT7 receptor.

To emphasize the involvement of 5-HT7 receptor in neurite elongation, subsequent experiments were conducted stimulating striatal cultures with the selective agonist LP-211.

The addition of 100 nM LP-211 to the culture medium, when compared to CTRL, did not have effect on neurite elongation at 30 min and 1 h, but caused a significant increase in the length of neurites after 2 h of stimulation (160%); the effect was still significant after 4 h (140%) and persisted up to 24 h (120%). As expected, co-treatment of the cells with LP-211 and SB-269970 for 2 h completely abolished neurite elongation, while addition of the antagonist alone for 2 h had no effect (Figure 7B).

We also repeated the application of the agonists to the cultures (at 30 min and 1 h for 8-OH-DPAT; at 2 h and 4 h for LP-211), but without significant modification of neurite length compared to single

application of the agonists (data not shown). These data indicate that a single application of the agonists is already producing the maximum stimulatory effect on neurite outgrowth, at least under our experimental conditions.

Other morphological parameters, such as the number of primary neurites, as well as the soma perimeter and the total area of each neuron were not significantly affected by 8-OH-DPAT or by LP-211 (data not shown).

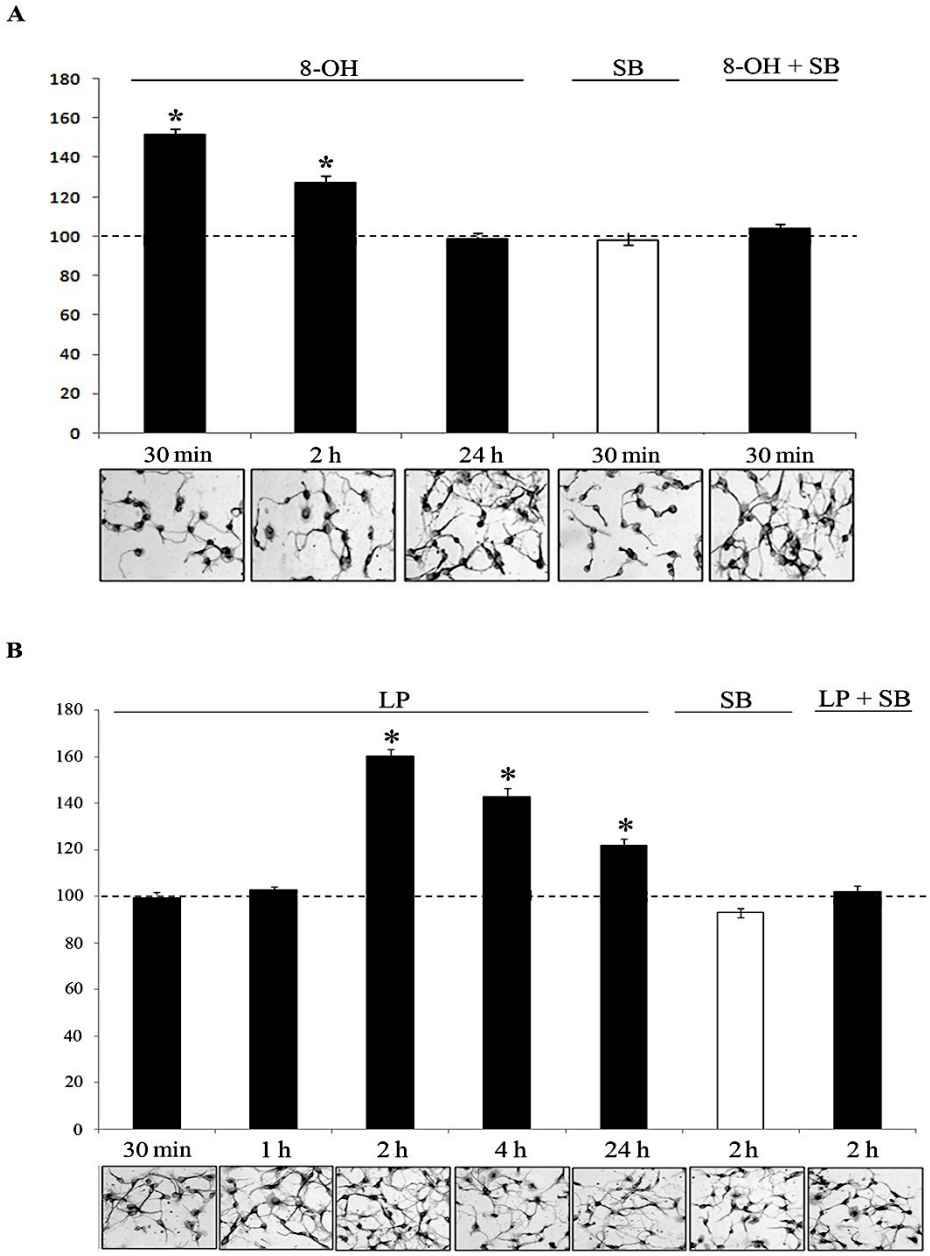

Figure 7. Agonists of 5-HT7R stimulate neurite outgrowth in striatal primary cultures. (A) Cells were treated for 30 min, 2 h and 24 h with the 5-HT7R agonist 8-OH-DPAT (8-OH, 100 nM), or for 30 min with the selective 5-HT7R antagonist SB-269970 (SB, 100 nM) with or without 8-OH-DPAT. (B) Striatal cells were treated for 30 min, 1 h, 2 h, 4 h and 24 h with the 5-HT7R selective agonist LP-211 (LP, 100 nM), or for 2 h with the selective 5-HT7R antagonist SB-269970 (SB, 100 nM) with or without LP-211. (A, B) Neurite length was measured on cells stained with anti-Tuj1 antibody, and expressed as percentage of the values measured in the corresponding vehicle-treated cultures (CTRL, set to 100%, dashed line). The bars represent means ± SEM from randomly selected fields for each cell culture condition (n= 12). * Significantly different from CTRL by Student's t-test ($p < 0.05$). The small box below each bar displays representative Tuj1 immunostaining of the striatal cells cultured in the corresponding condition (magnification 40x).

The 8-OH-DPAT is a mixed agonist with affinity for both 5-HT7R and 5-HT1A. To exclude the involvement of 5-HT1A receptor on agonists-induced neurite length, we stimulated striatal cultures with 8-OH-DPAT (30 min) or LP-211 (2 h) in presence of a potent and selective antagonist for 5-HT1A receptor (WAY-100635). As shown in Figure 8, co-treatment of the cells with agonist and WAY-100635 did not abolish agonist-induced neurite elongation. These results strengthen the involvement of 5-HT7 receptor in stimulating neurite outgrowth and exclude the contribution of 5-HT1A receptor.

To test the potential involvement of 5-HT7 receptor in remodeling cytoarchitecture of neurons from different areas of the CNS, we also prepared cortical primary cultures from E16 rat brains. Similarly to striatal neurons, dissociated cortical cells were plated at a density of 1.5 x 10^5 cells/cm^2 in a serum-free culture medium obtaining neuronal cultures virtually deprived of glial cells. Unlike striatal cultures however, cortical cultures survived well at cell density lower than 1.5 x 10^5/cm^2. Thus, for cortical neurons, neurite elongation induced by treatment with 100 nM LP-211 for 2 h was evaluated at various densities (1.5 x 10^5; 1 x 10^5; 7.5 x 10^4/cm^2) and was always significantly increased (Figure 9). This effect was completely abolished by co-treatment of the cells with LP-211 and SB-269970. As expected, neurites of both CTRL and LP-211-stimulated cells were longer when cells were plated at lower density. However, the extent of the increase of the neurite length induced by 5-HT7 receptor agonist when compared to the corresponding CTRL, was similar at all cell densities tested (Figure 9). These data suggest that stimulation of neurite outgrowth by 5-HT7 receptor activation is independent from cell density.

We also established striatal and cortical neuronal cultures dissociated from E15 mouse brain. Similarly to what was observed in rat primary cultures, we found that the neurites length was significantly increased by the application of 100 nM LP-211 for 2 h, and this increase was reversed by the co-treatment with SB-269970 (Figure 10).

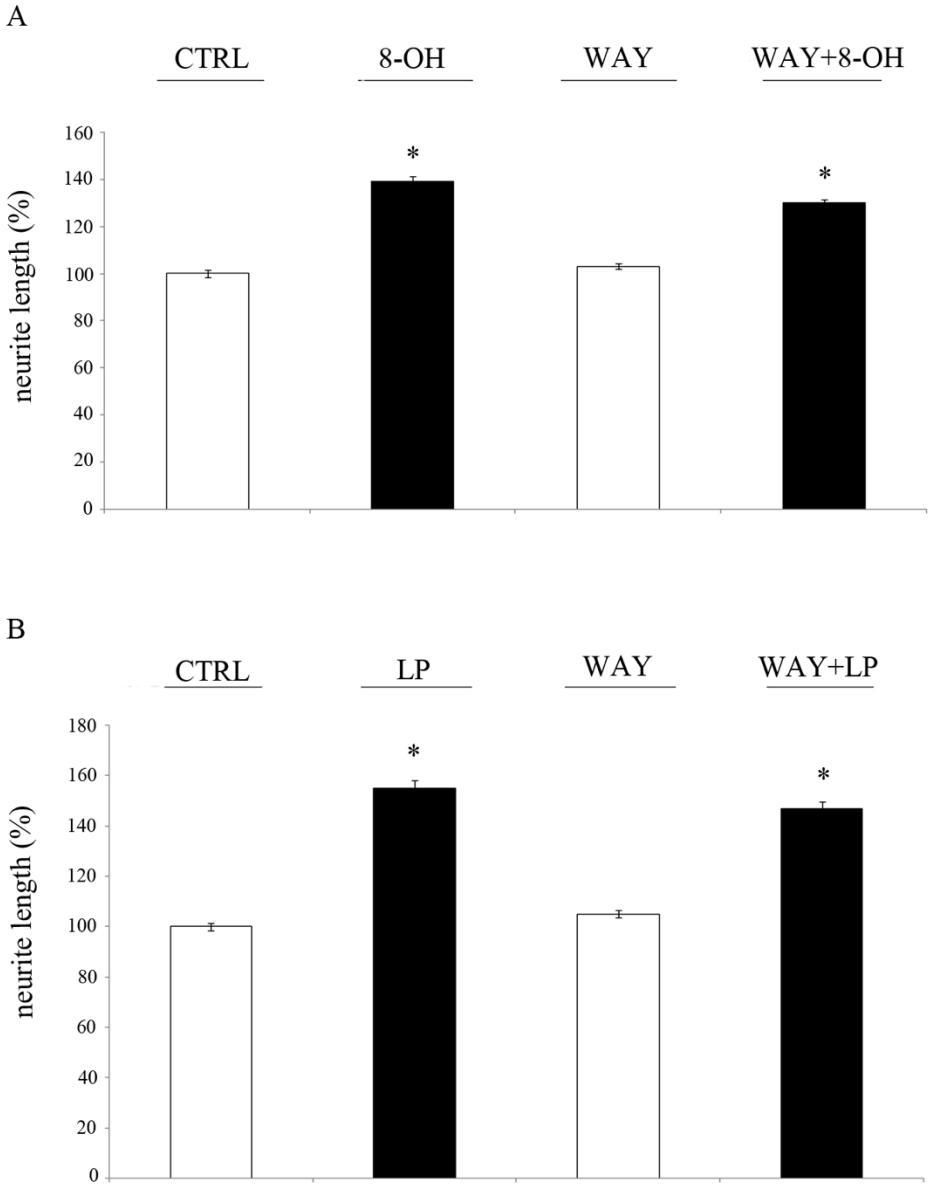

Figure 8. Neurite elongation induced by 8-OH-DPAT or by LP-211 is not dependent on 5-HT1A receptor. Cultured striatal neurons were treated for 30 min with 8-OH-DPAT (8-OH, 100 nM; A), or for 2 h with LP-211 (LP, 100 nM; B), with or without WAY-100635, a potent and selective antagonist for 5-HT1A receptor (WAY, 30 nM). Neurite length was measured on cells stained with anti-Tuj1 antibody, and expressed as percentage of the values measured in the corresponding vehicle-treated cultures (CTRL, set to 100%). The bars represent means ± SEM from randomly selected fields for each cell culture condition (n= 4). * Significantly different from CTRL by Student's t-test ($p < 0.05$).

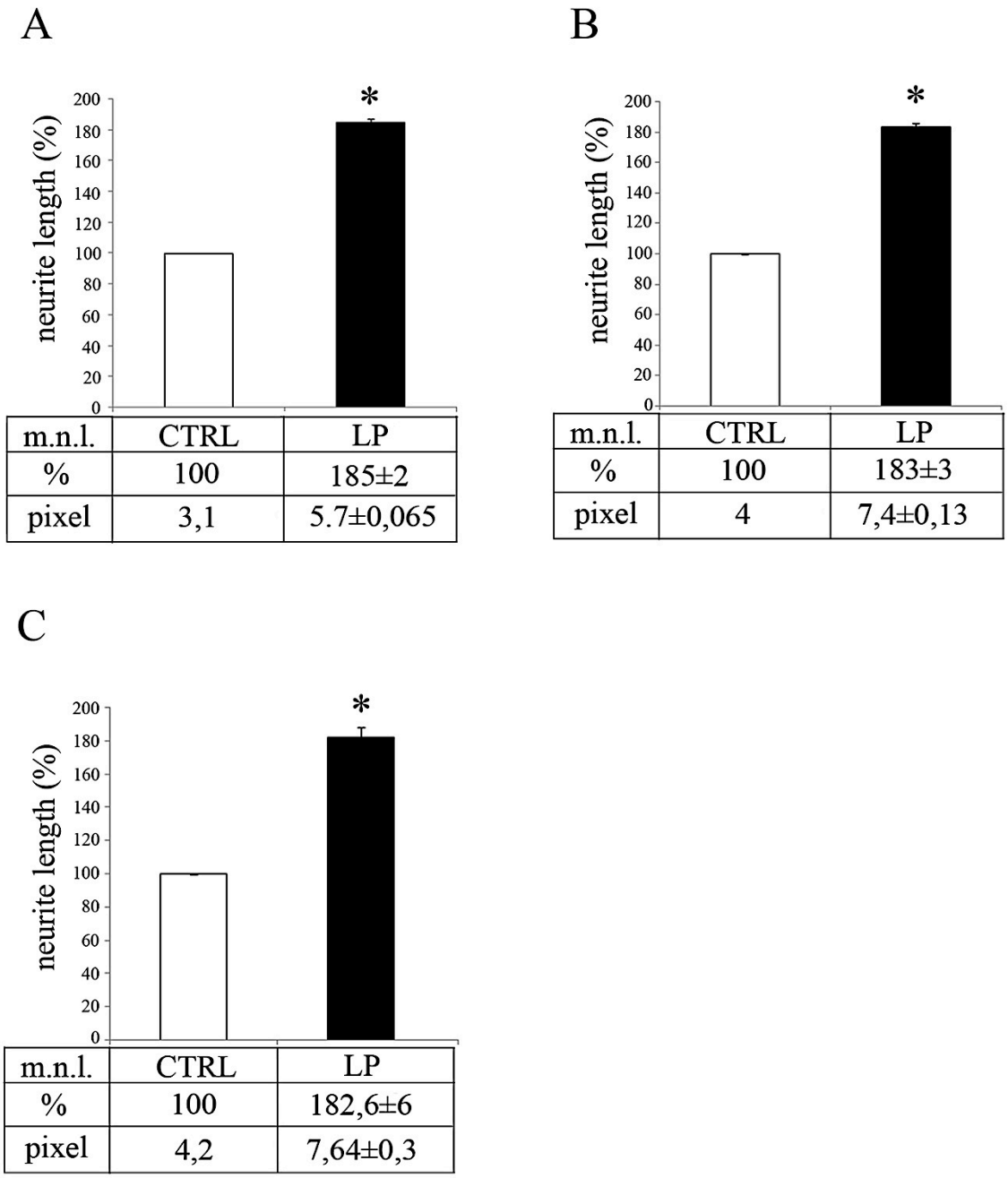

Figure 9. Neurite elongation induced by 5-HT7R stimulation in cortical neurons plated at different cell densities. Neurons dissociated from E16 cortex were plated at $1.5x10^5/cm^2$ (A), $1x10^5/cm^2$ (B) and $7.5x10^4/cm^2$ (C), and collected 2 h after the treatment with the 5-HT7R agonist LP-211 (LP, 100 nM). The graphs show the neurite length expressed as percent values in reference to the control values (CTRL). The bars represent means ± SEM from randomly selected fields for each cell culture condition (n= 8). The pixel values of mean neurite length (m.n.l.) for CTRL and LP-211 treated cultures are indicated in the table below each graph. *Significantly different from CTRL by Student's t-test ($p < 0.05$).

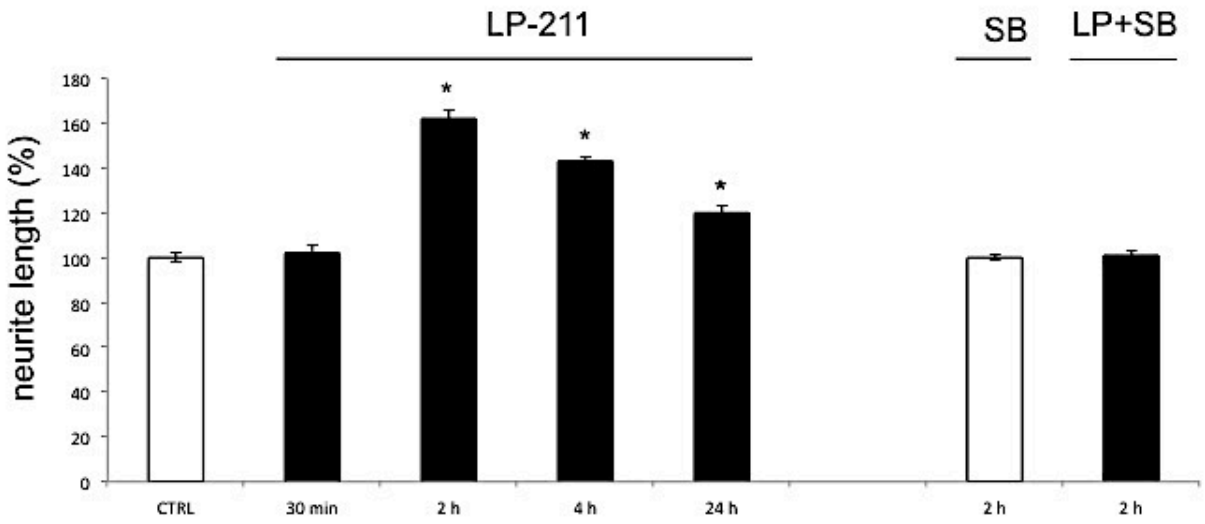

Figure 10. Agonist LP-211 stimulate neurite outgrowth in striatal primary cultures from E15 mice brain. Striatal cells were treated for 30 min, 1 h, 2 h, 4 h and 24 h with the 5-HT7R selective agonist LP-211 (LP, 100 nM), or for 2 h with the selective 5-HT7R antagonist SB-269970 (SB, 100 nM) with or without LP-211. Neurite length was measured on cells stained with anti-Tuj1 antibody, and expressed as percentage of the values measured in the corresponding vehicle-treated cultures (CTRL, set to 100%). The bars represent means ± SEM from randomly selected fields for each cell culture condition (n= 12). * Significantly different from CTRL by Student's t-test ($p < 0.05$).

4.3 Neurite elongation stimulated by 5-HT7 receptor activation requires ERK phosphorylation and Cdk5 activation.

G protein-coupled receptors are activated by a wide variety of external stimuli. One important mechanism to transduce mitogenic signals from the cell membrane to the cell nucleus is the engagement of the extracellular signal-regulated kinase (ERK)-mitogen-activated protein kinase (MAPK) cascade. A multitude of distinct signal transduction pathways are connecting G proteins with the ERK cascade.

Phosphorylation controls most cellular processes, including the cell cycle, proliferation, metabolism and apoptosis. Neural differentiation, including axon formation and elongation, is also regulated by a wide range of kinases and phosphatases (Arimura and Kaibuchi, 2007). In particular, the ERK signaling pathway is a well known point of convergence of distinct neurite outgrowth pathways (Colucci D'Amato et al., 2003; Buchser et al., 2010).

We thus tested whether 8-OH-DPAT and LP-211 were capable of stimulating ERK in rat striatal neuronal cultures. Activation of ERK was measured by quantitative Western blot experiments with an antibody detecting double phosphorylation of the kinase at threonine 202 and tyrosine 204. This signal was normalized with the western blot signal detecting unphosphorylated ERK.

ERK phosphorylation closely paralleled neurite elongation, stimulated by both 5-HT7 receptor agonists: when striatal cultures were treated with 8-OH-DPAT, a significant increase of ERK phosphorylation was observed at 30 min, but not at 24 h, compared to CTRL (Figure 11A). When striatal neurons were treated with LP-211, ERK phosphorylation was similar to CTRL at 1 h of stimulation, whereas it was significantly higher after 2 h; the induction, although reduced, significantly persisted at 24 h (Figure 11B).

ERK phosphorylation by 8-OH-DPAT and LP-211 was abolished by co-incubation with the 5-HT7 receptor antagonist (SB-269970), for 30 min and 2 h, respectively (Figure 11). Another set of experiments was performed using U0126, a highly selective inhibitor of MEK1 and MEK2 or ERK kinases. As expected, U0126 abolished ERK phosphorylation induced by both agonists, and treatment for 2 h with U0126 alone determined a significant reduction of ERK phosphorylation compared to CTRL (Figure 11).

Similar results were obtained on cortical neurons in culture (data not shown).

These data show that ERK activation is selectively due to stimulation of 5-HT7 receptor, and occurs at times when neurons are actively extending their neurites.

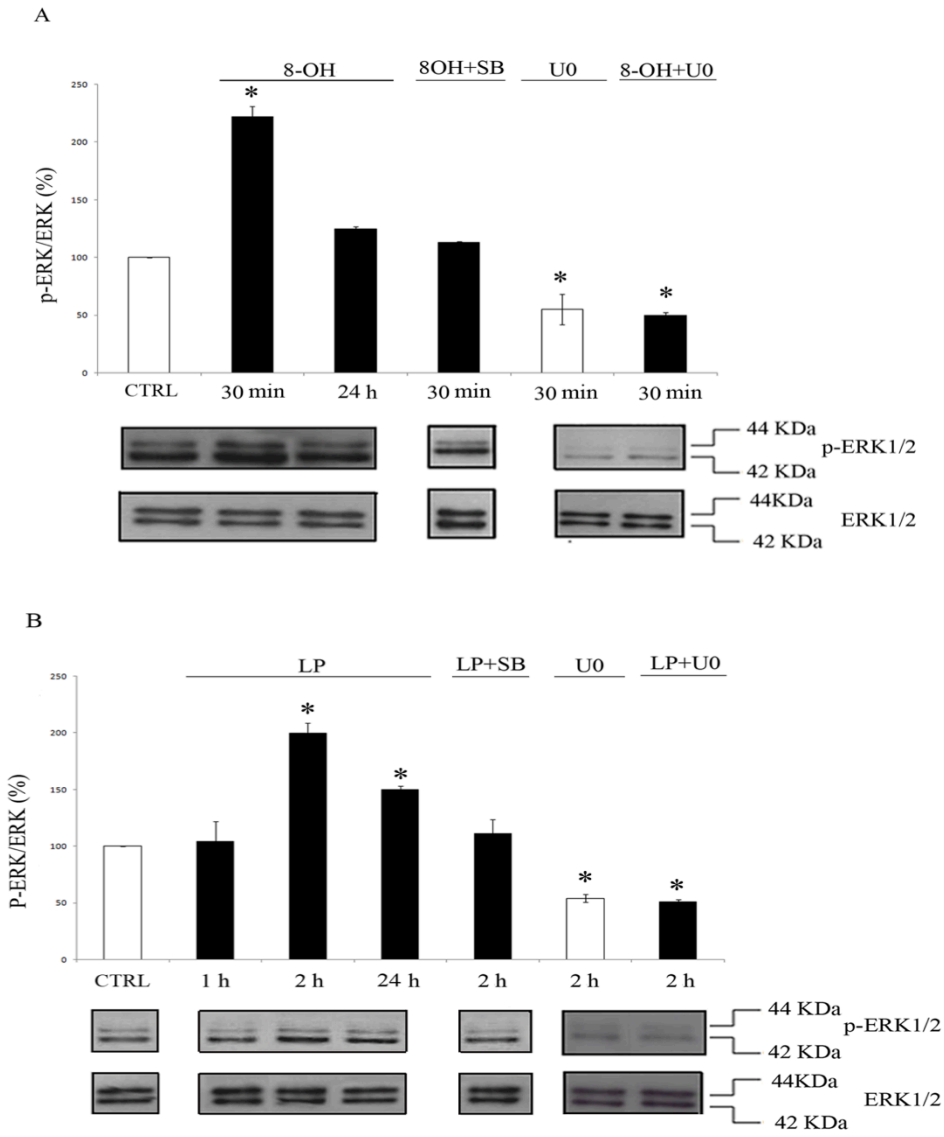

Figure 11. Agonist-induced activation of 5-HT7R stimulates ERK phosphorylation. (A) Striatal cultures were treated either with 5-HT7R agonist 8-OH-DPAT (8-OH, 100 nM, for 30 min and 24 h) alone, or in combination with the selective 5-HT7R antagonist SB-269970 (SB, 100 nM, for 30 min). Cells were also treated with the selective ERK inhibitor U0126 (U0, 10 μM) with or without 8-OH-DPAT for 30 min. (B) Cells were treated either with the selective 5-HT7R agonist LP-211 (LP, 100 nM, for 1 h, 2 h and 24 h) alone, or in combination with the selective 5-HT7R antagonist SB-269970 (100 nM, for 2 h). Cells were also treated with the selective ERK inhibitor U0126 (10 μM) with or without LP-211 for 2 h. (A, B) The level of ERK phosphorylation was measured as intensity of phosphorylated ERK (p-ERK 1/2) normalized with that of unphosphorylated ERK (ERK 1/2) in the same samples. ERK phosphorylation (means ± SEM n= 3) was expressed as percentage of values measured in the corresponding vehicle-treated control cultures (CTRL, set to 100%). *Significantly different from CTRL by Student's t-test ($p < 0.05$). The boxes below each graph display representative blots probed with antibody against p-ERK 1/2 and ERK 1/2.

To establish a casual relationship between ERK phosphorylation and 5-HT7 receptor-induced neurite outgrowth, rat striatal cultures were treated with the ERK inhibitor U0126 for 30 min prior to stimulation with the agonists, and then neuronal morphological alterations were examined. As shown in Figure 12, neurite growth stimulated by 30 min treatment with 8-OH-DPAT, or by 2 h treatment with LP-211 was completely abolished by 10 μM U0126. Treatment with U0126 alone determined a significant reduction of neurite length, when compared to CTRL (Figure 12), suggesting that ERK phosphorylation modulates neurite elongation also in absence of 5-HT7 receptor stimulation. These results show that ERK serve as a downstream effector of 5-HT7 receptor in inducing neurite extension.

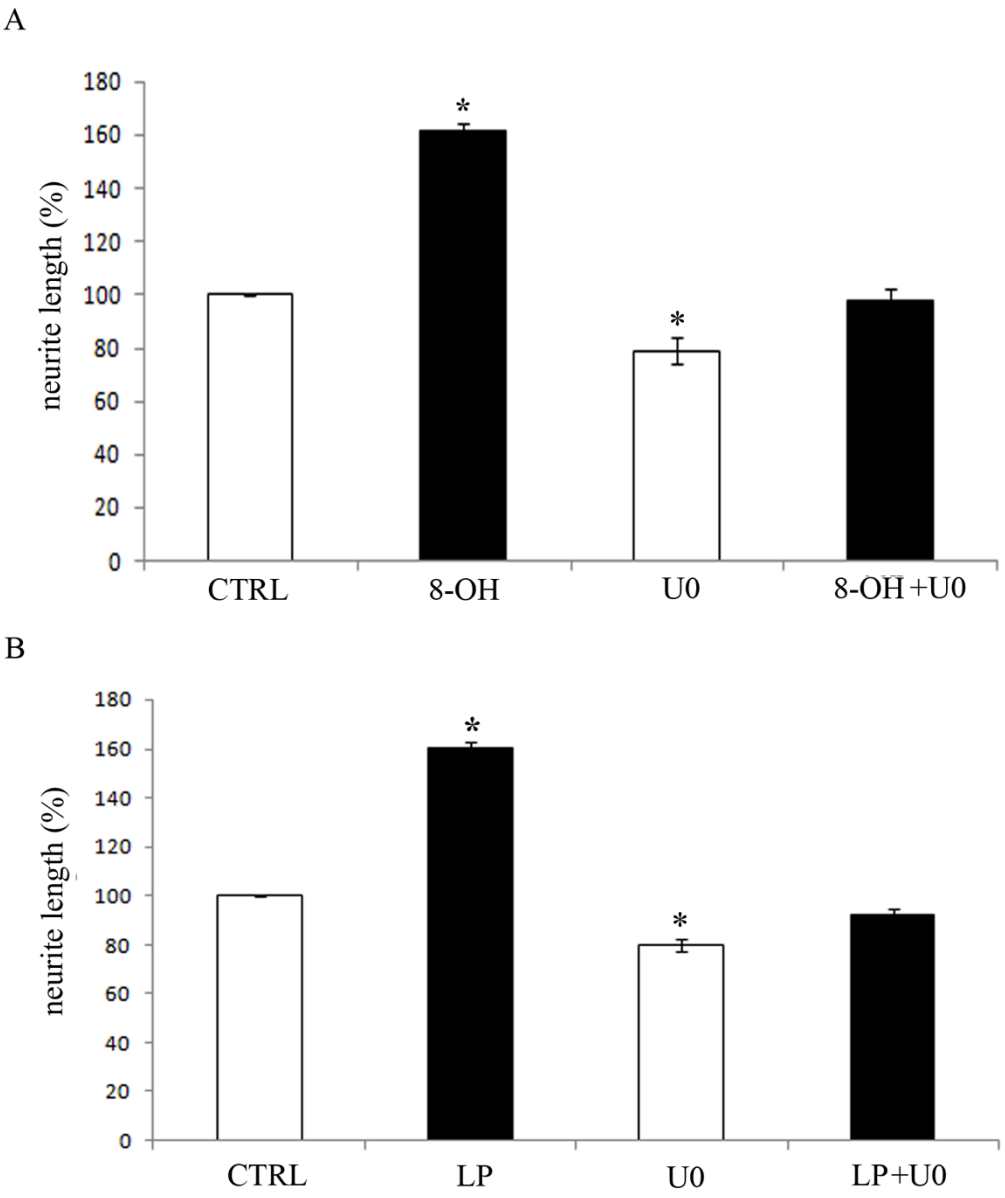

Figure 12. ERK phosphorylation is required for neurite elongation induced by 5-HT7R stimulation in neuronal primary cultures. (A) Striatal cells were treated for 30 min either with the 5-HT7R agonist 8-OH-DPAT (8-OH, 100 nM), or with the selective ERK inhibitor U0126 (U0, 10 µM), or with a combination of the two. (B) Cells were treated for 2 h either with the selective 5-HT7R agonist LP-211 (LP, 100 nM), or with U0126 (10 µM), or with a combination of the two. The graphs show the neurite length expressed as percent values in reference to the control values (CTRL). The bars represent means ± SEM from randomly selected fields for each cell culture condition (n= 8). *Significantly different from CTRL by Student's t-test ($p < 0.05$).

The ERK pathway is involved in "cross-talk" with various signal transduction pathways. Among these, we focused our attention on a serine/threonine protein kinase, the cyclin-dependent protein kinase 5 (Cdk5), that is highly expressed in the brain, and plays a key role in the regulation of microtubule dynamics and cytoskeletal reorganization necessary for neurite elongation (Nicolic et al., 1996; Cheung and Ip., 2007).

To evaluate the role of Cdk5 on neurite outgrowth induced by 5-HT7 receptor activation, we used roscovitine, a potent inhibitor of Cdks with limited selectivity between the Cdk5 and Cdk2 (Otyepka et al., 2006). In the CDK family, Cdk5 is the only member active in post-mitotic terminally differentiated neurons, where its activator proteins (p35 and p39) are localized (Otyepka et al., 2006). Differently, other members of the CDK family are activated by cyclins, critical regulators in proliferating cells. In our neuronal primary cultures, consisting of fully differentiated neurons we analyzed the gene expression level of Cdk5 and Cdk2 by Real-time quantitative RT-PCR analyses. As shown in Figure 13, we observed that the Cdk5 transcripts are approximately 4 fold more abundant than the Cdk2 transcripts, indicating that in our experimental conditions roscovitine can be considered a selective inhibitor of Cdk5 (Kim and Ryan, 2010).

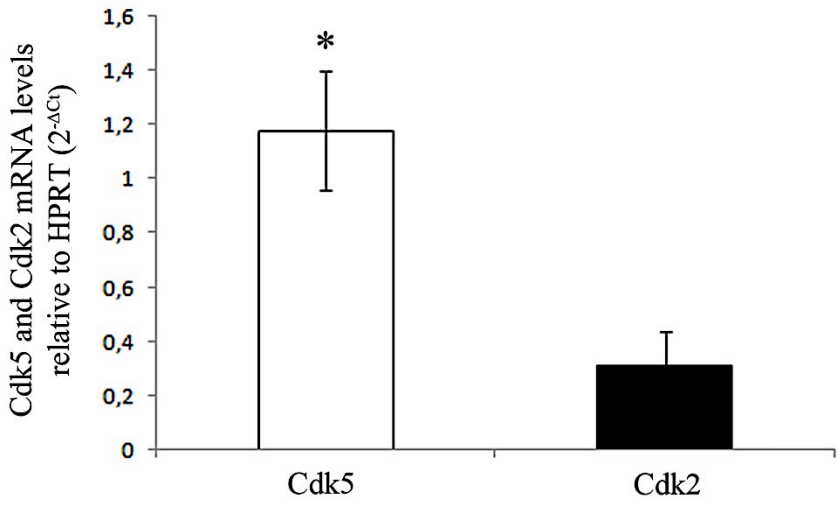

Figure 13. Expression levels of Cdk5 and Cdk2 mRNAs in striatal cultures. The levels of transcripts were determined by real time RT-PCR using the following forward (F) and reverse (R) primers: Cdk5 F, 5'-ATTGGGGAAGGCACCTA-3'; Cdk5 R, 5'-CTTGGCACACCCTCATCGTC-3'; Cdk2 F, 5'-TTGCGTTCCATCCCGAGCTA-3'; Cdk2 R, 5'-CCGGGAACCCTGACGAAAG-3'. The mRNA levels were normalized with those of the housekeeping gene HPRT (see Methods for details). The bars represent means ± SEM (n= 7). *Significantly different from CTRL by Student's t-test ($p < 0.05$).

Interestingly, treatment of neuronal rat striatal cultures with 20 μM roscovitine completely abolished neurite elongation induced by 2 h of treatment with 100 nM LP-211. Treatment of roscovitine alone for 2 h did not affect neurite length, compared to the CTRL (Figure 14). Similar results were obtained also with mouse neuronal primary cultures (data not shown).

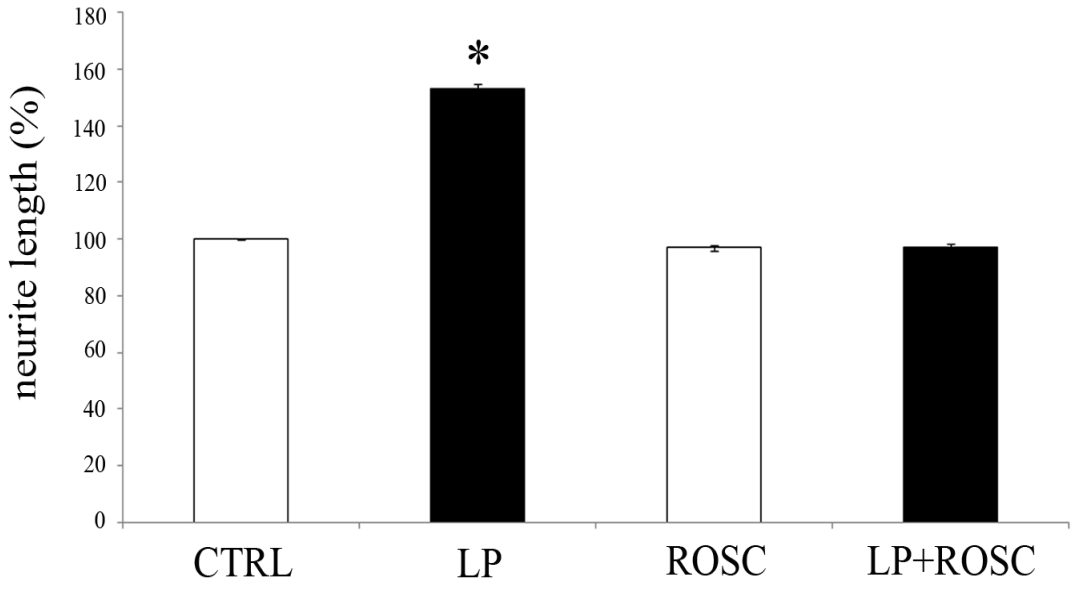

Figure 14. Neurite elongation induced by 5-HT7R stimulation in striatal primary cultures depends on Cdk5 activation. Striatal neurons were treated for 2 h either with the 5-HT7R selective agonist LP-211 (LP, 100 nM), or with the Cdk5 inhibitor roscovitine (ROSC, 20 μM), or with a combination of the two. Percent values of the neurite length (means ± SEM from randomly selected fields for each cell culture condition, n= 8) were calculated in reference to the control values (CTRL). *Significantly different from CTRL by Student's t-test ($p < 0.05$).

To analyze the possible interaction between ERK and Cdk5 pathways, we measured ERK phosphorylation by quantitative Western blot experiments, in cultures treated with LP-211 with or without roscovitine. Interestingly, the co-treatment abolished ERK phosphorylation stimulated by LP-211 (Figure 15.). All together, these results suggest that, in our culture conditions, neurite elongation stimulated by activation of 5-HT7 receptor requires ERK phosphorylation via Cdk5 activation.

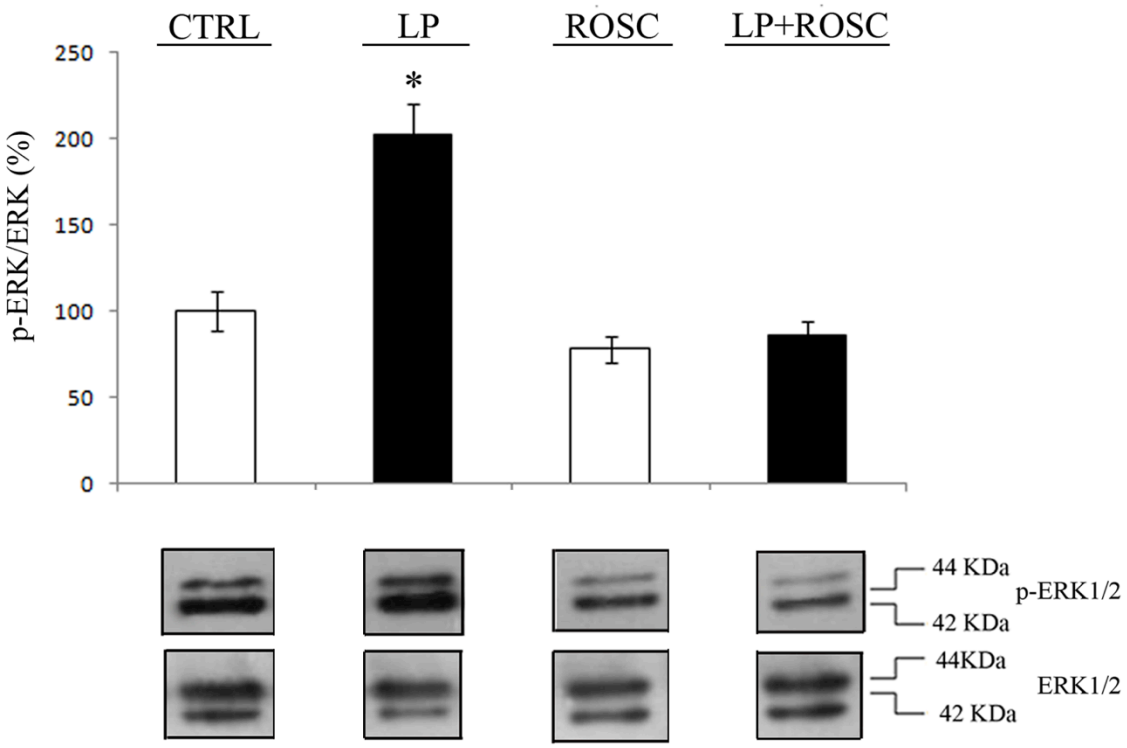

Figure 15. ERK phosphorylation induced by 5-HT7R stimulation is abolished by roscovitine. Cultured striatal neurons were treated for 2 h either with the selective 5-HT7R agonist LP-211 (LP, 100 nM), or with the Cdk5 inhibitor roscovitine (ROSC, 20 μM), or with a combination of the two. The level of ERK phosphorylation was measured as intensity of phosphorylated ERK (p-ERK 1/2) normalized with that of unphosphorylated ERK (ERK 1/2) in the same samples. ERK phosphorylation (means ± SEM; n= 3) was expressed as percentage of values measured in the corresponding vehicle-treated control cultures (CTRL, set to 100%). *Significantly different from CTRL by Student's t-test ($p < 0.05$). The boxes below each graph display representative blots probed with antibody against p-ERK 1/2 and ERK 1/2.

4.4 Neurite elongation stimulated by 5-HT7 receptor activation requires *de novo* protein synthesis and qualitative and quantitative changes in the expression of cytoskeletal proteins.

During the formation of the neural circuits of the mature nervous system, differentiating neurons acquire unique morphological and functional characteristics. The "neuronal differentiation" includes several processes such as neuritogenesis, neurite outgrowth, pathfinding, targeting and synaptogenesis. All of these processes are critically dependent on the reorganization of actin cytoskeleton presumably by several actin-binding proteins some of which may be newly synthesised.

To deepen our understanding of the biochemical machinery that underlies the 5-HT7 receptor-stimulated neurite outgrowth we investigated whether *de novo* protein synthesis was required. To this aim, neuronal striatal cultures were treated with LP-211 with or without 1 h pre-treatment with cycloheximide (CHX, an inhibitor of eukaryotic protein synthesis), and examined by morphometric analyses. As shown in Figure 16, neurite growth stimulated by 2 h treatment with LP-211 was completely abolished by co-incubation with 50 μM CHX. Treatment of CHX alone for 2 h did not affect neurite elongation, in comparison with the CTRL.

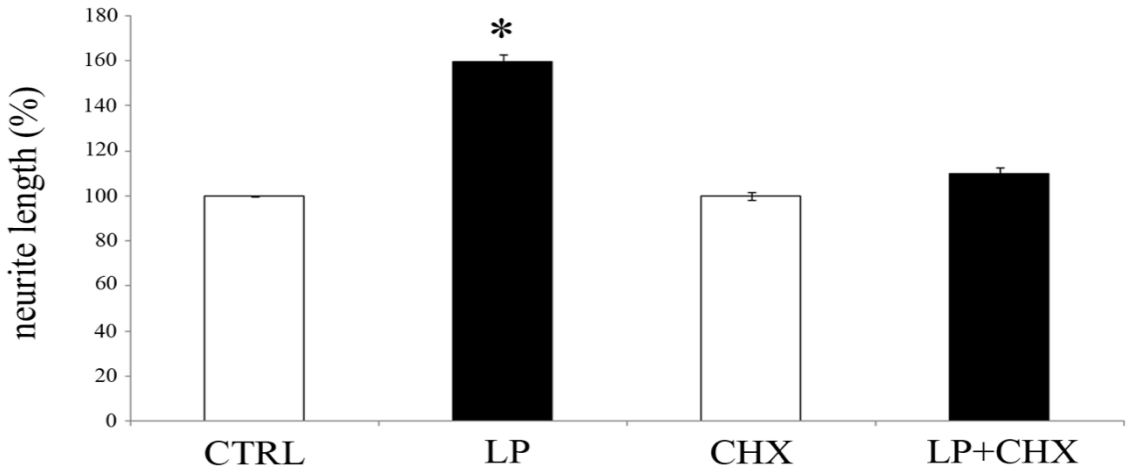

Figure 16. Neurite elongation induced by 5-HT7R stimulation in striatal primary cultures requires newly synthesized proteins. Striatal neurons were treated for 2 h either with the selective 5-HT7R agonist LP-211 (100 nM), or with the eukaryotic protein synthesis inhibitor cycloheximide (CHX, 50 μM) or with a combination of the two. Percent values of the neurite length (means ± SEM from randomly selected fields for each cell culture condition, n= 8) were calculated in reference to the control values (CTRL). *Significantly different from CTRL by Student's t-test ($p < 0.05$).

In order to understand the mechanism of neurite extension, it is particularly relevant to investigate the dynamics and organization of the cytoskeleton. Therefore, we analyzed whether LP-211 activation of the 5-HT7 receptor modulates the main components of the neuronal cytoskeleton, i.e. microtubules (constituted by α and β tubulin), neurofilaments and microfilaments (mainly constituted by actin). In addition to these major cytoskeletal elements, several additional proteins contribute to the organization of cytoskeletal structure cross-linking cytoskeletal proteins to each other or to cell membrane and modifying the polymerization of fibrillar structures from unassembled protein subunits. Such interactions may be controlled by enzymatic processes such as protein phosphorylation, which has been shown to regulate the interaction of actin with the microtubule-associated protein MAP2 (Selden and Pollard, 1983).

Following stimulation of striatal neurons with LP-211, we evaluated the expression of selected cytoskeletal genes, such as β-III-tubulin, vimentin, light and medium neurofilament subunits (NFL and NFM, respectively) and microtubule-associated proteins (MAPs) by Real-time quantitative RT-PCR analyses. Interestingly, significant variation between CTRL and agonist-stimulated striatal neurons was observed only for MAP1B transcripts, which were strongly up-regulated in rat striatal cultures treated with the agonist (Figure 17).

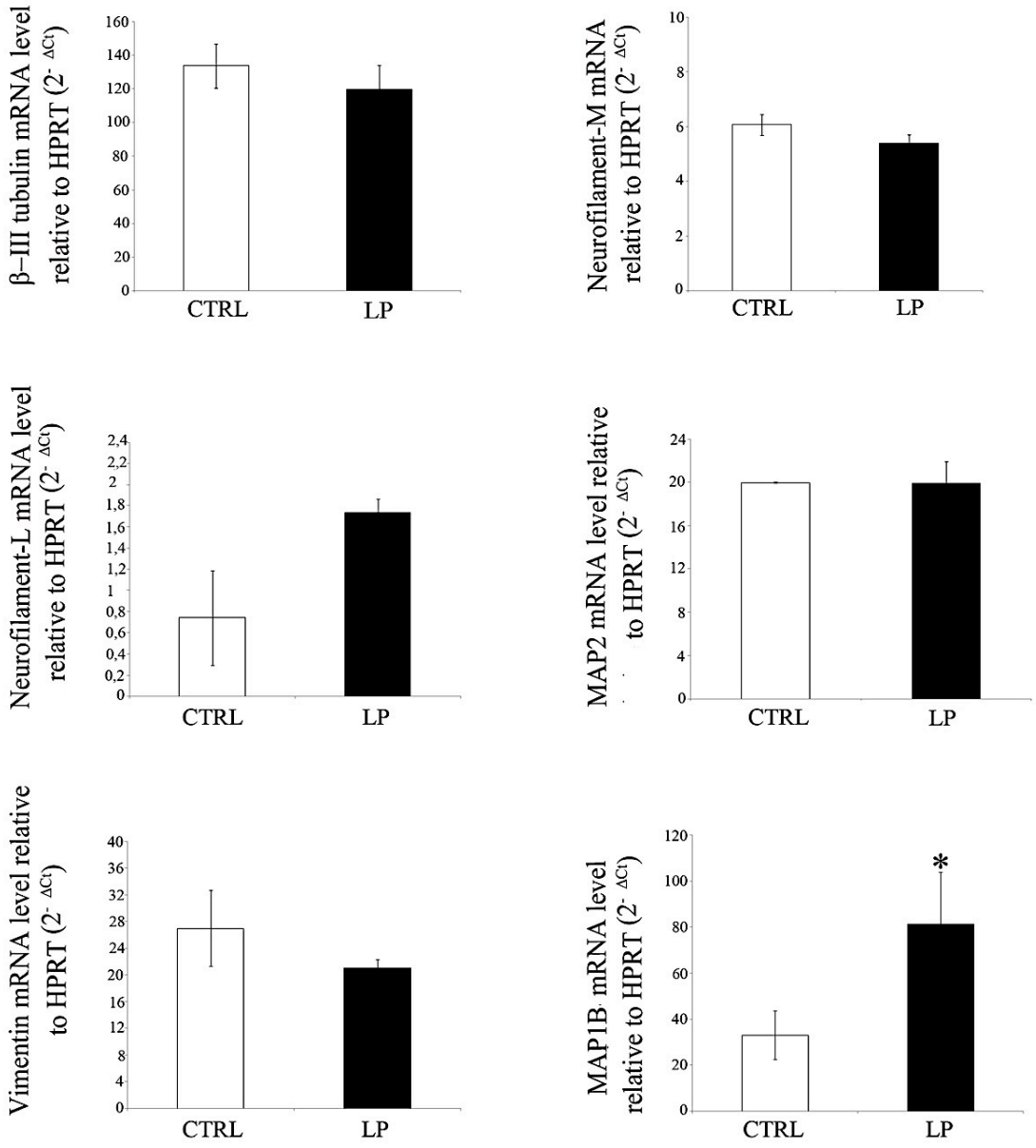

Figure17. Effect of LP-211 on expression levels of several mRNAs for cytoskeletal proteins in striatal neurons. Striatal cells were collected 2 h after the treatment with the selective 5-HT7R agonist LP-211 (LP, 100 nM). Expression levels of selected mRNAs were determined by Real time RT-PCR using specific primers for Tuj1, NF-M, vimentin, MAP2, and MAP1b. The mRNA levels were normalized with those of the housekeeping gene HPRT (see Methods for details). The bars represent means ± SEM (n= 4 for treated samples and n=3 for CTRL). *Significantly different from CTRL by Student's t-test ($p < 0.05$).

Although RT-PCR analyses provides insight on gene expression, changes occurring at the translational and post-translational levels are not detected.

Therefore, in collaboration with the laboratory directed by the Dr. A. Chambery, we analyzed the expression profiles of the same neuronal cytoskeleton proteins by Western blot analyses coupled to 2D-PAGE. The latter enabled us to obtain a higher resolution profile of these proteins and to evaluate possible posttranslational modifications. Immunostaining of 2D-gels of CTRL striatal cultures showed a marked stretching of β-tubulin spots (Figure 18), attesting a high level of tubulin heterogeneity. Interestingly, an overall down-regulation of β-tubulin was revealed in LP-211-treated cultures, compared to CTRL (Figure 18A). This reduction involved mostly the stretching of acidic tubulin spots, resulting in a marked reduction of β-tubulin heterogeneity in stimulated cells compared to CTRL. On the contrary, no expression changes of vimentin isoforms were observed between LP-211 and vehicle-treated control (Figure 18A). Similarly, no qualitative and quantitative expression changes were revealed for the main form at ~68 kDa of NFL (Figure 18B). However, a protein species with a slightly lower molecular weight that migrated as a satellite spot of NFL disappeared in LP-211 treated cells (Figure 18B). On the other hand, a down-regulation of the main component at 145 kDa of NFM was detected in LP-211-treated cultures, in comparison to CTRL (Figure 18B). On the contrary, a slight up-regulation of the main isoform of MAP2 (70 kDa) and of a satellite spot at acidic pI was observed in LP-211 treated cells together with the appearance of a lower molecular weight form (Figure 18C). Moreover, the high level of heterogeneity of MAP1B with several high molecular weight isoforms (ranging from 270 to 380 kDa) detected in control cultures, completely disappeared in LP-211-stimulated cells, whereas the 270 kDa isoform was slightly up-regulated (Figure 18C). Notably, in these cultures an evident qualitative change was detected regarding the appearance of an intense spot with molecular weight of about 34 kDa (Figure 18C).

This form corresponds to the MAP1B light chain (34 kDa), thought to play a role in regulating the neuronal cytoskeleton by binding to microtubules and inducing tubulin polymerization (Kuznetsov et al., 1986; Togel et al., 1998).

MAP1B is a developmentally regulated microtubule-associated phosphoprotein that is expressed at high levels in developing neurons and is generally down-regulated in the adult nervous system, although it persists in regions that show neuronal plasticity or regenerate after injury (Halpain and Dehmelt, 2006). MAP1B plays a role in axogenesis (Gordon-Weeks and Fisher., 2000) and participates in the cross-talk between microtubules and actin microfilaments to promote axonal elongation (Montenegro-Venegas et al., 2010). MAP1B precursor protein, encoded by a single gene consisting of seven exons, is proteolytically processed into 2 parts: a heavy chain (HC) and a light

chain (LC-1) corresponding to a 250 amino acid-long carboxy-terminal segment (Togel et al, 1998); both parts have microtubule binding domains (MTB) and the capacity to interact with both tubulin and actin (Lee et al., 2008).

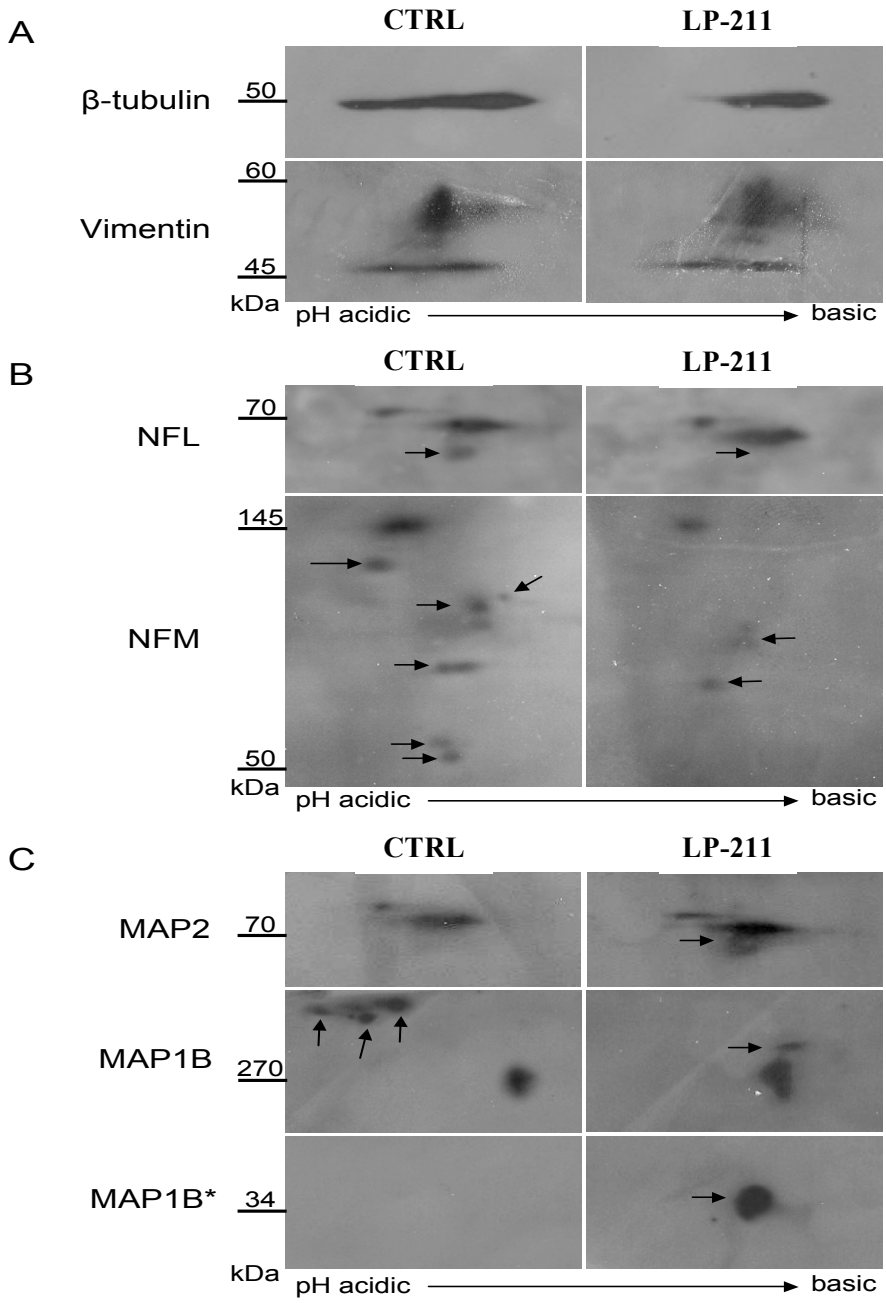

Figure 18. Effect of LP-211 on expression levels of several cytoskeletal proteins in striatal neurons. 2D immunoblots analyses were performed on striatal neurons treated with the 5-HT7R selective agonist LP-211 and on vehicle–treated cultures (CTRL). (A) β-tubulin and vimentin; (B) low- (NFL) and middle- (NFM) molecular weight neurofilaments; (C) microtubule-associated proteins (MAP2 and MAP1B). The molecular weights (kDa) are indicated on the left. Arrows represent qualitatively different spots between CTRL and LP-211 treated cultures.

To better analyze the involvement of actin cytoskeleton in LP-211 induced neurite outgrowth we extended our analysis to regulators of actin filament assembly/disassembly. Indeed, the dynamic of the actin cytoskeleton depends on the balance between assembly and disassembly of actin filament that is regulated by several factors, one of which is the protein cofilin, a major actin-depolymerizing factor (dos Remedios et al., 2003). Cofilin is activated by dephosphorylation at Ser3 and it is inactivated by phosphorylation at the same site (Morgan et al., 1993, Agnew et al., 1995). Active cofilin disassemble F-actin from the rear of the actin network to recycle actin monomers to the leading edge for further rounds of polymerization.

To examine the involvement of cofilin in 5-HT7 receptor-induced neurite outgrowth, we investigated, by 2D-PAGE, the expression profiles of β-actin and cofilin in striatal and cortical cultures from embryonic mice.

Immunostaining of 2D-gels of both control (CTRL) striatal and cortical cultures showed a marked stretching of actin spots at 42 kDa, attesting a high level of actin heterogeneity (Figure 19). No significant expression changes of the average actin content were observed upon treatment with LP-211 (Figure 19) as also confirmed by immunostaining of 1D-gel (data not shown).

Interestingly, LP-211 treatment was found to alter the cofilin expression profile in striatal and cortical cells. Indeed, a slight shift of the stretch of cofilin spots at 21 kDa toward acidic pH region was revealed following LP-211 treatment (Figure 19).

As previously reported for rat striatal neurons, also for mice striatal neurons, a down-regulation of acidic β-tubulin spots was revealed in LP-211-treated cultures, compared to CTRL (Figure 19A). This effect was not observed in cortical cells (Figure 19B). However, in both LP-211-treated samples, the appearance of lower molecular weight forms, possibly corresponding to β-tubulin degradation products was detected (Figure 19).

A

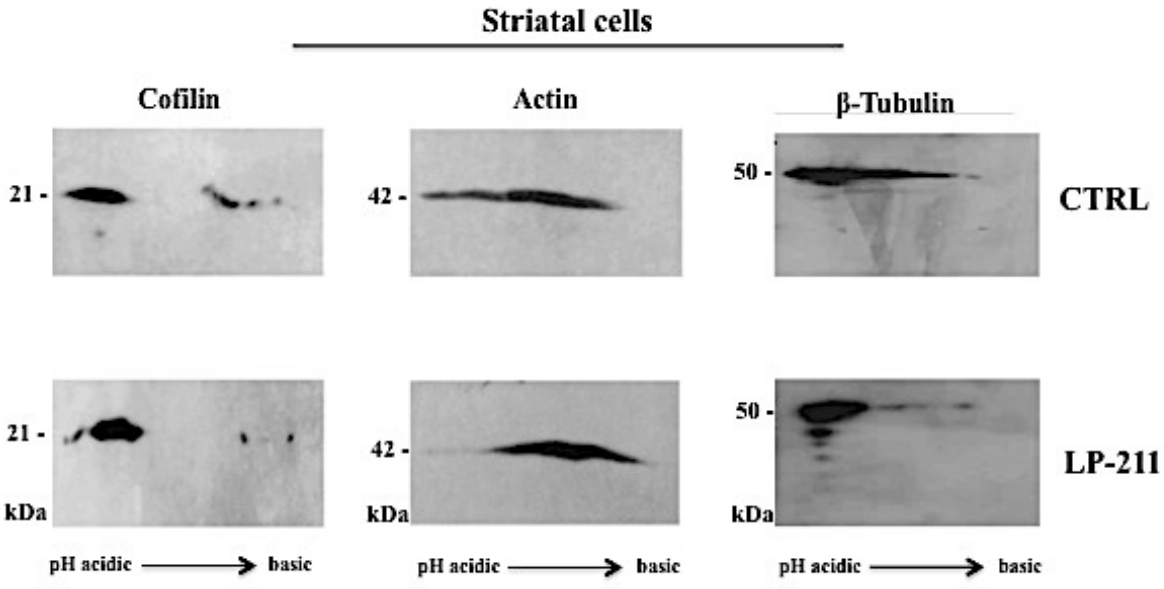

B

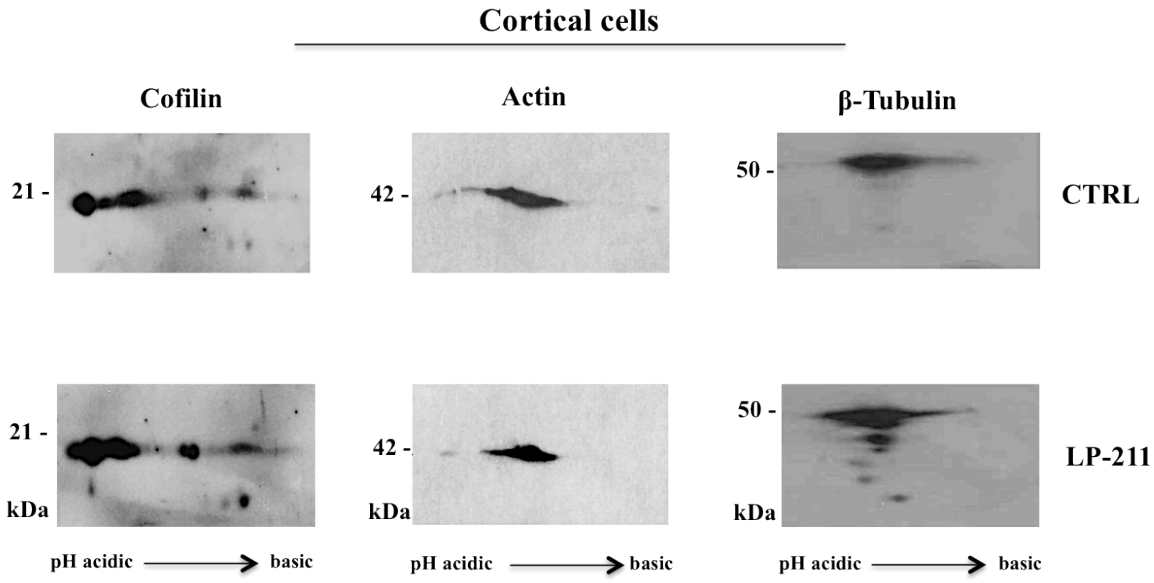

Figure 19. Effect of LP-211 on expression levels of cofilin, actin and β-tubulin in striatal and cortical neurons. 2D immunoblot analyses were performed on neurons treated with the 5-HT7R selective agonist LP-211 and on vehicle–treated cultures (CTRL). The molecular weights (kDa) are indicated on the left.

4.5 *In vitro* modulators of actin dynamics

Actin dynamics are essential for many cellular processes, including the control of cell shape, movement, and division (Ridley et al., 2003). To examine the role of actin dynamics in LP-211 neurite outgrowth, we used pharmacological compounds that interfere with polymerization and, depolymerization of the actin cytoskeleton. These compounds can be sorted into several classes. The first and most prevalent class of actin drugs includes those that interfere with actin polymerization by sequestering the free actin monomer pool (latrunculin) or by blocking the fast-growing barbed ends of actin filaments (cytochalasin; Cooper, 1987). A second class of actin drugs includes those that interfere with the disassembly of the actin network, as for instance jasplakinolide that binds actin filaments, blocks their disassembly and stabilizes their polymerization (Wilson et al, 2010). The striatal primary cultures from embryonic mice were treated for 2 hours with cytochalasin D (100 nM), latrunculin (2 μM), and jasplakinolide (2 μM) with or without the co-treatment with LP-211. When the neuronal cultures were stimulated with LP-211 in presence of cytochalasin D or latrunculin, inhibitors of actin polymerization, the stimulatory effect of LP-211 on neurite outgrowth was blocked, while the treatment with the inhibitors alone induced a reduction of neurite length.

In line with this, when the striatal neurons were exposed to jasplakinolide, agent promoting actin polymerization, a significant increase in neurite length was observed. When the striatal neurons were co-treated with jasplakinolide and LP-211 the effect was not cumulative and the neurites length was similar to the one obtained with LP-211 alone, suggesting that LP-211 is able to stimulate the outgrowing mechanism at its maximum level.
Taken together these results show that the neurite outgrowth induced by the selective stimulation of the endogenous 5-HT7 receptor is due by the remodelling of the actin cytoskeleton.

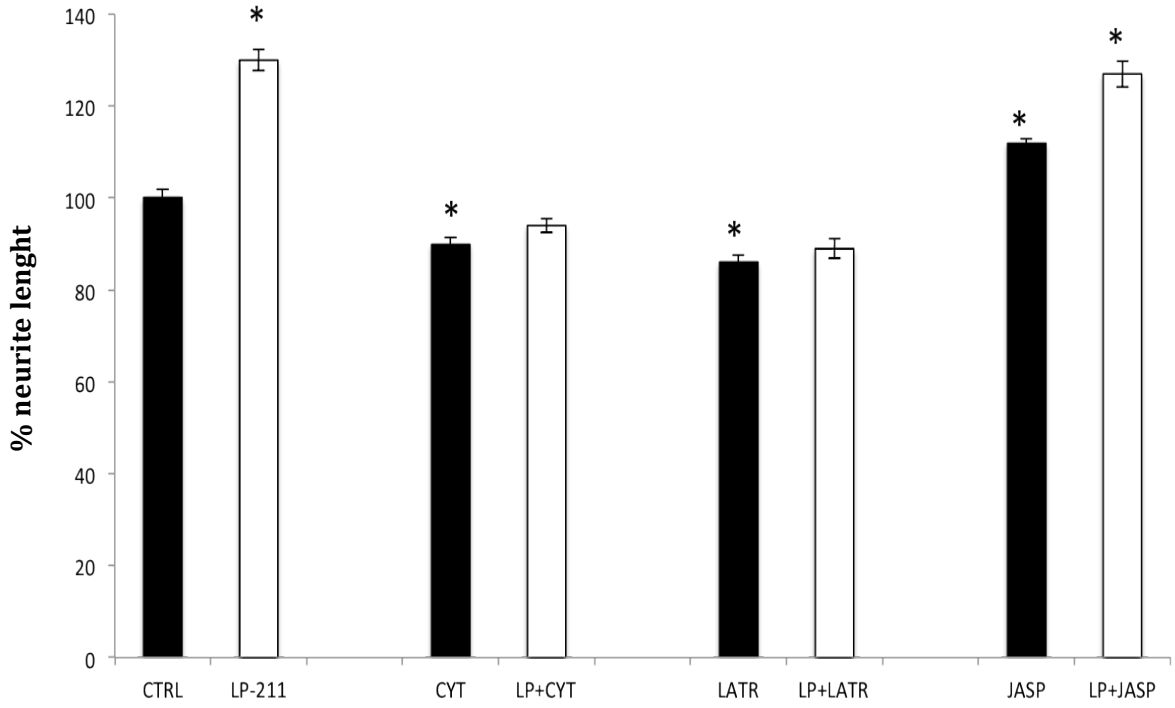

Figure 20. Effect of modulators of actin dynamics on the 5-HT7 receptor-induced neurite outgrowth. Striatal neurons from E15 mice were treated for 2 h either with the selective 5-HT7R agonist LP-211 (100 nM), or with the inhibitors of actin polymerization (cytochalasin D, 100 nM CYT; latrunculin, 2 μM LATR), or with the agent promoting actin polymerization (jasplakinolide, 2μM JASP) or with a combination of LP-211 and each of these compounds. The neurite length was expressed as means ± SEM from randomly selected fields for each cell culture condition, n= 8. *Significantly different from CTRL by Student's t-test ($p < 0.05$).

4.6 Activation of 5-HT7R induces axonal outgrowth

Neurons initially extend neuritis that are the precursors of axons and dendrites. Axons and dendrites can be distinguished by several morphological and biochemical properties and because they exhibit different growth rates during the development. The temporal pattern of neurite outgrowth from CNS neurons has been extensively examined in vitro using hippocampal neurons stained with antibodies against marker proteins specific for axons or dendrites. For instance, microtubule-associated protein 2 (MAP2) is expressed in neuronal cell bodies and dendrites and has been used as a marker to identify developing dendritic processes, while was more difficult to find an appropriate axonal marker (Pennypacker et al., 1991).

As axonal marker we chose to use MAP1B, the major microtubule associated protein in developing brain, highly concentrated at the distal tip of growing axons (Montenegro-Venegas et al., 2010).

We performed immunocytochemical analysis in cortical neurons dissociated from E15 mouse brains and cultured for 7 days, using antibodies against MAP2 and as show in Figure 21, the results are not clear, because several processes have double labelling, and therefore it is very difficult to distinguish axons from dendrites.

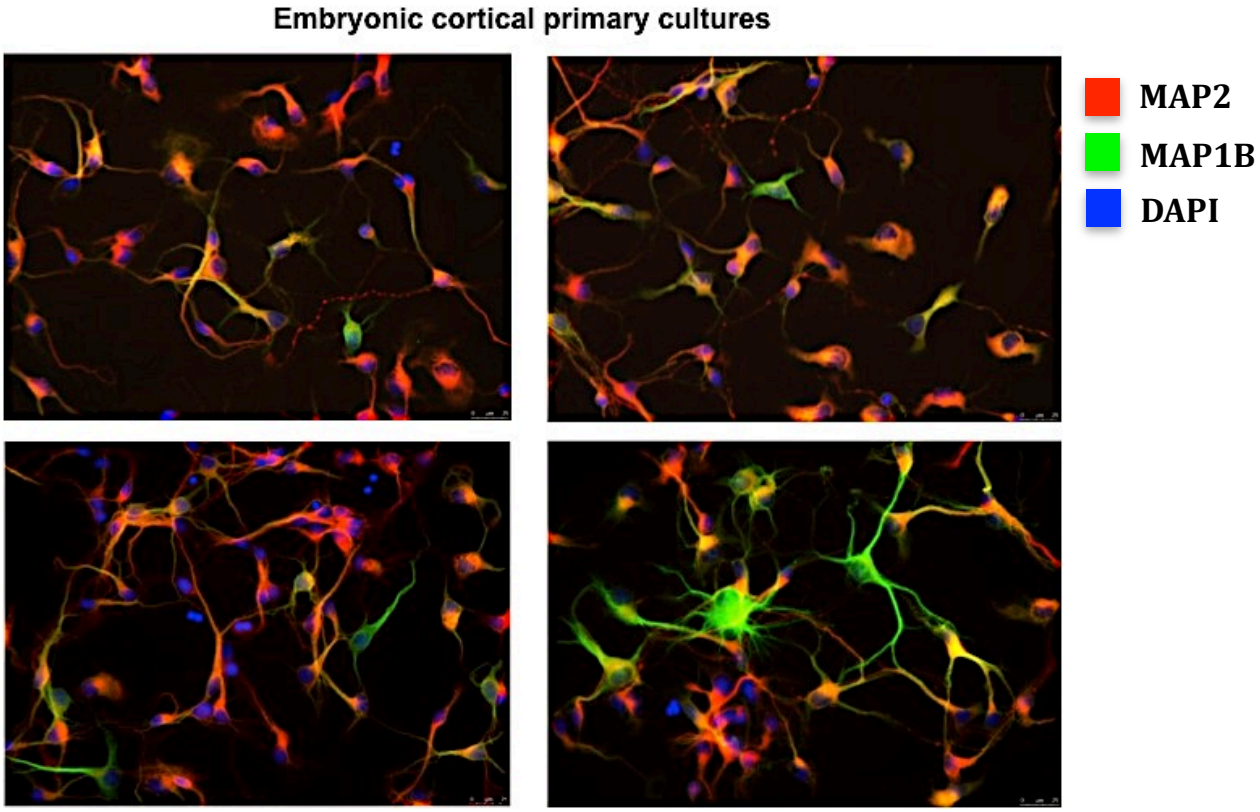

Figure 21. Representative photomicrographs of embryonic cortical cultures immunostained with specific antibodies against the axonal marker MAP1B (green), and dendritic marker MAP2 (red). Cell bodies were identified by counterstaining with the nuclear marker DAPI (blue). Magnification 40x

As alternative approach to identify as axons or dendrites the processes that are outgrowing following LP-211 treatment, we used microfluidic chambers. These chambers consist of a molded elastomeric polymer piece placed against a cell plate. Two mirror image compartments are separated by embedded microgrooves. The platform allows the fluidic isolation of axonal microenvironments by establishing a minute volume difference between the two compartments. The high fluidic resistance of the microgrooves produces a small but sustained flow between the compartments that counteracts diffusion.

Dissociated neurons, plated into one compartment of the microfluidic chamber (somal side), within 4 days in vitro begin to extend their processes through the microgrooves into the axonal compartment. Due to the dimensions of the cross-sectional area and the length of the microgrooves, only axons are able to elongate into the axonal compartment (Taylor et al 2005).

As previously reported, we confirm that the stimulation of cultured hippocampal neurons with LP-211 for 2 h induces neurite outgrowth that is completely abolished by co-treatment with the selective antagonist SB-269970 (Figure 22A). In collaboration with the laboratory directed by Dr. E. De Stefano, we incubated dissociated hippocampal cells in microfluidic chamber for 6 days with

or without the addition of 100 nM LP-211 to both compartments. Interestingly, LP-211 significantly increased the number of axons reaching the axonal compartment and their branching, starting from the third day up to the fifth day in culture. These results clearly indicate that the activation of 5-HT7R induced axonal outgrowth in hippocampal neurons in cultures.

A

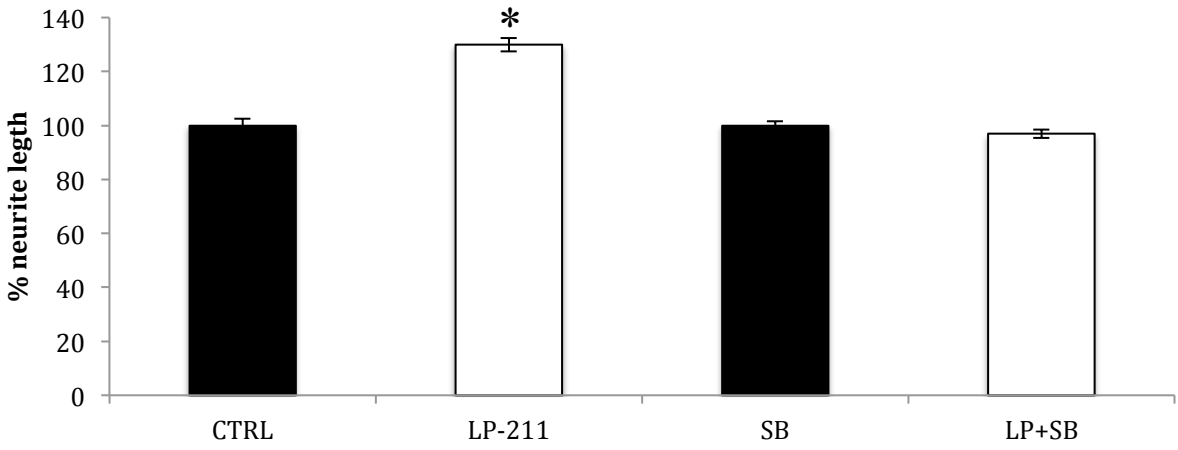

B

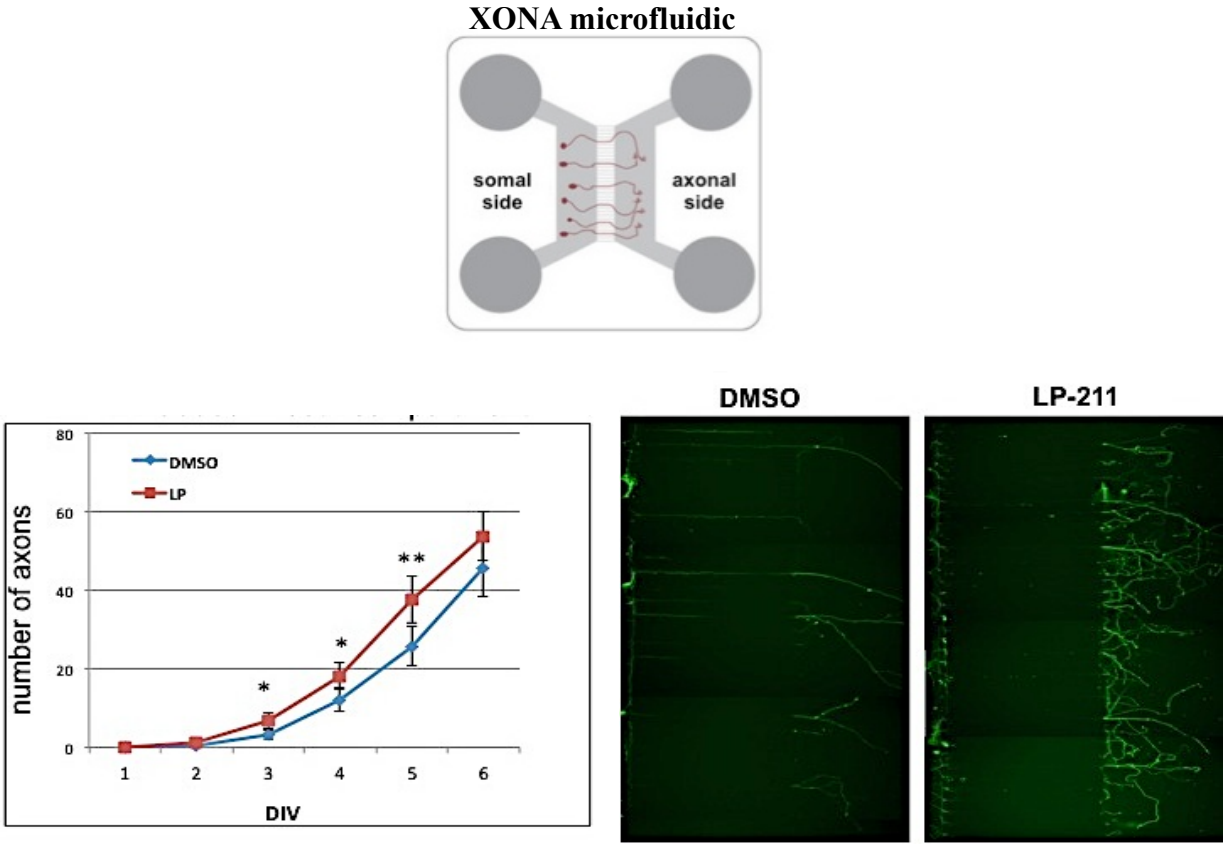

Figure 22. The selective 5-HT7R agonist stimulates neurite outgrowth in hippocampal primary cultures from E18 mice. (A) Cells were treated for 2 h with 100 nM LP-211, with or without the selective 5-HT7R antagonist SB-269970 (SB, 100 nM). Neurite length was measured on cells stained with anti-Tuj1 antibody, and expressed as percentage of the values measured in the corresponding vehicle-treated cultures (CTRL, set to 100%). (B) Hippocampal cultures were plated in microfluidic chamber and 100 nM LP-211was added to both compartments for 6 days. *Significantly different from CTRL by Student's t-test ($p < 0.05$).

4.7 Stimulation of 5-HT7 receptor modulates dendritic spine morphology in the CNS of living animals

A crucial point of my PhD project is to asses whether changes in neuronal cytoarchitecture observed on embryonic neuronal cultures are reproducible in rodent brain circuits in the postnatal period.

To address this aspect we first evaluated the expression levels of 5-HT7 receptor (mRNA and protein) at different developmental stages (embryonic, postnatal and adult) and in various areas of the CNS (striatum, cortex, hippocampus, midbrain and cerebellum) by RT-PCR and Western blot analyses. The results of these experiments show that the 5-HT7 receptor is expressed from embryonic to adult age at similar level in all the areas analyzed (data not shown).

To study the morphological effects induced by the activation of the endogenous 5-HT7 receptor in living animals, we analyzed the shape and density of dendritic spines in selected CNS neurons of P40 mice injected with the selective agonist LP-211. As first described by the beautiful camera-drawings of Ramon y Cajal at the end of 19th century, dendritic spines are small protrusions from the dendritic shaft; they receive and integrate predominantly excitatory presynaptic signals in most mammalian brain regions (Bhatt et al 2009), although recent data suggest that inhibitory synapses showing high levels of plasticity may also be located on dendritic spines (Chen et al 2012; van Versendaal et al 2012). Changes in spine densities or volume are interpreted as changes in synaptic strength.

Detailed analyses of dendritic arbors and their associated spines provide a basis for understanding synaptic function and plasticity in the brain (Rochefort N. and Konnerth A., 2012).

Detailed information about morphological characteristics of neurons and dendritic spines can be obtained by the Golgi-Cox impregnation, a widely employed method. More recently, visualization of dendrites by fluorescent labeling of neurons followed by confocal microscopy has allowed to analyze a large population of dendritic spines with a higher resolution.

A useful approach to the morphological identification of neurons is termed “DiOlistic labeling” (Gan et al., 2000). With this method, microparticles coated with a lipophilic dye (e.g. DiI) are applied to fixed tissue brain section. If a dye-coated particle is embedded in a neuron, the dye is incorporated into the membrane where the diffusion of the dye produces fluorescent Golgi-like labeling. Advantages of this labeling method are that it is compatible with a variety of tissues, is reliable and offers high-throughput neuronal analysis (Staffend N.A. and Meisel R.L., 2011).

In collaboration with the laboratory directed by the Dr. E. De Leonibus (IGB, CNR), we treated P-40 old mice with intra-peritoneal injections of the brain-penetrant 5-HT7 receptor agonist LP-211

(0.25 mg/Kg, once a day), which is brain-permeant. The animals were divided in two groups: the control group was treated with the veichle alone (DMSO), the other group was treated with LP-211. After 2 days of agonist administration, the animals were sacrified at the third day, perfused with PFA 4% and the brain post-fixed. Coronal brain slices from the dorsolateral striatum were cut by vibratome, and labeled with the fluorescent lipophilic tracer DiI for the morphological analyses of neurons. After 4 weeks of incubation, the morphology and density of dendritic spines was analyzed by using confocal microscopy.

Dendritic Z-stacks images were collected and dendritic shafts and spines were manually traced by using the Image J software. Accurate reconstruction of the diameter length, spine neck, head diameter and spine length was made possible using the freehand lines function. Representative 3D-reconstructions of the dorsolateral striatal dendritic shafts from neurons labeled with DiI are shown in Figure 23.

A

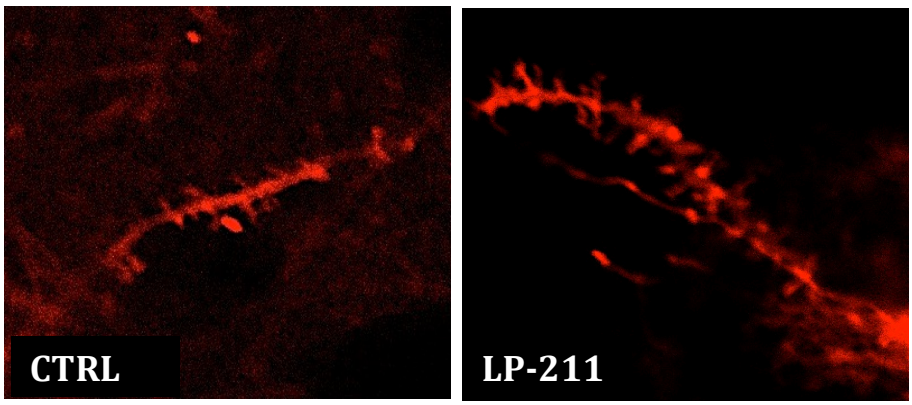

B

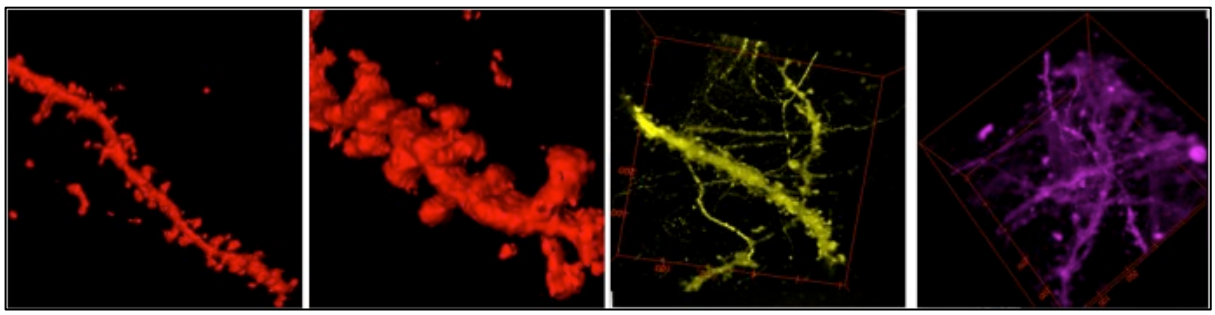

Fig 23. (A) Representative images of dendrites labeled by DiI tracer. The images were acquired after 4 weeks of incubation with DiI, using a confocal microscopy.
(B) In the small box there is a representative 3D-recostrunction of the dorsolateral striatal dendritic shafts labeled with DiI.

As shown in Figure 24, the total number of spines in neurons from the dorsolateral striatum is significantly increased in mice treated with LP-211 when compared to control animals.

Traditional methods of describing dendritic spines involve the classification and subsequent counting of spines into "Mushroom-like", "Stubby" and "Filipodial/long" spines (Harris et al., 1992; Arellano et al., 2007).

In accordance to their morphology, spines were classified into "Mushroom-like", "Stubby" and "filipodial/long" spines (Arellano et al., 2007) and further analyzed in LP-211 and CTRL-treated animals. We observed that the agonist treatment induces an increase of the spine length for all the spines categories, and an increase of the neck length only for the mushroom and thin spines. The head diameter and the neck diameter were not affected by the treatment (Figure 25).

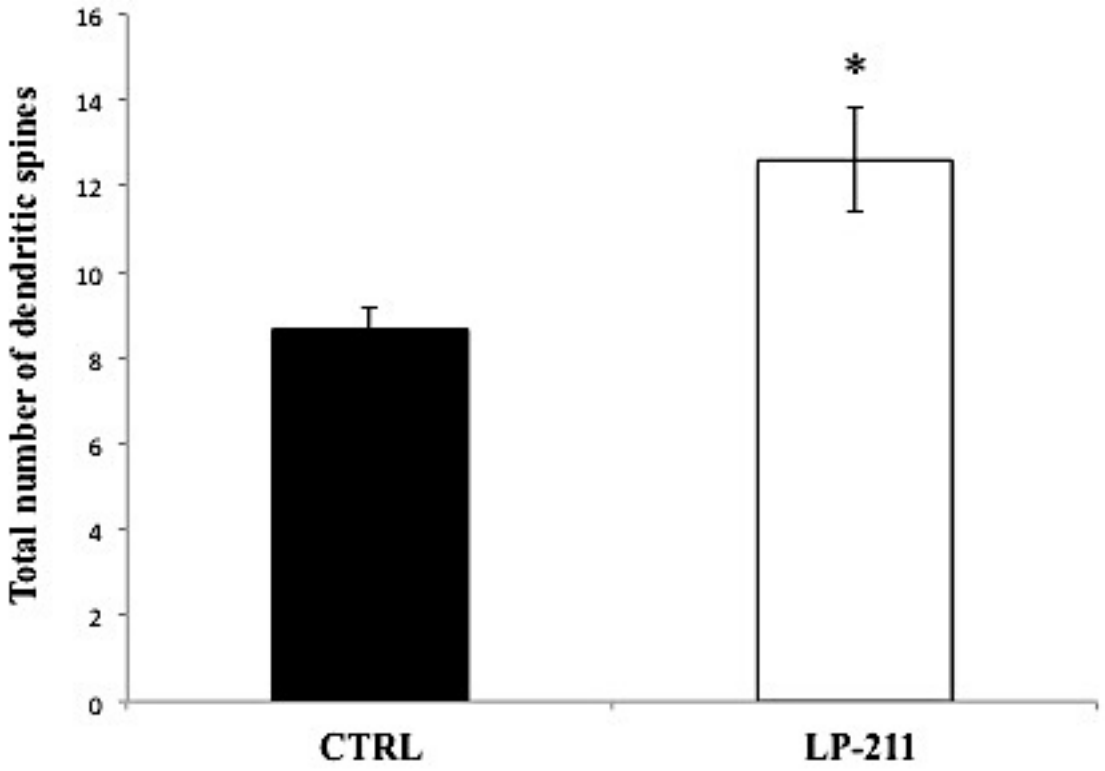

Figure 24. Agonist-stimulation of the 5-HT7 receptor *in vivo* affects dendritic spine morphology in CNS neurons.
The graph represents the number of dendritic spines in neurons of the dorsolateral striatum after treatment of mice with DMSO (CTRL) or with LP-211.
* Significantly different from CTRL by Student's t-test ($p < 0.05$).

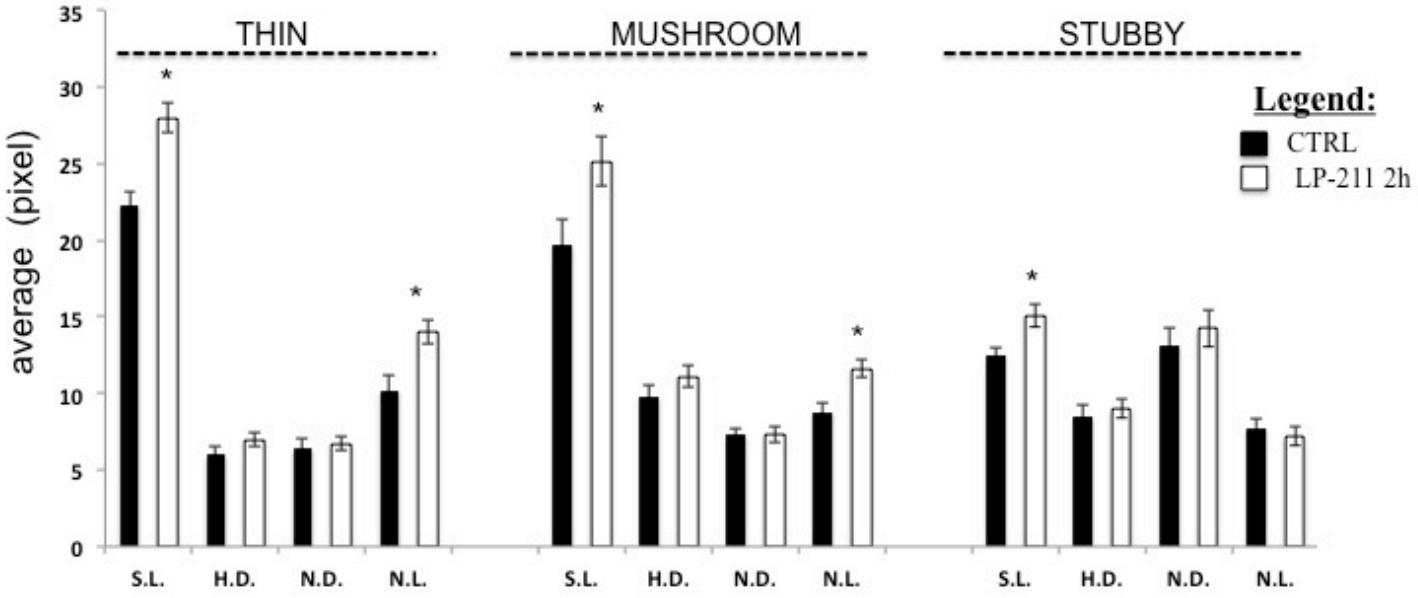

Figure 25. Morphogenic effects of LP-211 on dorsolateral striatal neurons.
The bar plots represent the average pixel of morphological parameters (S.L.= spine length, H.D. = head diameter, N-D. = neck diameter, N.L= neck length) for thin, mushroom and stubby spines after DMSO (CTRL) or LP-211 treatment *in vivo*.
* Significantly different from CTRL by Student's t-test ($p < 0.05$).

4.8 Stimulation of 5-HT7 receptor on neurons from animal models of a neurodevelopmental disease

Abnormalities in dendritic spines appears to be a common feature of many disorders characterized by mental disability during development. Dendritic pathology has been seen in human subjects with mental retardation, autism and Rett syndrome (RTT; Chang et al., 2013; Della Sala and Pizzorusso, 2013) and in animal models of X fragile mental retardation, Down syndrome and RTT (Belichenko et al 2009; Belichenko et al 2007; Kurt et al 2000).

Rett Syndrome (MIM 312750) is a severe form of X-linked neurodevelopmental disorder caused by mutations in the gene coding for the transcription regulator methyl CpG-binding protein 2 (MECP2, Amir, 1999).

Given the promising results obtained on the efficacy of the 5-HT7R activation to modulate the neuronal morphology, we used agonist stimulation treatment to contrast morphological alterations observed in CNS neurons of RTT mice. To this aim, in collaboration with the laboratory directed by Dr. M. D'Esposito (IGB, CNR), we tested the effect of 5-HT7 receptor agonist, LP-211, in neuronal primary cultures established from the cortex of wild type and Mecp2 null mouse (Mecp2-/y) embryos.

Confocal microscopy coupled to the use of selected immunofluorescent antibodies show that cultured neurons did not exhibit difference in the number of Tuj1, GAD2 or 5-HT7 receptor immunopositive cells (>90%, 85% and 80% respectively) between WT and Mecp2 null cultures (Figure 26).

A

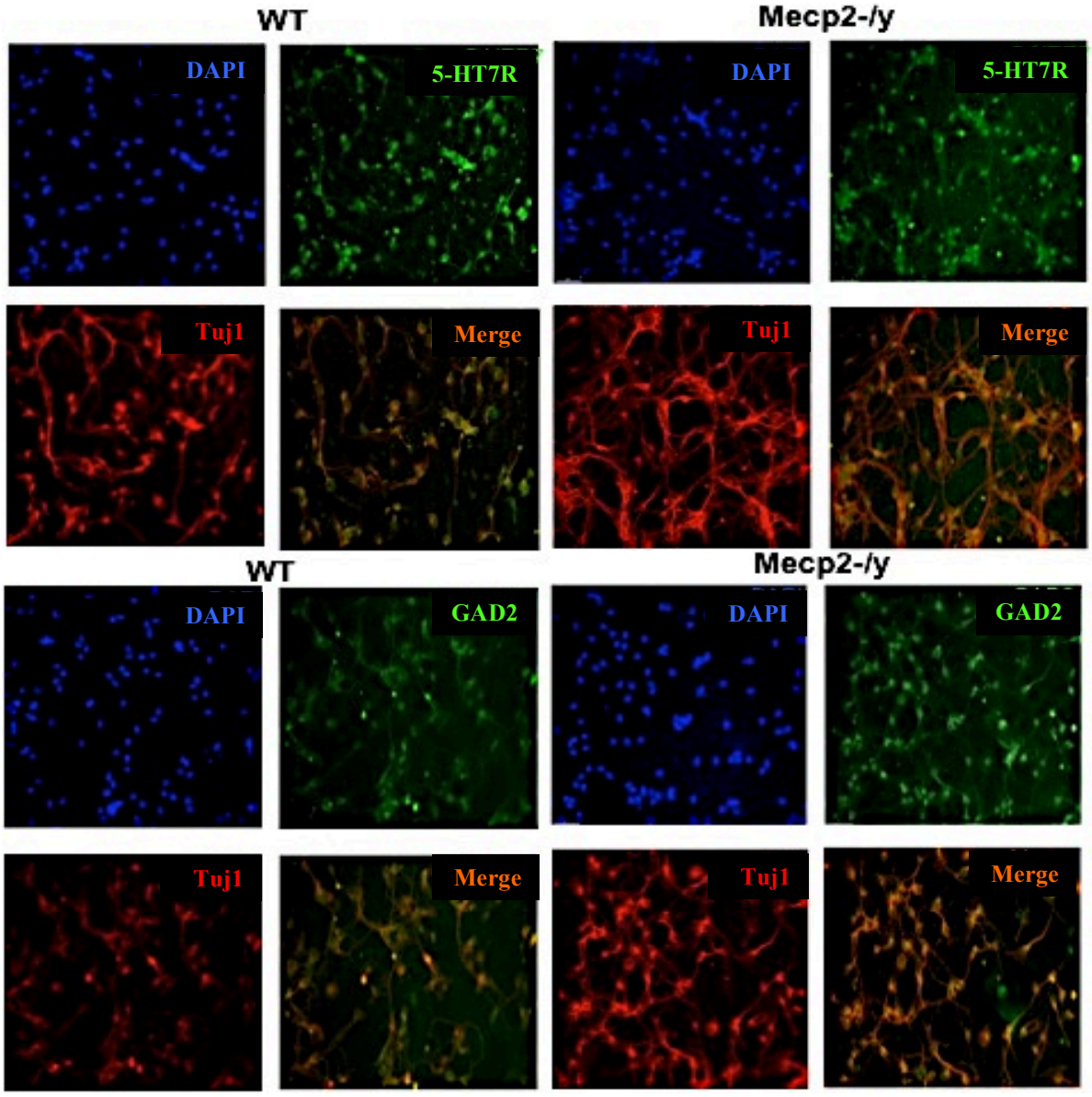
WT
Mecp2-/y
DAPI
5-HT7R
Tuj1
Merge
WT
Mecp2-/y
DAPI
GAD2
Tuj1
Merge

B

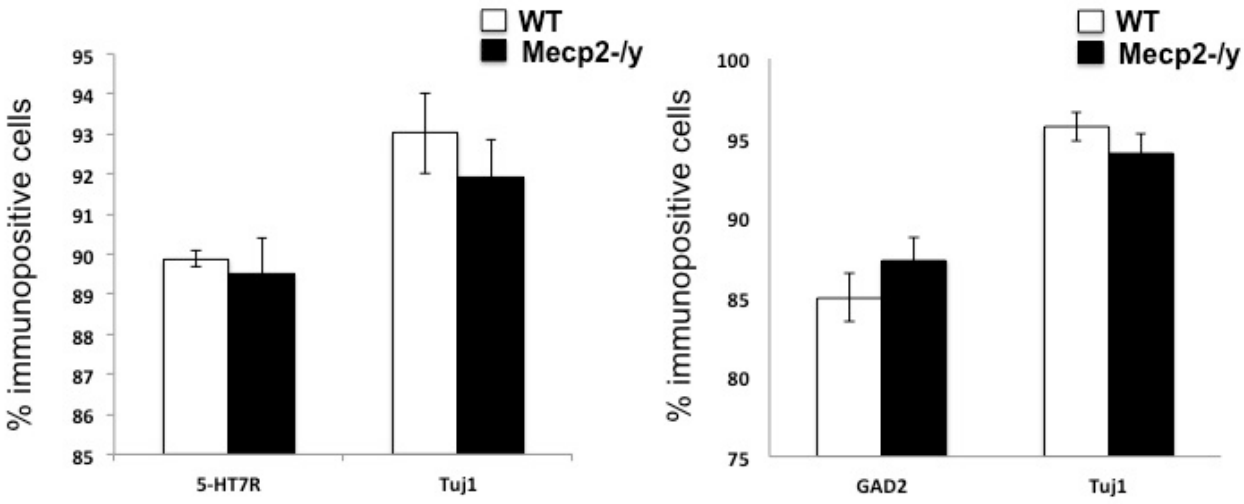
WT
Mecp2-/y
% immunopositive cells
95
94
93
92
91
90
89
88
87
86
85
5-HT7R
Tuj1
WT
Mecp2-/y
% immunopositive cells
100
95
90
85
80
75
GAD2
Tuj1

Figure 26. Characterization of cortical primary cultures from WT and Mecp2-/y E15 embryos (*previous page*).
(A) Cortical neurons were immunostained with specific antibodies against the neuronal marker Tuj1 (red), 5-HT7 receptor (green) or the GABAergic marker GAD2 (green). (B) The bar plots represent the percentage of cells immunopositive for the nuclear marker DAPI and for the indicated antibodies. The number of immunopositive cells did not show statistical differences between WT and Mecp2-/y cultures (means±SEM, n=100; Student t-test).

Exposure of cortical cultures to LP-211 resulted in significant increase of neurite length when compared to vehicle-treated cultures (CTRL, +130%). The agonist-stimulated enhancement of neurite outgrowth was similar in WT and Mecp2 null neurons. The effect was specifically due to 5-HT7 receptor stimulation, because co-treatment of the cells with LP-211 and SB-269970, the selective 5-HT7 receptor antagonist, completely abolished neurite elongation, while addition of the antagonist alone had no. Several other parameters, such as the number of primary neurites, as well as the soma perimeter and the total area of each neuron, were not affected by agonist treatment. Morphometrical analyses indicated that the length of neurites, in basal condition, did not differ between WT and Mecp2 null neuronal cultures. On the contrary, primary branching was significantly lower in Mecp2 null neurons compared to WT control (Figure 27A, compare upper and lower panels). Interestingly, treatment with LP-211 for 2 hours strongly increased branching in Mecp2 null neurons, while did not significantly affect WT cultures (Figure 27). Consequently, 5-HT7 receptor stimulation of cortical cultures did rescue the reduced branching of Mecp2 null neurons. The enhancement of both neurite outgrowth and branching was specifically due to 5-HT7 receptor stimulation, because co-treatment with LP-211 and SB-269970 abolished the morphological effects of the agonist, while the antagonist alone had no effect.

A

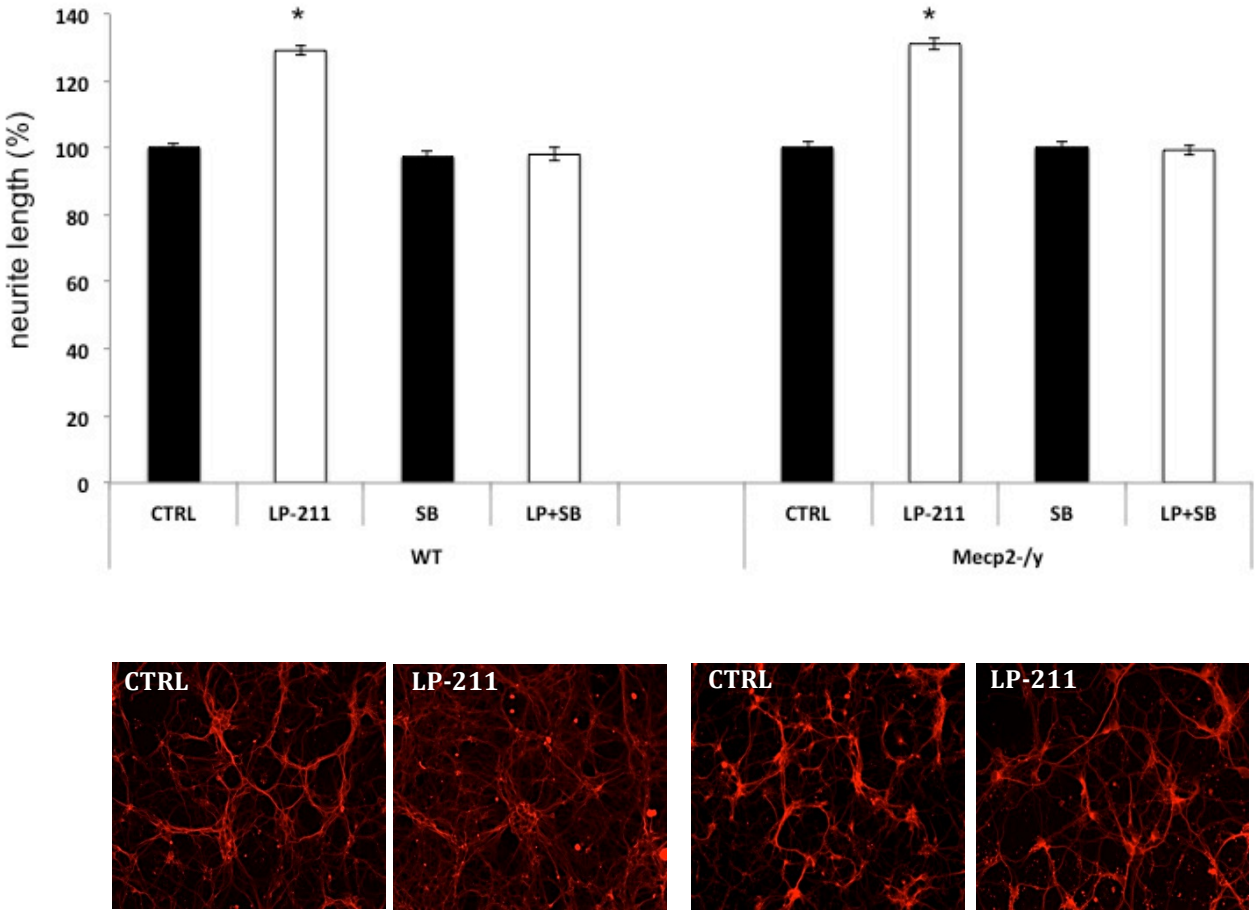
neurite length (%)
140
120
100
80
60
40
20
0
*
*
CTRL
LP-211
SB
LP+SB
WT
CTRL
LP-211
SB
LP+SB
Mecp2-/y
CTRL
LP-211
CTRL
LP-211

B

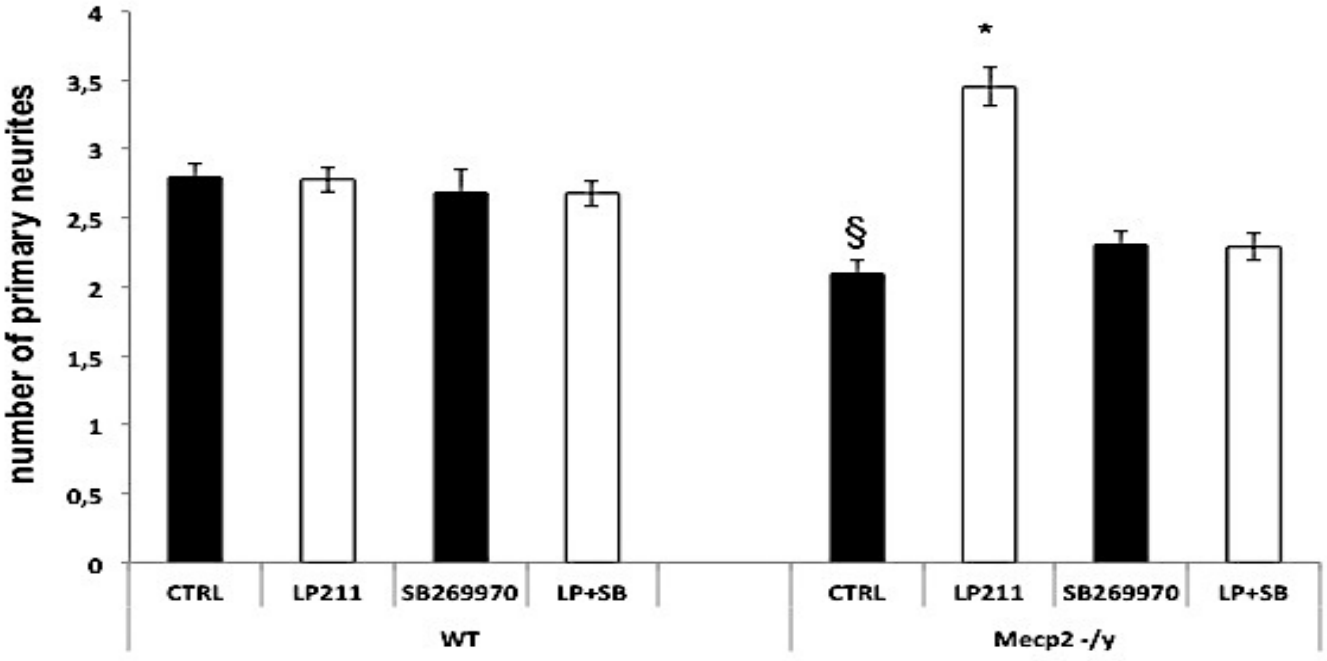
number of primary neurites
4
3,5
3
2,5
2
1,5
1
0,5
0
*
§
CTRL
LP211
SB269970
LP+SB
WT
CTRL
LP211
SB269970
LP+SB
Mecp2 -/y

Figure 27. (*Previous* page) LP-211 stimulates neurite outgrowth in cortical neurons from WT and Mecp2-/y embryos and rescues altered neurite branching in Mecp2 null neurons. Neuronal primary cultures were treated for 2 h with vehicle (CTRL) or with the 5-HT7 receptor selective agonist LP-211 (LP, 100 nM), alone or in combination with the selective 5-HT7R antagonist SB269970 (100 nM). (A) Neurite length was measured on cells stained with anti-Tuj1 antibody (ImageJ software). (B) Branching was evaluated by Sholl analysis. The bars represent means ± SEM from randomly selected fields for each cell culture condition (n=8). * $p<0,05$ LP-211-treated neurons versus genotype-matched CTRL, § $p<0,05$ LP-211 null treated neurons versus WT CTRL, Student's t-test.

4.9 Stimulation of endogenous 5-HT7 receptor partially rescues molecular alterations in embryonic cortical cultures from Mecp2 null mice.

To gain insights on how Mecp2 deficiency could affect embryonic neurons at a molecular level, and how LP-211 treatment may drive morphological changes, we used RNA-sequencing (RNA-seq) technology (Morozova et al., 2009) to sequence, map, and quantify the entire population of transcripts in cortical primary cultures.

Functional bioinformatics analyses on the rough RNA-seq data are still in progress.

RNA sequencing was performed in parallel to morphological analyses on 12 samples: each sample was a pool of RNAs derived from 3 independent neuronal cultures. Three pools had a WT genotype and three other were from Mecp2-/y. Each of the three replicates was treated with LP-211 or with vehicle (DMSO).

Sequencing data (short reads) have been filtered, based on their base call and mapping quality. All differentially expressed genes have been analyzed between the two different genotypes (null vs. WT), both under treatment or in vehicle-treated condition. As a first preliminary observation, we obtained a dataset of 491 DE genes that are possibly regulated directly or indirectly by MeCP2 at E15 developmental stage in cortical neurons, as they were DE in null vs. WT, prior of any treatment. Among these genes, 80% were up-regulated. Enriched GO (gene ontology) terms were identified in the whole group of the DE genes. Upon LP-211 treatment the null neurons differed from WT ones in 466 transcripts, with 357 genes in common to dataset of untreated null vs. WT. Thus, there are 357 genes that are not influenced by agonist treatment and 192 genes that respond to LP-211. Interestingly, among these unique genes, 134 genes resulted deregulated in the null and recovered a level of physiological expression as consequence of LP-211 administration (Figure 28A).

DAVID (**D**atabase for **A**nnotation, **V**isualization and **I**ntegrated **D**iscovery v6.7) analysis for functional annotation chart and classification clustering was then applied to the list of 134 genes rescued (Figure 27B). Clusters with the higher enrichment score were preferentially selected also because they were made of subset of genes involved in regulation of neurogenesis, or functionally related to regulation of cytoskeleton, intracellular signal transduction, receptor mediated pathways, based on cues from GO and KEGG (*Kyoto Encyclopedia of Genes and Genomes*) pathways analysis.

Ongoing experiments will validate by Real-time PCR the most interesting transcripts deregulated in cortical neurons of Mecp2 null mice, and rescued by LP-211 treatment.

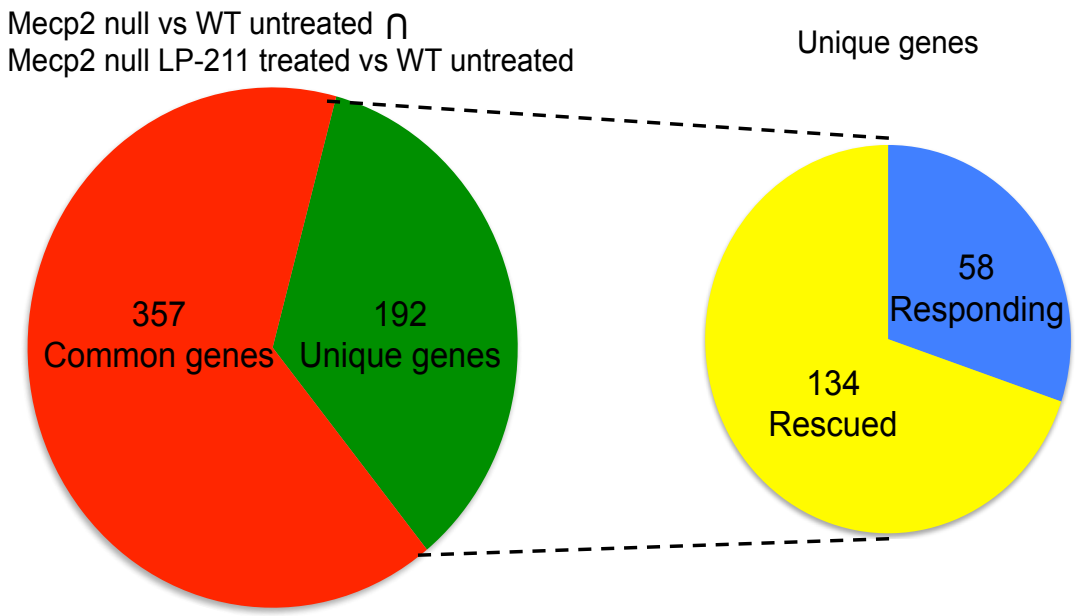

Figure 28. Representative RNA-seq dataset of cortical primary cultures from WT and Mecp-/y E15 embryos upon LP-211 treatment. Neuronal primary cultures were treated with vehicle or with the 5-HT7R selective agonist LP-211. Total RNA was extracted, sequenced and differentially expression analysis was conducted at gene level. The intersection of differentially expressed (DE) genes in untreated Mecp2 null neurons (compared to WT) with the DE genes in LP-211 treated Mecp2 null neurons (compared to WT) show 357 shared genes and 192 unique genes. The first group includes the genes not influenced by the agonist. On the contrary, 192 genes respond to LP-211 and 134 genes of them, which were deregulated in Mecp2 null neurons, rescue a level of physiological expression as a consequence of LP-211 administration.

All together these data show that stimulation of endogenous 5-HT7R selectively affects neurite elongation in embryonic cortical cultures from WT and RTT animal models, and rescues deficits of neurite branching observed in cortical cultures from Mecp2 null mice. These changes appear to be sustained by deep modifications of the transcriptome. In addition these results suggest that alteration of neuronal branching and gene expression can be observed in RTT animal models already at early embryonic stage.

5. SUMMARY RESULTS

In summary, the experimental results obtained during my PhD show that:

1) The stimulation of 5-HT7 receptor with agonists (8-OH-DPAT and LP-211), significantly promotes the neurite outgrowth in neuronal cultures obtained from cortex, hippocampus and striatal complex of rodents during embryonic development and in early postnatal period. The 5-HT7 receptor-induced neurite outgrowth requires ERK phosphorylation and Cdk5 activation.
2) The neurite outgrowth stimulated by 5-HT7 receptor requires *de novo* protein synthesis and qualitative and quantitative changes in some selected neuronal cytoskeletal proteins and some regulator of actin polymerization (MAP1B, cofilin).
3) The stimulation of 5-HT7 receptor with the selective agonist LP-211 promotes the axonal growth in embryonic hippocampal cultures.
4) *In vivo* treatment of one month-old mice with LP-211 modulates the morphology and density of dendritic spines, in dorsolateral striatum.
5) The stimulation of 5-HT7 receptor selectively affects neurite elongation in embryonic cortical cultures from WT and RTT animal models, and rescues deficit of neurite branching observed in cortical cultures from Mecp2 null mice.
6) The 5-HT7R-induced morphological changes in cortical cultures of Mecp2 null mice appear to be sustained by deep modifications of the transcriptome. Preliminary RNA-seq analyses reveals 134 genes which were deregulated in Mecp2 null neurons compared to WT and were rescued to a physiological expression level following LP-211 administration.

All together, these data show that the 5-HT7 receptor has an important role during embryonic development in shaping the morphology of various classes of telencephalic neurons, pinpointing key signaling transduction pathways and cytoskeletal proteins involved.
In addition, preliminary results show that stimulation of 5-HT7 receptor modulates dendritic spine morphology in the CNS of living animals, and partially rescues morphological alterations of cultured CNS neurons obtained from animal models of Rett syndrome, a severe form of mental retardation.

6. DISCUSSION AND CONCLUSIONS

During development, neuronal precursors differentiate, migrate, extend long processes, and finally establish connections with their targets. Over the past years, the initial steps of neurite formation have been widely studied using primarily *in vitro* approaches such as dissociated culture of rodent CNS neurons. Using these models important progress has been made towards the identification of the physiological signals and molecular mechanisms regulating neurite outgrowth (Arimura and Kaibuchi, 2007; Calabrese, 2008). Along this line, our data show that the endogenous 5-HT7R strongly stimulates neurite elongation in cultured embryonic neurons from rodent striatal complex and cortex. A selective role of the 5-HT7R in promoting neurite outgrowth was confirmed by specific agonists and by the inhibition of the effects in presence of a selective 5-HT7R antagonist (SB-269970; Hagan et al., 2000). Moreover, we could exclude the involvement of 5-HT1A receptor, since its selective antagonist (WAY-100635; Corradetti et al., 1998) did not alter agonists-induced neurite elongation. Other parameters, such as the number of primary neurites, as well as the soma perimeter and the total area of each neuron, were not affected by agonist treatment, in accordance with the hypothesis that mechanisms underlying neurite length determination are different than those controlling other morphological aspects (Shelly et al., 2010).

The stimulation of neurite outgrowth was achieved using the commonly used promiscuous agonist 8-OH-DPAT and the novel and highly potent selective agonist, LP-211 (Hedlund et al., 2010). Interestingly the effect of LP-211 on neurite outgrowth was more persistent than that of 8-OH-DPAT, but required more time (2 h) to be evident. This difference could be due to the action of the two agonists on different sites of the receptor, which in turn could activate the same signal transduction pathways (see below) with a different kinetic.

A role for the 5-HT7R in the regulation of neuronal morphology is consistent with previous results obtained in mouse hippocampal neurons *in vitro* (Kvachnina et al., 2005), and extends our preliminary observations on rat striatal cultures (Leo et al., 2009). All together, these results demonstrate that this receptor plays a key role in stimulating neurite outgrowth from different neurons *in vitro* and suggest its involvement in CNS connectivity. Indeed, a prominent role for the 5-HT7R in the morphological and functional maturation of hippocampal circuits is supported by recent data by Kobe and coworkers. These authors show that the activation of 5-HT7R stimulates formation of dendritic spines and neuronal excitability in organotypic preparations from the hippocampus of juvenile mice, while in preparations from older mice where the expression of the receptor was down-regulated, the effect was not present (Kobe et al., 2012). Therefore it is possible that critical developmental stages for the modulation of neuronal circuits depend from the variable

expression and activation of 5-HT7R. In addition, psychostimulant administration to adolescent rats triggered a strong and persistent up-regulation of the 5-HT7R in discrete regions of the reward circuits, which paralleled with structural modifications of synaptic contacts and alterations of impulsive behavior, as we showed in previous experiments. In these animals, 5-HT7R modulation caused alterations of reward-based behavior (Cavaliere et al., 2011; Leo et al., 2009).

Our new findings that ERK phosphorylation is required for 5-HT7R-dependent neurite elongation are consistent with the knowledge that 5-HT7R can be functionally coupled to G_s or Gα-12 G-proteins, which in turn can activate ERK (Errico et al., 2001; Kvachnina et al., 2005; Lin et al., 2003). It is likely that the activation of the Gα-12 subunit is involved in ERK-dependent neurite outgrowth also in our cultures, since in hippocampal neurons from Gα-12-deficient mice the 5-HT7R-mediated effects do not occur (Kobe et al., 2012). It is noteworthy that neurite elongation mirrored the time course of ERK phosphorylation stimulated by either 8-OH-DPAT or LP-211.

With this work we also unravel the essential role of Cdk5 activity in 5-HT7R-dependent neurite elongation in CNS primary cultures, supporting literature data on Cdk5 involvement in neurite outgrowth and remodeling (Nikolic et al., 1996; Zhang et al., 2010). To this aim, we used roscovitine, a potent inhibitor of CDKs with limited selectivity between the CDK5 and CDK2 (Otyepka et al., 2006). However, in our cultures consisting of fully differentiated neurons, roscovitine can be considered a selective inhibitor of Cdk5 (Kim and Ryan, 2010). In addition, we observed that Cdk5 transcripts were approximately 4 fold more abundant than Cdk2 transcripts. Indeed, this kinase, differently from other known cyclin-dependent family members, is active in non proliferating cells and is highly expressed in differentiated neurons, where it can phosphorylate various proteins of the neuronal cytoskeleton. Cdk5 plays important roles in various aspects of neural development including neuronal migration, axon guidance and regeneration, synapse development, and plasticity (Cheung and Ip, 2007; Lai and Ip, 2009). Its activity is dependent upon association with the p35 cofactor. Interestingly, mice with dysregulation of Cdk5/p35 activity during development display improperly established meso-cortico-limbic circuitry and a locomotor profile and pharmacological responses reminiscent of ADHD (Drerup et al., 2010), a well known developmental disease associated to altered connectivity of neural circuits (Liston et al., 2011). The involvement of altered connectivity in ADHD has been supported by independent genome-wide association studies showing that top-ranked ADHD candidate genes, including ERK and MAP1B, encode proteins regulating neurite outgrowth (Poelmans et al., 2011).

As expected, 5-HT7R-dependent neurite elongation in CNS primary cultures was accompanied by qualitative and quantitative expression changes on selected components of the neuronal cytoskeleton (i.e. β -tubulin, vimentin, and selected neurofilaments and microtubule associated

proteins). In particular, the high level of heterogeneity of β -tubulin observed in untreated striatal neurons matched previous data reporting up to 21 isoelectric variants of this protein in the brain and in cultured neurons, mainly due to variable number of phosphates that cause variable shifts towards acidic pI (Edde et al., 1989). The absence of stretching of acidic tubulin spots in cultures treated with the 5-HT7R agonist suggests a marked reduction of phosphorylated isoforms. This observation confirms that neurite elongation requires changes in cytoskeleton function and dynamics, depending on post-translational modifications of key proteins (Fukushima et al., 2009). In addition, the down-regulation of the NFM main component and the up-regulation of MAP2 main isoform in stimulated cultures highlights a role of 5-HT7R in modulating the amount of proteins involved in neurite outgrowth. On the contrary, no relevant expression changes of spots corresponding to vimentin isoforms or to NFL were observed.

The most striking expression changes induced by 5-HT7R stimulation were observed for MAP1B, a protein essential to regulate microtubule dynamics, thus playing an important role in dendritic spine formation, synaptic maturation and axonal elongation (Black et al., 1994; Tortosa et al., 2011; Tymanskyi et al., 2012). MAP1B is present as a full-length protein, or may be fragmented into a heavy chain and a light chain, and its function is modulated by phosphorylation (Riederer, 2007). The high molecular weight isoforms (above 270 up to 380 kDa) identified in CTRL cultures completely disappeared in LP-211-treated cultures, whereas the 270 kDa form was slightly upregulated. Interestingly, stimulation of the 5-HT7R was able to selectively induce the appearance of a 34 kDa protein corresponding to the MAP1B light chain (34 kDa; Kuznetsov et al., 1986). This protein plays a key role in regulating the crosstalk between microtubules and actin microfilaments during neurite elongation (Togel et al., 1998). Therefore our findings strongly suggest that MAP1B light chain may act as an important effector in enhancing neurite outgrowth stimulated by 5-HT7R.

The up-regulation of MAPs in agonist-stimulated neurons is consistent with the finding that 5-HT7R-dependent neurite elongation requires *de novo* protein synthesis, and with their synergistic role in regulating the dynamics of the cytoskeleton in neuronal processes (Matus, 1991). The modulation of cytoskeleton dynamics requires modification of actin polymerization. Therefore, a key role is played by several actin filament assembly/disassembly regulators, such as cofilin.

My experiments indicate that the stimulation of striatal and cortical neurons with LP-211 is able to induce cofilin phosphorylation, a regulatory event recently showed to be important in the neuronal outgrowth phenomenon (Figge et al., 2012). The same authors showed also the interaction of phosphorylated cofilin with the neural cell adhesion molecule L1, suggesting a possible mechanism to explain its action (Figge et al., 2012). In particular, consistently with previous studies on neurite outgrowth elicited by NGF and laminin (Endo et al. 2007; Endo et al. 2003), it has been

demonstrated that both activation of cofilin by dephosphorylation and inactivation by phosphorylation are essential for L1-stimulated neurite outgrowth (Figge et al. 2012).

My data also indicate a difference in the response to LP-211 treatment of striatal and cortical cell cultures, mainly related to basal differences in the post-translational modification of specific proteins such as β-tubulin.

Interesting results were obtained from embryonic hippocampal cultures where we showed that selective stimulation of 5-HT7 receptor is able to modulate axonal growth (Park et a., 2006). Structural changes of neuronal morphology can help to predict functional variations in brain physiology and pathology. Activity-induced modification of neuronal connectivity is essential for the development of the nervous system and several brain pathologies, such as ADHD, autism and Rett syndrome, are associated with altered neuronal connectivity (Poelmans G. et al, 2011; Dani V.S. and Nelson S.B., 2009). From this point of view the second goal of my project aimed to verify if the administration of the 5-HT7R selective agonist *in vivo* may modulate the structure of nervous circuits and correct the altered connectivity often observed in neurodevelopmental diseases.

An interesting approach to study brain connectivity is to analyze the dendritic spines density, morphology and distribution. Dendritic spines are major sites of synaptic transmission in the central nervous system (Yuste and Bonhoeffer, 2004). Changes in their density and morphology occur during development, learning, aging and various types of mental disorders. The morphology of spines reflect their structure and function, thus the variety in their shape and size, suggests a high degree of functional diversity. Based on their morphology the spines are commonly classified into three types: thin, mushroom and stubby. Importantly, on the same dendrite a continuum of different shapes can be observed and the morphology of a spine can change rapidly through activity-dependent and independent mechanisms. New insights into dendritic spine structure and function, resulting from the use of imaging techniques, have significantly increased our knowledge of synaptic function, ranging from a better understanding of the molecular mechanisms of experience-dependent plasticity to the dendritic organization. Some of the recent technical advances, such as time-lapse microscopy and the use of fluorescent reporters in transgenic mouse lines, coupled with the two-photon (2P) laser scanning microscopy have recently allowed the detection of stimulus-induced changes in dendritic spines shape and number and has considerably contributed to deepen our knowledge about the connectivity of the CNS.

To reveal a possible relationship between 5-HT7 receptor activation and structural plasticity changes into the brain, I used the fluorescent reporter DiI coupled with laser scanning microscopy, to analyze the stimulus-induced changes in spines shape and number. Following intraperitoneal administration of LP-211 to 30-days old mice, I found an increased spine length and density, in

dorsolateral striatum of adult mice. These data show that the activation of the 5-HT7 receptor by selective brain-permeant agonists can affect the morphology of synaptic contacts in the adult brain, and thus could correct the altered connectivity often observed in neurodevelopmental diseases.
We thus performed preliminary experiments by using an animal model of the Rett syndrome, it is an autism spectrum disorder caused by mutation in the X-linked MECP2 gene.
Our results show that in RTT animal models the stimulation of endogenous 5-HT7R selectively affects neurite elongation in embryonic cortical cultures and rescues deficits of neurite branching. These changes appear to be sustained by deep modifications of the transcriptome. In addition these results suggest that alteration of neuronal branching and gene expression can be observed in RTT animal models already at early embryonic stage.
These results are consistent with recent studies, showing a clear link between activation of 5-HT7R and modulation of hippocampal synaptic plasticity both in WT as well as in X- fragile syndrome mouse models (Costa et al., 2012). These data suggest that the 5-HT7R may modulate the functional properties of synapses and neuronal networks, both in physiological and pathological conditions.

In summary, my results show that agonist-dependent activation of the endogenous 5-HT7R in CNS neuronal primary cultures stimulates ERK- and Cdk5-dependent neurite outgrowth, sustained by *de novo* protein synthesis and modifications of cytoskeletal proteins (Speranza et al., 2013) indicating that 5-HT7R may exert a crucial role in the regulation of neuronal morphology and in the structural organization of behaviorally relevant brain circuits during the early phases of development. These results were confirmed by the *in vivo* treatment on adult mice with LP-211, indicating that the agonist -dependent stimulation of the 5-HT7 receptor modulates the neuronal connectivity inducing changes both in the morphology of dendritic spines.
In line with this data, experiments performed using animal model of Rett syndrome, show that the stimulation of cortical neurons from WT and Mecp2-/y mice, induces neurite growth and rescues the observed branching defects in KO mice.
Taken together, the results of my project highlight the key role played by 5-HT7R in the regulation of neuronal cytoarchitecture and may provide insights for innovative pharmacological treatments of neurodevelopmental disorders characterized by altered brain connectivity.

7. REFERENCES

Abbass A., HedlundPB., Huang XP., Tran TB., Meltzer HY., Roth BL. (2009) Amisulpride is a potent 5-HT7 antagonist: relevance for antidepressant actions *in vivo*. Psychopharm. 1:119-28.

Abramowski D., Staufenbiel M.(1995) Identification of the 5-hydroxytryptamine2C receptor as a 60-KDa N-glycosilated protein in choroid plexus and hippocampus. J Neurochem 65: 782-790.

Agnew BJ., Minamide LS., Bamburg JR. (1995) Reactivation of phosphorylated actin depolymerizing factor and identification of the regulatory site. J Biol Chem; 270:17582-17587.

Amir R.E., Van de Veyver I.B., Wan B., Tran C. Q., Francke U., Zoghbi H.Y. (1999) Rett syndrome is caused by mutations in X-linked MECP2, encoding methyl-CpG-binding protein 2. Nature America Inc. 23(2):185-8

Arimura N., Kaibuchi K. (2007) Neuronal polarity: from extracellular signals to intracellular mechanisms. Nat. Rev. Neurosci. 8, 194-205.

Azmitia E.C., and Whitaker-Azmitia P.M. (1997). Mutations causing syndromic autism define an axis of synaptic pathophysiology. Nature 480, 63-68.

Auer P.L. and Doerge R.W. (2010) Statistical design and analysis of RNA sequencing data. Genetics 185: 405-416.

Azmitia E.C. and Nixon R. (2008) Dystrophic serotonergic axons in neurodegenerative diseases. Brain Res. 1217, 185-194.

Backstrom JR., Price RD., Reasoner DT., Sanders-Bush E. (2000) Deletion of the serotonin 5-HT_{2C} receptor PDZ recognition motif prevents receptor phosphorylation and delays resensitization of receptor responses. J Biol Chem 275: 23620-23626.

Bard J.A., et al. (1993) Cloning of a novel human serotonin receptor (5-HT7) positively linked to

adenylate cyclase. J. Biol. Chem. 268, 23422-23426.

Barnes N.M., Sharp T. (1999) A review of central 5-HT receptors and their function. Neuropharmacol. 38, 1083-1152.

Beattie DT., Smith JA., Marquess D., Shaw JP., Vickery RG., Humphrey PP. (2008) The *in vitro* pharmacological profile of TD-5108, a selective 5-HT(4) receptor agonist with high agonist with intrinsic activity. Naunyn-Schmiedeberg's Archives of Pharmacology, Vol 378, issue1, pp 125-137

Belenky M.A., and Pickard G.E. (2001) Subcellular distribution of 5-HT1b and 5-HT7 receptors in the mouse suprachiasmatic nucleus. J. Comp. Neurol, 432, 371-388.

Benninghoff J et al (2012) The complex role of the serotonin transporter in adult neurogenesis and neuroplasticity. A critical review. World J Biol Psychiatry: Off J World Fed Soc Biol Psychiatry 13(4):240-247.

Bertulat B., De Bonis M.L., Della Ragione F., Lehmukuhl A., Milden Manuela, Storm C., Jost K.L., Scala S., Hendrich B., D'Esposito M., Cardoso M.C. (2012) MeCP2 dependent heterochromatin reorganization during neural differentiation of a novel Mecp2-deficient embryonic stem cell reporter line. PLOS ONE, Vol7, issue 10, e47848.

Bickmeyer U., et al (2002) Differential modulation of I_h by 5-HT receptors in mouse CA1 hippocampal neurons. Eur. J. Neurosci. 16, 209-218.

Black M.M., Slaughter T., Fischer I. (1994). Microtubule-associated protein 1b (MAP1b) is concentrated in the distal region of growing axons. J. Neurosci. 14, 857-870.

Blakemore SJ. (2008) The social brain in adolescence. Neuroscience 9:268.

Bonaventure P., et al. (2002) Reconsideration of 5-hydroxytryptamine (5-HT)(7) receptor distribution using [(3)H]5-carboxamidotryptamine and [(3)H]8-hydroxy-2-(di-n-propylamino)tetraline:analysis in brain of 5-HT(1A) knockout and 5- HT(1A/1B) double-knockout mice. J. Pharmacol. Exp. Ther. 302, 240-248.

Bonaventure P., Nepomuceno D., Hein L., Sutcliffe Jg., Lovenberg T., Hedlund PB. (2004) Radioligand binding analysis of knockout mice reveals 5-hydroxytryptamine (7) receptor distribution and uncovers 8-hydroxy-2-(di-n-propylamino)tetralin interaction with α_2-adrenergic receptors. Neuroscience 124:901-911.

Bonaventure P., Kelly L., Aluisio L., Shelton J., Lord B., Galici R., Miller K., Atack J., Lovenberg T.W., Dugovic C. (2007) Selective blockade of 5-hydroxytryptamine (5-HT)7 receptors enhances 5-HT transmission, antidepressant-like behavior, and rapid eye movement sleep suppression induced by citalopram in rodents. J. Pharmacol. Exp. Ther. 321, 690-698.

Buchser W.J., Slepak T.I., Gutierrez-Arenas O., Bixby,J.L., Lemmon V.P. (2010) Kinase/phosphatase overexpression reveals pathways regulating hippocampal neuron morphology. Mol. Syst. Biol. 6, 391.

Bulenger S., Marullo S., Bouvier M. (2005) Emerging role of homo- and heterodimerization in G-protein-coupled receptor biosynthesis and maturation. Trends Pharmacol Sci 26: 131-137.

Calabrese E.J. (2008) Enhancing and regulating neurite outgrowth. Crit. Rev. Toxicol. 38, 391-418.

Calizo L.H., Akanwa A., Ma X., Pan Y.Z., Lemos J.C., Craige C., Heemstra L.A., and Beck S.G. (2011) Raphe serotonin neurons are not homogenous:electrophysiological, morphological and neurochemical evidence. Neuropharmacology 61, 524-543.

Cavaliere C., Cirillo G., Bianco M.R., Adriani W., De Simone A., Leo D., Perrone-Capano C., Papa M. (2012) Methylphenidate administration determines enduring changes in neuroglial network in rats. Eur. Neuropsychopharmacol. 22, 53-63.

Chen JJ. et al (2001) Maintenance of serotonin in the intestinal mucosa and ganglia of mice that lack the high-affinity serotoni transporter: abnormal intestinal motility and the expression of cation transporter. J. Neurosci 21(16):b 6348-6361.

Cheung Z.H., Ip N.Y. (2007) The roles of cyclin-dependent kinase 5 in dendrite and synapse development. Biotechnol. J. 2, 949-957.

Cifariello A., Pompili, A., Gasbarri, A., (2008) 5-HT(7) receptors in the modulation of cognitive processes. Behav. Brain Res. 195, 171-179.

Colucci-D'Amato, G.L., Perrone Capano C., di Porzio U. (2003) Chronic activation of ERK and neurodegenerative diseases. BioEssays 25, 1085-1095.

Contesse V., Lefebvre H., Lenglet S., Kuhn JM., Delarue C., Vaudry H. (2000) Role of 5-HT in the regulation of the brain-pituitary- adrenal axis: effects of 5-HT on adrenocortical cells. Can J Physiol Pharmacol 78(12):967–983

Cooper JA. (1987) Effects of cytochalasin and phalloidin on actin. J. Cell. Biol. Vol. 105, p.1473-1478.

Corradetti R., Laaris N., Hanoun N., Laporte AM., Le Poul E., Hamon M., Lanfumey L. (1998) Antagonist properties of (-)-pindolol and WAY 100635 at somatodendritic and postsynaptic 5-HT1A receptors in the rat brain. Br J Pharmacol Feb;123(3):449-62.

Coss RG, Perkel DH. (1985) The function of dendritic spines: areview of theoretical issues. Behav Neural Biol.; 44:151-185.

Costa L., Spatuzza M., D'Antoni S., Bonaccorso CM., Trovato C., Sebastiano A., Musumeci A., Leopoldo M., Lacivita E., Catania MV., Ciranna L. (2012) Activation of 5-HT7 serotonin receptors reverses metabotropic glutamate receptor-mediated synaptic plasticity in Wild-Type and Fmr1 Knockout mice, a model of Fragile X syndrome. Biol Psychiatry 72:924-933.

Dalva M.B., McClelland A.C., and Kayser M.S. (2007) Cell adhesion molecules: signalling functions at the synapse. Nat. Rev. Neurosci. 8, 206-220.

Daubert E.A. and Condron B.G., (2010) Serotonin: a regulator of neuronal morphology and circuitry. Trends in Neurosciences, Vol.33 N°9.

Dani VS. and Nelson SB. (2009) Intact LTP but reduced connectivity between neocortical Layer 5 pyramidal neurons in a mouse model of Rett Syndrome. J. Neurosci 29(36): 11263-11270.

De Martelaere K., Lintermans B., Haegeman G., Vanhoenacker P. (2007) Novel interaction between the human 5-HT7 receptor isoforms and PLAC-24/eiF3k. Cell Signal 19 (2):278–288.

Devi LA.(2001) Heterodimerization of G-protein-coupled receptors: pharmacology, signaling and trafficking. Trends Pharmacol Sci 22, 532-537.

di Porzio U., Daguet M.C., Glowinski J., Prochiantz A., (1980) Effect of striatal cells on in vitro maturation of mesencephalic DA neurons grown in serum-free conditions. Nature 288, 370-373.

Dos Remedios CG., Chhabra D., Kekic M., Dedova IV., Tsubakihara M., Berry DA., Nosworthy NJ.; (2003) Actin binding proteins: regulation of cytoskeletal microfilaments. Physiol Rev; 83:433-473.

Drerup J.M., Hayashi K., Cui H., Mettlach G.L., Long M.A., Marvin M., Sun X., Goldberg M.S., Lutter M., Bibb J.A. (2010) Attention-deficit/hyperactivity phenotype in mice lacking the cyclin-dependent kinase 5 cofactor p35. Biol. Psychiatry 68, 1163-1171.

Dutton AC., Massoura AN., Dover TJ., Andrews NA., Barnes NM. (2008) Identification and functional significance of N-glycosylation of the 5-ht_{5A} receptor. Neurochem Int 52: 419-425.

Edde B., Denoulet P., de Nechaud B., Koulakoff A., Berwald-Netter Y., Gros F. (1989) Posttranslational modifications of tubulin in cultured mouse brain neurons and astroglia. Biol. Cell. 65, 109-117.

Endo M., Ohashi K., Sasaki Y., Goshima Y., Niwa R., Uemura T., Mizuno K. (2003). Control of growth cone motility and morpholgy by LIM kinase and slingshot via phosphorylation and dephosphorylation of cofilin. J. Neurosci.23, 2527-2537.

Endo M., Ohashi K, Mizuno K. (2007). LIM kinase and slingshot are critical for neurite extension. J. Biol. Chem., 282, 13692-13702.

Erickson JD., et al (1996) Distinct pharmacological properties and distribution in neurons and endocrine cells of two isoforms of the human vesicular monoamine transporter. Proc Natl Acad Sci 93(10):5166-5171.

Eriksson, T.M., Golkar, A., Ekström, J.C., Svenningsson, P., Ogren, S.O. (2008) 5-HT7 receptor stimulation by 8-OH-DPAT counteracts the impairing effect of 5-HT(1A) receptor stimulation on contextual learning in mice. Eur. J. Pharmacol. 596, 107-110.

Errico M., Crozier R.A., Plummer M.R., Cowen D.S. (2001) 5-HT(7) receptors activate the mitogen activated protein kinase extracellular signal related kinase in cultured rat hippocampal neurons. Neuroscience 102, 361-367.

Figge C., Loers G., Schachner M., Tilling T. (2012) Neurite outgrowth triggered by the cell adhesion molecule L1 requires activation and inactivation of the cytoskeletal protein cofilin. Molecular and Cellular Neuroscience 49, 196-204.

Filip M., Bader M. (2009) Overview on 5-HT receptors and their role in physiology and pathology of the central nervous system. Pharmacol Rep 61(5):761-777.

Fiszman ML:, Zuddas A., Masana MI., Barker JL., di Porzio U. (1991) Dopamine synthesis precedes dopamine uptake in embryonic rat mesencephalic neurons. J. Neurochem. 56, 392-399.

Franco R. (2009) G-protein-coupled receptor heteromers or how neurons can display differently flavoured patterns in response to the same neurontrasmitters. Br. J. Pharmacol. 158, 23-31.

Fukushima N., Furuta D., Hidaka Y., Moriyama R., Tsujiuchi T., (2009) Post-translational modifications of tubulin in the nervous system. J. Neurochem. 109, 683-693.

Fuller and Wong DT. (1990) Serotonin uptake and serotonin uptake inhibition. Ann N Y Acad Sci 600:68-80.wade

Gan WB., Grutzendler J., Wong WT., Wong RO., Lichtman JW. (2000) Multicolor “DiOlistic” labeling of the nervous system using lipophilic dye combinations. Neuron; 27: 219-225.

Gasbarri A., Cifariello A., Pompili A., Meneses A. (2008) Effect of 5-HT(7) antagonist SB-269970 in the modulation of working and reference memory in the rat. Behav. Brain Res. 195, 164-170.

Gaspar P. (2003) The neurodevelopmental role of serotonin: news from mouse molecular genetics. Nat. Rev. Neurosci. 4, 1002-1012.

Gellynck E., Laenen K., Andressen KW., Lintermans B., De Martelaere K., Matthys A., Levy FO., Haegeman G., Vanhoenacker P., Van Craenenbroeck K. (2008) Cloning, genomic organization and functionality of 5-HT(7) receptor splice variants from mouse brain. Gene 426(1–2):23–31.

Gellynck E., Andressen K.W., Lintermans B., Haegeman G., Levy F.O., Vanhoenacker P., Van Craenenbroeck K. (2012). Biochemical and pharmacological study of N-linked glycosylation of the human serotonin 5-HT$_{7(a)}$ receptor. FEBS journal 279.

Gellynck E., Heyninck K., Andressen KW., Haegeman G., Levy F.O., Vanhoenacker P., Craenenbroeck K.V. (2013) The serotonin 5-HT$_7$ receptors: two decades of research. Exp Brain Res 230(4):555-68

Geurts FJ., De Schutter E., Timmermans JP. (2002) Localization of 5-HT2A, 5-HT3, 5-HT5A and 5-HT7 receptor-like immunoreactivity in the rat cerebellum. J Chem Neusoanat 24:65-74.

Glass J.D., et al (2003) Midbrain raphe modulation of nonphotic circadian clock resetting and 5-HT release in the mammalian suprachiasmatic nucleus. J. Neurosci. 23, 7451-7460.

Graveleau C., et al. (2000) Presence of a 5-HT7 receptor positively coupled to adenylate cyclase activation in human granulosa-lutein cells. J. Clin. Endocrinol. Metab. 85, 1277-1286.

Guscott M., Bristow LJ., Hadingham K., Rosahl TW., Beer MS., Stanton JA., Bromidge F., Owens A.P., Huscroft I., Myers J., Rupniak NM:, Patel S., Whiting PJ., Hutson PH., Fone KC., Biello SM., Kulagowski JJ., McAllister G., (2005) Genetic knockout and pharmacological blockade studies of the 5-HT7 receptor suggest therapeutic potential in depression. Neuropharmacol. 48, 492-502.

Gustafson E.L., et al (1996) A receptor autoradiographic and in situ hybridization analysis of the distribution of the 5-HT7 receptor in rat brain. Br. J. Pharmacol. 117, 657-666.

Guthrie CR., Murray AT., Franklin AA., Hamblin MW. (2005) Differential agonist-mediated internalization of the human 5-hydroxytryptamine 7 receptor isoforms. J Pharmacol Exp Ther 313:1003-1010.

Hagan J.J., Price G.W., Jeffrey P., Deeks N.J., Stean T., Piper D., Smith M.I., Upton N., Medhurst A.D., Middlemiss D.N., Riley G.J., Lovell P.J., Bromidge S.M., Thomas D.R. (2000). Characterization of SB-269970-A, a selective 5-HT_7 receptor antagonist. Br.J.Pharmacol. 130, 539-548.

Hay-Schmidt A. (2000). The evolution of the serotonergic nervous system. Proc. Biol. Sci. 267, 1071-1079.

Hedlund P.B., Danielson P.E., Thomas E.A., Slanina K., Carson M.J., Sutcliffe J.G., (2003). No hypothermic response to serotonin in 5-HT7 receptor knockout mice. Proc. Natl. Acad. Sci. U S A. 100, 1375-1380.

Hedlund P.B., Kelly L., Mazur C., Lovenberg T., Sutcliffe J.G., Bonaventure P., (2004). 8-OH-DPAT acts on both 5-HT1A and 5-HT7 receptors to induce hypothermia in rodents. Eur. J. Pharmacol. 487, 125-132.

Hedlund P.B., Sutcliffe J.G., (2004). Functional, molecular and pharmacological advances in 5-HT7 receptor research. Trends Pharmacol. Sci. 25, 481-486.

Hedlund P.B., Huitron-Resendiz S., Henriksen S.J., Sutcliffe J.G., (2005). 5-HT7 receptor inhibition and inactivation induce antidepressantlike behavior and sleep pattern. Biol. Psychiatry. 58, 831-837.

Hedlund P.B. (2009). The 5-HT7 receptor and disorders of the nervous system: an overview. Psychopharmacol.(Berl). 206, 345-354.

Hedlund P.B., Leopoldo M., Caccia S., Sarkisyan G., Fracasso C., Martelli G., Lacivita E., Berardi F., Perrone R., (2010). LP-211 is a brain penetrant selective agonist for the serotonin 5-HT(7) receptor. Neurosci. Lett. 481, 12-16.

Heidmann DE., Metcalf MA., Kohen R., Hamblin MW. (1997). Four 5-hydroxytryptamine7 (5-HT7) receptor isoforms in human and rat produced by alternative splicing: species differences due to altered intron-exon organization. J. Neurochem 68:1372-1381.

Heidmann DE., Szot P., Kohen R., Hamblin MW. (1998) Function and distribution of three rat 5-hydroxytryptamine7 (5-HT7) receptor isoforms produced by alternative splicing. Neuropharmacology 37(12):1621–1632.

Hensler J.G. (2006). Serotonergic modulation of the limbic system. Neurosci. 19, 10348-10356.

Hoyer D., Clarke DE., Fozard JR., Hartig PR., Martin GR., Mylecharane EJ., Saxena PR., Humphrey PP. (1994) International union of pharmacology classification of receptors for 5-hydroxytryptamine (serotonin). Pharmacol Rev 56:157-203.

Hoyer D., Martin.(1997). 5-HT receptor classification and nomenclature: towards a harmonization with the huan genome. Neuropharmacology 36: 419-428.

Inoue M., Kitazawa T., Cao J., Taneike T. (2003) 5-HT7 receptor- mediated relaxation of the oviduct in nonpregnant proestrus pigs. Eur J Pharmacol 461(2–3):207–218.

Jahnichen S., Glusa E., Pertz HH. (2005) Evidence for 5-HT2b and 5-HT7 receptor-mediated relaxation in pulmonary arteries of weaned pigs. Naunyn-Schmiedeberg's Arch Pharmacol 371(1):89–98.

Janssen P., Prins NH., Moreaux B., Meulemans AL., Lefebvre RA. (2005) Characterization of 5-HT7-receptor-mediated gastric relaxation in conscious dogs. Am J Physiol Gastrointest Liver Physiol 289(1):G108–G115.

Kasai H., Fukunda M., Watanabe S., Hayashi-Takagi A., Noguchi J. (2010). Structural dynamics of dendritic pines in memory and cognition. Trends Neurosci; 33:121-129.

Kim S.H., Ryan T.A., (2010). CDK5 serves as a major control point in neurotransmitter release. Neuron. 67, 797-809.

Kitazawa T., Nakagoshi K., Teraoka H., Taneike T. (2001) 5-HT(7) receptor and beta(2)-adrenoceptor share in the inhibition of porcine uterine contractility in a muscle layer-dependent manner. Eur J Pharmacol 433(2–3):187–197.

Kiuchi T., Nagai T., Ohashi K., Mizuno K. (2011). Measurements of spatiotemporalchanges in G-actin concentration reveal its effect on stimulus-induced actin assembly and lamellipodium extension. J Cell Biol 193, 365-380.

Kobe F., Guseva D., Jensen TP., Wirth A., Renner U., Hess D., Muller M., Medrihan L., Zhang W., Zhang M., Braun K., Westerholz S., Herzog A., Radyushkin K., El-kordi A., Ehrenreich H., Richter DW., Rusakov DA., Ponimaskin E. (2012) 5-HT7R/G12 signaling regulates neuronal morphology and function in an age-dependent manner. J. Neurosci. 32, 2915-2930.

Krobert KA., Bach T., Syversveen T., Kvingedal AM., Levy FO (2001). The cloned human 5-HT7 receptor splice variants: a comparative characterization of their pharmacology, function and distribution. Naunyn Schmiedebergs Arch Pharmacol 363: 620-632.

Krobert KA., Levy FO. (2002) The human 5-HT7 serotonin receptor splice variants: constitutive activity and inverse agonist effects. Br J Pharmacol 135(6):1563–1571.

Kuznetsov S. A., Rodionov V. I., Nadezhdina E. S., Murphy D. B., Gelfand VI. (1986) Identification of a 34-kD polypeptide as a light chain of microtubule-associated protein-1 (MAP-1) and its association with a MAP-1 peptide that binds to microtubules. J. Cell Biol. 102, 1060-1066.

Kvanchina E., Liu G., Dityatev A., Renner U., Dumuis A., Richter D.W., Dityateva G., Schachner M., Voyno-Yasenetskaya T.A., Ponimaskin EG. (2005) 5-HT7 receptor is coupled to Gα-subunits

of heterotrimeric G12-protein to regulate gene transcription and neuronal morphology. J. Neurosci. 25, 7821-7830.

Laenen K., Haegeman G., Vanhoenacker P. (2007) Structure of the human 5-HT7 receptor gene and characterization of its promoter region. Gene 391(1–2):252–263.

Lai KO., Ip NY. (2009) Recent advances in understanding the roles of Cdk5 in synaptic plasticity. Biochim. Biophys. Acta 1792, 741–745.

Leo D., Adriani W., Cavaliere C., Cirillo G., Marco E.M., Romano E., di Porzio U., Papa M., Perrone-Capano C., Laviola G. (2009). Methylphenidate to adolescent rats drives enduring changes of accumbal Htr7 expression: implications for impulsive behavior and neuronal morphology. Genes Brain Behav. 8, 356-368.

Leon-Ponte M., Ahern GP., O'Connell PJ. (2007) Serotonin provides an accessory signal to enhance T-cell activation by signaling through the 5-HT7 receptor. Blood 109(8):3139–3146.

Leopoldo M. (2004) Serotonin7 receptors (5-HT7Rs) and their ligands, Curr. Med. Chem. 11 629–661.

Leopoldo M., Lacivita E., De Giorgio P., Fracasso C., Guzzetti S., Caccia S., Contino M., Colabufo N.A., Berardi F., Perrone R. (2008) Structural modifications of N-(1,2,3,4tetrahydronaphthalen-1-yl)-4-aryl-1-piperazinehexanamides: influence on lipophilicity and 5-HT7 receptor activity. Part III, J. Med. Chem. 51, 5813–5822.

Leopoldo M., Lacivita E., Berardi F., Perrone R., Hedlund P.B. (2011). Serotonin 5-HT7 receptor agents: Structure-activity relationships and potential therapeutic applications in central nervous system disorders. Pharmacol. Ther. 129, 120-148.

Lieb K. Biersack L., Waschbisch A., Orlikowski S., Akundi RS., Candelario-Jalil E., Hull M., Fiebich BL. (2005) Serotonin via 5- HT7 receptors activates p38 mitogen-activated protein kinase

and protein kinase C epsilon resulting in interleukin-6 synthesis in human U373 MG astrocytoma cells. J Neurochem 93(3):549–559.

Lin S.L., Johnson-Farley N.N., Lubinsky D.R., Cowen D.S. (2003) Coupling of neuronal 5-HT7 receptors to activation of extracellular-regulated kinase through a protein kinase A-independent pathway that can utilize Epac. J. Neurochem. 87, 1076-1085.

Liston C., Malter Cohen M., Teslovich T., Levenson D., Casey B.J. (2011). Atypical prefrontal connectivity in attention-deficit/hyperactivity disorder: pathway to disease or pathological end point? Biol. Psychiatry 69, 1168-1177.

Lovenberg TW., Baron BM., de Leces L., Miller JD., Prosser RA., Rea MA., Foye PE., Racke M., Slone Al., Siegel BW., et al (1993). A novel adenylyl cyclase-activating serotonin receptor (5-HT7) implicated in the regulation of mammalian circadian rhythms. Neuron11:449-458.

Mahe C., Loetscher E., Dev KK., Bobirnac I., Otten U., Schoeffter P. (2005) Serotonin 5-HT7 receptors coupled to induction of interleukin-6 in human microglial MC-3 cells. Neuropharmacol-ogy 49(1):40–47.

Marston OJ., Garfield AS., Heisler LK.(2011) Role of central serotonin and melanocortin system in the control of energy balance. Eur J Pharmacol 660(1):70-79.

Martin-Cora F.J., and Pazos A. (2004) Autoradiographic distribution of 5-HT7 receptors in the human brain using [3H]mesulergine: comparison to other mammalian species. Br. J. Pharmacol. 141, 92-104.

Matthys A., Haegeman G., Van Craenenbroeck K., Vanhoenacker P. (2011). Role of the 5-HT7 receptor in the central nervous system: from current status to future perspectives. Mol. Neurobiol. 43, 228-253.

Matus A. (1991) Microtubule-associated proteins and neuronal morphogenesis. J. Cell. Sci. Suppl. 15, 61-67.

Mnie-Filali O., Dahan L., Zimmer L., Haddjeri N. (2007). Effects of the serotonin 5-HT(7) receptor antagonist SB-269970 on the inhibition of dopamine neuronal firing induced by amphetamine. Eur. J. Pharmacol. 570, 72-76.

Mnie-Filali O., Faure C., Lambas-Senas L., El Mansari M., Belblidia H., Gondard E., Etiavant A., Scarna H., Didier A., Berod A., Blier P., Haddjeri N. (2011) Pharmacological blockade of 5-HT7 receptors as a putative fast acting antidepressant strategy. Neuropsychopharmacol. 36, 1275-1288.

Monk SA., Williams JM., Hope AG., Barnes NM. (2004) Identification and importance of N-glycolysation of the human 5-hydroxytryptamine3A receptor subunit. Biochem Pharmacol 68:1787-1796.

Montenegro-Venegas C., Tortosa E., Rosso S., Peretti D, Bollati F., Bisbal M., Jausoro I., Avila J., Caceres A., and Gonzalez-Billault C. (2010) MAP1B Regulates axonal development by modulating Rho-GTPase Rac1 activity.Molecular Biology of the Cell. Vo. 21, 3518-3528.

Morozova O., Marra H. and Marra M.A. (2009) Applications of new sequencing technologies for transcriptome analysis. Annu. Rev. Genomics. Hum. Genet. 10:135-151.

Mullins U.L., Gianutsos G., Eison A.S. (1999). Effects of antidepressants on 5-HT7 receptor regulation in the rat hypothalamus. Neuropsychopharmacol. 21, 352-367.

Muneoka K.T., and Takigawa M. (2003) 5-Hydroxytryptamine7 (5-HT7) receptor immunoreactivity-positive “stigmoid body’-like structure in developing rat brains. Int. J. Dev. Neurosci. 21, 133-143.

Nandam LS., Jhaveri D., Bartlett P. (2007) 5-HT7, neurogenesis and antidepressants: a promising therapeutic axis for treating depression. Clin. Exp. Pharmacol. Physiol. 34, 546-551.

Neumaier J.F., et al (2001) Localization of 5-HT7 receptors in rat brain by immunocytochemistry, in situ hybridization, and agonist stimulated cFos expression. J.Chem.Neuroanat. 21, 63-73.

Nikolic, M., Dudek, H., Kwon, Y.T., Ramos, Y.F.M., Tsai, LH. (1996). The cdk5/p35 kinase is essential for neurite outgrowth during neuronal differentiation. Genes Dev. 10, 816-825.

Nichols D.E. and Nichols C.D. (2008) Serotonin receptors. Chem Rev. 108, 1614-1641.

Nikolic M., Dudek H., Kwon Y.T., Ramos Y.F.M., Tsai LH. (1996) The cdk5/p35 kinase is essential for neurite outgrowth during neuronal differentiation. Genes Dev. 10, 816-825.

Norum JH., Hart K., Levy FO. (2003) Ras-dependent ERK activation by the human g(s)-coupled serotonin receptors 5- HT4(b) and 5-HT7(a). J Biol Chem 278(5):3098–3104.

Otyepka M., Bártová I., Kríz Z., Koca J. (2006) Different mechanisms of CDK5 and CDK2 activation as revealed by CDK5/p25 and CDK2/cyclin A dynamics. J Biol Chem. 281, 7271-7281.

Papageorgiou A., Denef C. (2007) Stimulation of growth hormone release by 5-hydroxytryptamine (5-HT) in cultured rat anterior pituitary cell aggregates: evidence for mediation by 5-HT2b, 5- HT7, 5-HT1b, and ketanserin-sensitive receptors. Endocrinology 148(9):4509–4522.

Park TH., Shuler ML.(2003) Integration of cell culture and microfabrication technology. Biotechnol. Prog 19: 243-253.taylor

Parker LL., Backstrom JR., Sanders-Bush E., Shieh BH. (2003) Agonist-induced phosphorylation of the serotonin 5-HT_{2C} receptor regulates its interaction with multiple PDZ protein 1. J Biol Chem 278: 21576-21583.

Pennypacker K., Fischer I., Pat Levitt P. (1991) Early in Vitro genesis and differentiation of axons and dendrites by hippocampal neurons analyzed quantitatively with neurofilament-H and microtubule-associated protein 2 antibodies. Experimental Neurology 111, 23-35.

Pittalà V., Salerno L., Modica M., Siracusa M.A., Romeo G. (2007) 5-HT7 receptor lig- ands: recent developments and potential therapeutic applications, Mini Rev. Med. Chem. 7, 945–960.

Poelmans G., Pauls DL., Buitelaar JK., Franke B. (2011) Integrated genome-wide association study findings: identification of a neurodevelopmental network for attention deficit hyperactivity disorder. Am. J. Psychiatry 168, 365-377.

Pollard T.D., and Earnshaw W.C. (2007) Cell Biology. Second Edition. W.B. Saunders, New York, NY.

Ponimaskin E., Voyno-Yasenetskaya T., Richter D.W., Schachner M., Dityatev A. (2007) Morphogenic signaling in neurons via neurotransmitter receptors and small GTPases. Mol. Neurobiol. 35, 278-287.

Pytliak, M., Vargová, V., Mechírová, V., Felšöci, M. (2011) Serotonin receptors - from molecular biology to clinical applications. Physiol. res. 60, 15-25.

Raikhlin NT., Kvetnoy IM., Tolkachev VN. (1975) Melatonin may be synthesised in enterochromaffin cells. Nature 255(5506):344-345.

Read K.E., et al. (2003) Evidence for the involvement of central 5-HT7 receptors in the micturition reflex in anaesthetized femal rats. Br. J. Pharmacol. 140, 53-60.

Recio P., Barahona MV., Orensanz LM., Bustamante S., Martinez AC., Benedito DS., Garcia-Sacristan A., Prieto D., Hernandez M. (2009) 5-Hydroxytryptamine induced relaxation in the pig urinary bladder neck. Br J Pharmacol 157(2): 271-280.

Renner U., Zeug A., Woehler A., Niebert M., Dityatev A., Dityateva G., Gorinski N., Guseva D., Abdel-Galil D., Fröhlich M., Döring F., Wischmeyer E., Richter DW., Neher E., Ponimaskin EG. (2012) Heterodimerization of serotonin receptors 5-HT1A and 5-HT7 differentially regulates receptor signalling and trafficking. J Cell Sci. Feb 22.

Ridley AJ., Schwartz MA., Burridge K., Firtel RA., Ginsberg MH., Borisy G., Parson JT., Horwitz AR. (2003) Cell migration: integrating signals from front to back. Science 302, 1704-1709.

Riederer B.M. (2007). Microtubule-associated protein 1B, a growth-associated and phosphorylated scaffold protein. Brain Res. Bull. 71, 541-558.

Roberts AJ., et al.(2004) Mice lacking 5-HT7 receptors show specific impairments in contextula learning. Eur. J. Neurosci. 19, 1913-1922.

Roth B.L., Craigo S.C., Choudhary M.S., Uluer A., Monsma F.J. Jr, Shen Y., Meltzer H.Y., Sibley D.R. (1994) Binding of typical and atypical antipsychotic agents to 5-hydroxytryptamine-6 and 5-hydroxytryptamine-7 receptors. J. Pharmacol. Exp. Ther. 268, 1403-1410.

Rozenfeld R., and Devi LA. (2011) Exploring a role for heteromerization in GPCR signaling specificity. Biochem J. 433, 11-18.

Sarkisyan G., Hedlund PB. (2009) The 5-HT7 receptor is involved in allocentric spatial memory information processing. Behav. Brain Res. 202, 26-31.

Schmittgen T.D., Livak K.J. (2008) Analyzing real-time PCR data by the comparative C(T) method. Nat. Protoc. 3, 1101-1108.

Severino V., Chambery A., Vitiello M., Cantisani M., Galdiero S., Galdiero M., Malorni L., Di Maro A., Parente A. (2010) Proteomic analysis of human U937 cell line activation mediated by Haemophilus influenzae type b P2 porin and its surface-exposed loop 7. J. Proteome Res. 9, 1050-1062.

Shelly M., Lim B.K., Cancedda L., Heilshorn S.C., Gao H., Poo M.M. (2010) Local and long-range reciprocal regulation of cAMP and cGMP in axon/dendrite formation. Science 327, 547–552.

Shen Y., Monsma FJ Jr., Metcalf MA., Jose PA., Hamblin MW., Sibley DR. (1993) Molecular cloning and expression of a 5-hydroxytryptamine7 serotonin receptor subtype. J. Biol. Chem. 268:18200-18204.

Sjogren B., Hamblin MW., Svenningsson P. (2006) Cholesterol depletion reduces serotonin binding and signaling via human 5-HT7 receptor isoforms and PLAC-24/eiF3k. Cell Signal 19 (2):278-288.

Sjogren B., Svenningsson P. (2007) Depletion of the lipid raft constituents, sphingomyelin and ganglioside, decreases serotonin binding at human 5-HT7(a) receptors in HeLa cells. Acta Physiol (Oxf) 190(1):47–53.

Staffend N.A. and Meisel R.L. (2011) DiOlistic labeling in fixed brain slices: phenotype, morphology and dendritic spines. Curr Protoc Neurosci; Unit2.13.

Steinbusch HWM. (1981) Distribution of serotonin-immunoreactivity in the central nervous system of the rat cell bodies and terminals. Neuroscience 6:557-618.

Stoltenberg SF., Glass JM., Chermack ST., Flynn HA., Li S., Weston ME, Burmeister M (2006) Possible association between response inhibition and a variant in the brain-expressed tryptophan hydroxylase-2 gene. Psychiatr Genet 16: 35-38.

Taylor AM., Blurton-Jones M., Rhee SW., Cribbs DH., Cotman CW., Jeon NL. (2005) A microfluidic culture platform for CNS axonal injury, regeneration and transport. Nat Methods (8):599-605.

Teitler M., Klein M.T. (2012) A new approach for studying GPCR dimers: drug-induced inactivation and reactivation to reveal GPCR dimer function in vitro, in primary culture, and in vivo. Pharmacol Ther. 133, 205-217.

Thomas D.R., Melotto S., Massagrande M., Gribble A.D., Jeffrey P., Stevens A.J., Deeks N.J., Eddershaw P.J., Fenwick S.H., Riley G., Stean T., Scott C.M., Hill M.J., Middlemiss D.N., Hagan J.J., Price G.W., Forbes I.T. (2003) SB-656104-A, a novel selective 5-HT7 receptor antagonist, modulates REM sleep in rats. Br. J. Pharmacol. 139, 705-714.

Tögel M., Wiche G. Propst F. (1998) Novel features of the light chain of microtubule-associated protein MAP1B: microtubule stabilization, self interaction, actin filament binding, and regulation by the heavy chain. J. Cell Biol. 143, 695-707.

Tortosa E., Montenegro-Venegas C., Benoist M., Härtel S., González-Billault C., Esteban J.A., Avila J. (2011) Microtubule-associated protein 1B (MAP1B) is required for dendritic spine development and synaptic maturation. J. Biol. Chem. 286, 40638-40648.

Turner JH., Raymond JR (2005). Interaction of calmodulin with the serotonin 5-hydroxytryptamine2A receptor. A putative regulator of G protein coupling and receptor phosphorylation by protein kinase C. J Biol Chem 280: 30741-30750.

Tymanskyj S.R., Scales T.M.E., Gordon-Weeks P.R. (2012) MAP1B enhances microtubule assembly rates and axon extension rates in developing neurons. Mol. Cell. Neurosci. 49, 110-119.

Vanhoenacker P., Haegeman G., Leysen JE (2000). 5-HT7 receptors: current knowledge and future prospects. Trends Pharmacol Sci 21:70-77.

Wade PR. et al (1996) Localization and function of a 5-HT transporter in crypt epithelia of the gastrointestinal tract. J Neurosci 16(7):2352-2364.

Walther D.J. et al. (2003). Serotonylation of small GTPases is a signal transduction pathway that triggers platelet α-granule release. Cell 115, 851-862.

Wilson CA., Tsuchida MA., Allen GM., Barnhart EL., Applegate KT., Yam PT., Ji L, Keren K., Danuser G., Theriot JA. (2010) Myosin II contributes to cell-scale actin network treadmilling through network disassembly. Nature 465, 373-377.

Wu X., Kushwaha N., Albert PR., Penington NJ. (2002) A critical protein kinase C phosphorylation site on the 5-HT_{1A} receptor controlling coupling to N-type calcium channels. J Physiol 538: 41-51.

Yamagata M., Sanes J.R., and Weiner J.A. (2003) Synaptic adhesion molecules. Curr. Opin. Cell Biol. 15, 621-632.

Yuste R. and Bonhoeffer T. (2004) Genesis of dendritic spines: insights from ultrastructural and imaging studies. Nat. Rev. Neurosci. 5, 24-34.

Yu PL., Fujimura M., Okumiya K., Kinoshita M., Hasegawa H.and Fujimiya M.(1999) Immunohistochemical localization of tryptophan hydroxylase in the human and rat gastrointestinal tracts. The journal of comparative neurology 411:654-665.

Zhang P., Yu PC., Tsang A.H.K., Chen Y., Fu A.K.Y., Fu WY., Chung K.K., Ip N.Y. (2010) S-nitrosylation of cyclin-dependent kinase 5 (Cdk5) regulates its kinase activity and dendrite growth during neuronal development. J Neurosci. 30, 14366-14370.

8. LIST OF ABBREVIATIONS

A

AADC	L-amino acid decarboxylase
AC	Adenylyl cyclase
AP2	Adipocyte protein 2
ATP	*Adenosine triphosphate*

B

bp	Base pair
BSA	*Bovine serum albumine*

C

CA	*Cornu Ammonis*
cAMP	3'-5'-cyclic adenosine monophosphate
CDK	Cyclin-dependent kinase
Cdk2	Cyclin-dependent kinase 2
Cdk5	Cyclin-dependent kinase 5
cDNA	Complementary DNA
CHX	Cycloheximide
CLi	Caudal linear nucleus
CNS	Central Nervous System
CTRL	Control
CTX	Cortex
CYT	Cytochalasin D

D

DAPI	4',6-diamidino-2-phenylindole
DAVID	Database for Annotation, Visualization and Integrated Discovery

DE	
DiI	1,1=-dioctadecyl-3,3,3=,3=-tetramethylindocarbo- cyanine perchlorate
DMSO	Dimethyl sulfoxide
DNA	Deoxyribonucleic acid
DR	Dorsal raphe nucleus
DTT	Dithiothreitol

E

E	Embryonic age
EC cells	Enterochromaffin cells
Egr-1	Early growth response 1
ERK	Extracellular signal-regulated kinase

G

GABA	Gamma-aminobutyric acid
GAD	Glutamate decarboxylase
Gch1	GTP cyclohydrolase 1
Gfrp	GTP cyclohydrolase I feedback regulatory protein
GO	Gene ontology
GPCR	G-protein coupled receptor
Gs	Activating adenylyl cyclase
GTP	*Guanosine-5'-triphosphate*

H

h	Hours
HIPP	Hippocampus
HPRT	Hypoxanthine-guanine phosphoribosyltransferase

I

IEF	Isoelectrofocusing
IL2	Interleukin 2
IP3	Inositol trisphosphate
IPG	Immobilized pH gradient

J

JASP	Jasplakinolide

K

KEGG	*Kyoto Encyclopedia of Genes and Genomes*
KO	Knockout

L

LAS	Leica application suite
LATR	Latrunculin
LGIC	Ligand-gated ion channel
LP-211	N-(4-cyanophenylmethyl)-4-(2-diphenyl)-1-piperazinehexanamide
LTD	Long-term depression

M

MAOA	Monoamino oxidase A
MAPK	Mitogen activated protein kinase
MAPs	Microtubule-associated protein
MAP1B	Microtubule-associated protein 1B
MAP2	Microtubule-associated protein 2
MAP1B-HC	Microtubule-associated protein 1B-heavy chain
MAP1B-LC1	Microtubule-associated protein 1B-light chain
MAPK	Mitogen-activated protein kinase
MAZ	MYC-associated zinc finger protein
MeCp2	Methyl CpG-binding protein 2
Mecp2-/y	Mecp2 null mice
MFB	Medial frontal bundle
mGluR	Metabotropic glutamate receptors
MR	Median raphe nucleus

N

NFL	Neurofilament light chain
NFM	Neurofilament medium chain
NGS	Normal goat serum
NGS	Next generation sequencing

P

p-ERK	Posphorilated-Extracellular signal-regulated kinases
PAGE	Polyacrylamide gel electrophoresis
PBS	*Phosphate buffered saline*
PCR	Polymerase chain reaction
PFA	Paraformaldehyde
PKA	Protein kinase A
PKCε	Protein kinase Cε
Ptps	Protein tyrosine phosphatases
PVDF	Polyvinylidene fluoride

Q

Qdpr	Quinoid dihydropteridine reductase

R

RNA	Ribonucleic acid
RNA-seq	RNA sequencing
ROSC	Roscovitine
RT-PCR	Reverse transcription polymerase chain reaction
RTT	Rett syndrome

S

SB-258719	(R)-3,N-dimethyl-N-[1-methyl-3-(4-methyllpiperidin-1-yl)propyl]benzene sulfonamide
SB-269970	(2R)-1-[3-hydroxy-phenyl)sulfonyl]-2-[2-(4-methyl-1-piperidinyl)ethyl]pyrrolidine
SCN	Suprachiasmatic nucleus
SDS	Sodium dodecyl sulfate
SEM	Standard error of mean
SERT	Serotonin reuptake transporter

Sp1	Specificity protein 1
Sp3	Specificity protein 3
SRE	Serum response element
STR	Striatum

T

TRYP	Tryptophan
Tph	Tryptophan 5-hydroxylase
TBS	Tris-buffered saline
TBST	Tris buffered saline + Tween

U

U0126	MEK inhibitor U0126

V

V	Volt
VMAT	Vesicular monoamine transporter

W

WAY100635	(N-[2-[4-(2-methoxyphenyl)-1-piperazinyl]ethyl]-N (2pyridyl)cyclohexanecarboxamide
WB	Western blot
WT	Wild type

2D-WB	2 dimensional western blot
5-CT	5-carboxamidotryptamine
5-HIAA	5-hydroxyindoleacetic acid
5-HT	5-hydroxytryptamine
5-HTP	5-hydroxy-L-tryptophan
5-HTR	5-HT receptor
5-HT7R	5-HT receptor 7
5-MeOT	5-Methoxytryptamine

8-OH-DPAT 8-hydroxy-N,N-dipropylaminotetraline